

**Synthesis and Solubility of Arsenic Tri-sulfide and
Sodium Arsenic Oxy-sulfide Complexes in Alkaline
Sulfide Solutions**

by

Wen Li

B. Sc., (Materials Engineering), Hebei University of Technology, China, 2006

A THESIS SUBMITTED IN PARTIAL FULFILLMENT OF THE
REQUIREMENTS FOR THE DEGREE OF

MASTER OF APPLIED SCIENCE

in

THE FACULTY OF GRADUATE STUDIES

(Materials Engineering)

THE UNIVERSITY OF BRITISH COLUMBIA

(Vancouver)

June 2013

© Wen Li, 2013

Abstract

Alkaline sulfide leaching (ASL) at approximately 100 °C has been used to selectively extract arsenic and antimony from enargite and tetrahedrite concentrates. Sodium thio-arsenate has been postulated to crystallize from alkaline sulfide leaching solutions upon cooling. However, literature data on the solubility of sodium thio-arsenate as well as proof of its crystallization from ASL solutions is scant. In this thesis, the solubility of leach-produced and synthetic sodium thio-arsenate is studied.

To determine arsenic solubility in ASL solutions, sodium thio-arsenate and sodium arsenic oxide sulfide complexes are synthesized by various means and characterized by EDX, QXRD, and ICP.

The synthesis of amorphous As_2S_3 , sodium arsenic oxy-sulfide complexes, and sodium thio-arsenate is first presented. For amorphous As_2S_3 synthesis, the effect of concentration of sodium sulfide (0.1 M) and hydrochloric acid (1 M), temperature (40 ~ 60 °C), and aging time (48 hours) was optimized. The solubility of synthetic sodium arsenic oxy-sulfide complexes and sodium thio-arsenate in ASL solutions increases significantly as temperature is increased to 95 °C. More importantly, the solubility of sodium thio-arsenate at certain temperatures is significantly affected by the concentration of sodium hydroxide and sulfide in solution. Due to the common ion effect, if NaOH and HS^- concentrations are very high, the solubility of sodium thio-arsenate decreases.

Enargite leaching tests were done to characterize the precipitate that occurred upon cooling and to verify the arsenic saturation point, which should be between 38.5 ~ 58 g/L (0.51 M ~ 0.78 M) As depending on the NaOH and HS^- concentration. Comparison with

solubility experiments of pure sodium thio-arsenate shows that arsenic solubility in ASL solutions is supersaturated. However, direct comparison of saturation in ASL solutions and the solubility as obtained by the synthetic solutions/crystallites prepared here is not possible given the complex nature of the ASL crystallites that appear not to contain the often discussed “sodium thio-arsenate”.

Preface

This dissertation is original, unpublished, independent work by the author, W. Li.

Table of Contents

Abstract	i
Preface	iii
Table of Contents.....	iv
List of Tables.....	viii
List of Figures	x
Acknowledgments.....	xiv
Chapter 1 Introduction	1
Chapter 2 Literature Review	7
2.1 Copper arsenic minerals	7
2.2 Metallurgical processing of enargite	11
2.2.1 <i>Pyrometallurgical treatment</i>	14
2.2.2 <i>Alkaline sulfide leaching of enargite</i>	17
2.2.3 <i>Arsenic removal and precipitate analysis</i>	20
2.2.4 <i>Sodium thio-arsenate solubility</i>	24
2.3 Synthesis of amorphous As_2S_3	25
2.4 Synthesis of sodium thio-arsenate	26
2.5 Solubility of amorphous As_2S_3	30
Chapter 3 Objectives.....	33
Chapter 4 Experimental Procedures	34
4.1 Preliminary solubility study on arsenic trioxide	34
4.2 Synthesis of amorphous As_2S_3	34
4.2.1 <i>Concentration effect</i>	37
4.2.2 <i>Temperature effect</i>	39
4.2.3 <i>Effect of hydrochloric acid addition rate</i>	39
4.2.4 <i>Aging time effect</i>	40
4.3 Solubility of amorphous As_2S_3 in sodium sulfide solution.....	40

4.4 Synthesis of sodium thio-arsenate	40
4.4.1 <i>Synthesis of precursor sodium arsenate by hydrogen peroxide oxidation of As (III)</i>	40
4.4.1.1 Synthesis of sodium thio-arsenate from sodium arsenate and sodium sulfide solution	42
4.4.1.2 Synthesis of sodium thio-arsenate from sodium arsenate and solid sodium sulfide	42
4.4.1.3 Synthesis of sodium thio-arsenate from sodium arsenate and hydrogen sulfide gas.....	43
4.4.2 <i>Synthesis of sodium thio-arsenate by reaction of arsenic tri-sulfide with elemental sulfur</i>	45
4.5 Solubility of synthetic sodium arsenic oxy-sulfide complexes and sodium thio-arsenate.....	46
4.6 Solubility accuracy calibration test	47
4.7 Precipitation from an enargite leaching test	48
Chapter 5 Results and Discussion	52
5.1 Solubility of As_2O_3 in Na_2S and $NaOH$ solution.....	52
5.2 Characterization of synthesized amorphous As_2S_3	55
5.2.1 <i>Effect of reagent concentrations</i>	56
5.2.2 <i>Effect of temperature</i>	57
5.2.3 <i>Effect of hydrochloric acid solution flow rate</i>	59
5.2.4 <i>Effect of aging time</i>	60
5.3 Solubility of As_2S_3 in Na_2S solution.....	61
5.4 Characterization of synthetic crystalline products.....	63
5.4.1 <i>Attempts to synthesize sodium arsenic oxy-sulfide from sodium arsenate precursor</i>	63
5.4.2 <i>Synthesis of sodium thioarsenate by reaction of As_2S_3 with elemental sulfur</i>	67
5.4.3 <i>Arsenic content determination by ICP analysis</i>	69
5.5 Solubility of synthesized sodium thio-arsenate products	70
5.5.1 <i>Sodium arsenate precursor synthesized by oxidation of As (III) with hydrogen peroxide</i>	70
5.5.1.1 Sodium thio-arsenate synthesized by the addition of sodium sulfide solution to dissolved sodium arsenate precursor (product #1)	70
5.5.1.2 Sodium thio-arsenate synthesized by the addition of solid sodium sulfide to dissolved sodium arsenate precursor (product #2).....	70
5.5.1.3 Sodium thio-arsenate synthesized by the addition of hydrogen sulfide to dissolved sodium arsenate precursor (product #3).....	72
5.5.2 <i>Synthesis of thio-arsenate by oxidation of As (III) with elemental sulfur</i>	73

5.5.2.1 Solubility of sodium thio-arsenate (product #4) in leach solution under air atmosphere and argon atmosphere	73
5.5.2.3 Solubility of synthetic crystal #4 (sodium thio-arsenate) at constant hydroxide (2.5 M/100 g/L) and varying hydrosulfide content (0 M ~ 1.0 M/0 ~ 56 g/L) in argon.....	75
5.6 Solubility accuracy calibration test	78
5.7 Solubility of As in ASL solutions originating from an enargite leaching test	78
Chapter 6 Conclusion.....	82
Chapter 7 Future Work	83
References	84
Appendix	90
Part A. Tables of solubility data by experiment and OLI systems software for amorphous As_2S_3 and synthetic crystals	90
<i>A.1 Solubility data of orpiment in literature and amorphous As_2S_3 by experiment and OLI systems software</i>	<i>90</i>
<i>A.2 Solubility data of synthetic crystal #2, #3, #4 (sodium thio-arsenate) by experiment.....</i>	<i>96</i>
A.2.1 Solubility of synthetic crystal #2 in air	96
1. In 100 ml 2.5 M sodium hydroxide and 1.0 M sodium sulfide solution.....	96
2. In 100 ml 2.5 M sodium hydroxide and 0.5 M sodium sulfide solution.....	96
3. In 100 ml 1.0 M sodium hydroxide and 1.0 M sodium sulfide solution.....	96
A.2.2 Solubility of synthetic crystal #3 in air	97
1. In 10 ml 2.5 M sodium hydroxide and 1.0 M sodium sulfide solution.....	97
2. In 10 ml 2.5 M sodium hydroxide and 0.5 M sodium sulfide solution.....	97
3. In 10 ml 1.0 M sodium hydroxide and 1.0 M sodium sulfide solution.....	98
A.2.3 Solubility of synthetic crystal #4 (sodium thio-arsenate) in air	98
1. In 20 ml 2.5 M sodium hydroxide and 1.0 M sodium sulfide solution under air atmosphere	98
2. In 20 ml 2.5 M sodium hydroxide and 0.5 M sodium sulfide solution under air atmosphere	98
3. In 20 ml 1.0 M sodium hydroxide and 1.0 M sodium sulfide solution under air atmosphere	99
A.2.4 Solubility of synthetic crystal #4 (sodium thio-arsenate) in argon.....	99
1. In 10 ml 2.5 M sodium hydroxide and 1.0 M sodium sulfide solution under argon atmosphere	99

2.	In 10 ml 2.5 M sodium hydroxide and 0.5 M sodium sulfide solution under air atmosphere	100
3.	In 10 ml 1.0 M sodium hydroxide and 1.0 M sodium sulfide solution under air atmosphere	100
A.2.5 Solubility of synthetic crystal #4 (sodium thio-arsenate) at constant hydroxide and varying hydrosulfide content in argon		
		101
1.	In 10 ml 2.5 M sodium hydroxide and 1.0 M sodium hydrosulfide solution	101
2.	In 10 ml 2.5 M sodium hydroxide and 0.5 M sodium hydrosulfide solution	101
3.	In 10 ml 2.5 M sodium hydroxide and 0 M sodium hydrosulfide solution	101
Part B. EDX analysis of synthetic complexes		102
Part C. Quantitative x-ray diffraction result of arsenic precipitate from enargite leaching		105

List of Tables

TABLE 1.1 MAJOR ARSENIC MINERALS OCCURRING IN NATURE (WTO ARSENIC COMPOUNDS, 2001)	1
TABLE 1.2 ARSENIC DEPOSITS OF THE WORLD (WTO ARSENIC COMPOUNDS, 2001)	2
TABLE 1.3 SUMMARY OF TOXIC EFFECTS IN HUMANS AFTER OCCUPATIONAL INHALATION EXPOSURE TO INORGANIC ARSENIC COMPOUNDS (EUROPEAN COMMISSION 2001)	4
TABLE 2.1 THE MOST COMMONLY FOUND (OR ANTICIPATED) ARSENIC COMPOUNDS IN AIR (EUROPEAN COMMISSION 2001)	8
TABLE 2.2 THE MOST COMMON CU-AS-SB-S MINERALS AND THEIR PHYSICAL PROPERTIES (BARTHELMY 2004) ...	9
TABLE 4.1 CONDITIONS OF AS ₂ S ₃ SYNTHESIS CONCENTRATION TESTS	37
TABLE 4.2 CONDITIONS OF AS ₂ S ₃ SYNTHESIS TEMPERATURE TESTS	39
TABLE 4.3 CONDITIONS OF AS ₂ S ₃ SYNTHESIS FLOW RATE TESTS	39
TABLE 4.4 CONDITIONS OF AS ₂ S ₃ SYNTHESIS AGING TIME TESTS	40
TABLE 4.5 THREE DIFFERENT LEACH SOLUTIONS FOR SOLUBILITY TESTS	47
TABLE 4.6 THREE CONDITIONS FOR VARYING HYDROSULFIDE AND CONSTANT NaOH	47
TABLE 4.7 ELEMENTAL ANALYSIS OF THE ENARGITE SAMPLE	49
TABLE 4.8 QUANTITATIVE PHASE ANALYSIS OF THE ENARGITE SAMPLE	49
TABLE 5.1 EDX RESULT FOR EFFECT OF CONCENTRATION	56
TABLE 5.2 EDX RESULT FOR EFFECT OF TEMPERATURE	58
TABLE 5.3 EDX RESULT FOR EFFECT OF HYDROCHLORIC ACID FLOW RATE	59
TABLE 5.4 EDX RESULT FOR EFFECT OF AGING TIME	60
TABLE 5.5 ELEMENTAL ANALYSIS OF SYNTHETIC SODIUM ARSENATE BY EDX	63
TABLE 5.6 EDX ANALYSIS FOR SYNTHETIC CRYSTAL #1, #2, AND #3	64
TABLE 5.7 ELEMENTAL ANALYSIS OF SYNTHETIC CRYSTALLINE PRECIPITATE #4 BY EDX	67
TABLE 5.8 QXRD RESULT AND CRYSTAL PARAMETERS OF SYNTHETIC SODIUM THIO-ARSENATE	67
TABLE 5.9 ICP ANALYSIS FOR ARSENIC CONTENT IN PRECIPITATES #2, 3 AND 4	69
TABLE 5.10 SOLUBILITY DATA FOR ACCURACY CALIBRATION	78
TABLE 5.11 ARSENIC CONCENTRATION OF SOLUTION A. AND B. BY ICP	79
TABLE 5.12 QXRD RESULT FOR ARSENIC PRECIPITATE FROM ENARGITE LEACHING TESTS (SEE XRD SPECTRA IN APPENDIX FIGURE C-1, 2, 3)	80
TABLE A-1 ORPIMENT SOLUBILITY IN SOLUTIONS TO WHICH NO SULFIDE HAS BEEN ADDED (WEBSTER 1990)	90
TABLE A-2 ORPIMENT SOLUBILITY IN SOLUTIONS TO WHICH SULFIDE HAS BEEN ADDED (WEBSTER 1990)	91

TABLE A-3 SOLUBILITY PREDICTION OF As_2S_3 IN 1 WT% OF 1 L Na_2S SOLUTION.....	93
TABLE A-4 SOLUBILITY PREDICTION OF As_2S_3 IN 2 WT% OF 1 L Na_2S SOLUTION.....	94
TABLE A-5 SOLUBILITY PREDICTION OF As_2S_3 IN 3 WT% OF 1 L Na_2S SOLUTION.....	95
TABLE A-6 SOLUBILITY OF As_2S_3 IN 1 WT%, 2 WT%, AND 3 WT% OF 80 ML Na_2S SOLUTION.....	95
TABLE A-7 SOLUBILITY OF IN 2.5 M $NaOH$ AND 1.0 M Na_2S SOLUTION.....	96
TABLE A-8 SOLUBILITY OF IN 2.5 M $NaOH$ AND 0.5 M Na_2S SOLUTION.....	96
TABLE A-9 SOLUBILITY OF IN 1.0 M $NaOH$ AND 1.0 M Na_2S SOLUTION.....	97
TABLE A-10 SOLUBILITY OF IN 2.5 M $NaOH$ AND 1.0 M Na_2S SOLUTION.....	97
TABLE A-11 SOLUBILITY OF IN 2.5 M $NaOH$ AND 0.5 M Na_2S SOLUTION.....	97
TABLE A-12 SOLUBILITY OF IN 1.0 M $NaOH$ AND 1.0 M Na_2S SOLUTION.....	98
TABLE A-13 SOLUBILITY OF $Na_3AsS_4 \cdot 8H_2O$ IN 2.5 M $NaOH$ AND 1.0 M Na_2S SOLUTION	98
TABLE A-14 SOLUBILITY OF $Na_3AsS_4 \cdot 8H_2O$ IN 2.5 M $NaOH$ AND 0.5 M Na_2S SOLUTION	99
TABLE A-15 SOLUBILITY OF $Na_3AsS_4 \cdot 8H_2O$ IN 1.0 M $NaOH$ AND 0.5 M Na_2S SOLUTION	99
TABLE A-16 SOLUBILITY OF $Na_3AsS_4 \cdot 8H_2O$ IN 2.5 M $NaOH$ AND 1.0 M Na_2S SOLUTION	100
TABLE A-17 SOLUBILITY OF $Na_3AsS_4 \cdot 8H_2O$ IN 2.5 M $NaOH$ AND 0.5 M Na_2S SOLUTION	100
TABLE A-18 SOLUBILITY OF $Na_3AsS_4 \cdot 8H_2O$ IN 1.0 M $NaOH$ AND 0.5 M Na_2S SOLUTION	100
TABLE A-19 SOLUBILITY OF $Na_3AsS_4 \cdot 8H_2O$ IN 2.5 M $NaOH$ AND 1.0 M $NaHS$ SOLUTION	101
TABLE A-20 SOLUBILITY OF $Na_3AsS_4 \cdot 8H_2O$ IN 2.5 M $NaOH$ AND 0.5 M $NaHS$ SOLUTION	101
TABLE A-21 SOLUBILITY OF $Na_3AsS_4 \cdot 8H_2O$ IN 2.5 M $NaOH$ AND 0 M $NaHS$ SOLUTION	101

List of Figures

FIGURE 2.1 CONVENTIONAL PROCESSING OF PRIMARY COPPER SULFIDE ORES (SAFARZADEH ET AL. 2012).....	11
FIGURE 2.2 A CLASSIC HYDROMETALLURGICAL ROUTE FOR COPPER PRODUCTION FROM OXIDE ORES.....	12
FIGURE 2.3 A HYDROMETALLURGICAL ROUTE FOR ENARGITE OR TENNANTITE	13
FIGURE 2.4 A COMPARISON OF WORLDWIDE COPPER PRODUCTION BY COMBINED METHODS (TOTAL) AND SOLVENT EXTRACTION/ELECTRO-WINNING (SX/EW) BETWEEN 1980 AND 2005 (REPLOTTED FROM MOATS 2005)	14
FIGURE 2.5 A SIMPLIFIED FLOWSHEET OF THE EL INDIO ENARGITE ROASTER DRAWN WITH DATA	16
BY SMITH 1986.....	16
FIGURE 2.6 SIMPLIFIED EH-PH DIAGRAM FOR THE CU-AS-S-H ₂ O SYSTEM WITH 1 MOL/L DISSOLVED SPECIES AT 25 °C AND 1 ATM (FILIPPOU ET AL. 2007)	18
FIGURE 2.7 SIMPLIFIED EH-PH DIAGRAM FOR THE CU-S-AS-H ₂ O SYSTEM WITH 1 MOL/L DISSOLVED SPECIES AT 25 °C AND 1 ATM (FILIPPOU ET AL. 2007)	19
FIGURE 2.8 AN ARSENIC DISPOSAL OPTION 1 BY ADDING H ₂ SO ₄ (NADKARNI ET AL. 1975)	21
FIGURE 2.9 ARSENIC DISPOSAL OPTIONS 2 AND 3 BY ADDING CO ₂ AND SO ₂ (NADKARNI ET AL. 1975)	22
FIGURE 2.10 FINAL ARSENIC ROUTE BY SCORODITE PRECIPITATE (NADKARNI ET AL. 1975).....	23
FIGURE 2.11 SOLUBILITY OF SODIUM THIOARSENATE AND STIBNITE IN AQUEOUS SODIUM SULFIDE (2.2~2.4M) (REPLOTTED FROM NADKARNI AND KUSIK, 1988).....	25
FIGURE 2.12 SCHEMATIC ILLUSTRATION OF THE CU ₃ AS ₄ -NAHS-NAOH LEACHING AND NA ₃ ASS ₄ PRECIPITATION PROCESS FOR ARSENIC REMOVAL AND CIRCULATION OF WASTE WATER TO LEACHING AND PRECIPITATION STAGES FOR RE-USE (TONGAMP ET AL. 2010A, 2010B).....	27
FIGURE 2.13 THE SOLUBILITY OF ORPIMENT IN 3.43 WT % NA ₂ S SOLUTIONS AT 52, 100, 150 AND 200 °C, AS A FUNCTION OF PRESSURE (REPLOTTED FROM WEISSBERG ET AL. 1966)	32
FIGURE 4.1 THE DELTA GIBBS ENERGY OF AS ₂ S ₃ SYNTHESIS REACTIONS BY HSC.....	35
FIGURE 4.2 AS ₂ S ₃ SOLUBILITY PREDICTED BY OLI AT PH RANGE 0~12 AT 25 °C.....	36
FIGURE 4.3 EXPERIMENT SETUP FOR AS ₂ S ₃ SYNTHESIS	37
FIGURE 4.4 SYNTHETIC ARSENIC TRI-SULFIDE POWDER.....	38
FIGURE 4.5 SYNTHETIC SODIUM ARSENATE	41
FIGURE 4.6 CRYSTALLINE PRECIPITATE #1 SYNTHESIZED BY ADDITION OF SODIUM SULFIDE SOLUTION TO SODIUM ARSENATE SOLUTION.....	42
FIGURE 4.7 CRYSTALLINE PRECIPITATE #2 SYNTHESIZED BY ADDITION OF SOLID SODIUM SULFIDE TO SODIUM ARSENATE SOLUTION.....	43

FIGURE 4.8 EXPERIMENTAL SETUP FOR SYNTHESIS OF SODIUM ARSENIC OXY-SULFIDE COMPLEXES BY H ₂ S	44
FIGURE 4.9 CRYSTALLINE PRECIPITATE #3 SYNTHESIZED BY H ₂ S GAS ADDITION TO SODIUM ARSENATE SOLUTION	45
FIGURE 4.10 CRYSTALLINE PRECIPITATE #4 SYNTHESIZED BY REACTION OF ELEMENTAL SULFUR (12.8 G) WITH ARSENIC TRISULFIDE (50 G) IN 200 ML AT 3M SODIUM SULFIDE	46
FIGURE 4.11 CRYSTALLINE PRECIPITATE #4 SYNTHESIZED BY REACTION OF ELEMENTAL SULFUR WITH ARSENIC TRISULFIDE AFTER FILTRATION.....	46
FIGURE 4.12 ENARGITE MINERAL SAMPLES	48
FIGURE 4.13 CRYSTAL PRECIPITATED FROM PREGNANT ASL SOLUTION AFTER ENARGITE LEACHING	50
FIGURE 4.14 SIZE OF CRYSTALLITES OBTAINED UPON COOLING OF ASL PREGNANT LEACH SOLUTION	51
FIGURE 5.1 SOLUBILITY OF AS ₂ O ₃ IN 0.5 M SODIUM SULFIDE SOLUTIONS.....	52
FIGURE 5.2 SOLUBILITY OF AS ₂ O ₃ IN 0.5 M SODIUM HYDROXIDE SOLUTIONS	54
FIGURE 5.3 PSD RESULT FOR EFFECT OF CONCENTRATION ON THE PRECIPITATION OF AS ₂ S ₃ FROM AS ₂ O ₃ -NA ₂ S SOLUTION	57
FIGURE 5.4 PSD RESULT FOR EFFECT OF TEMPERATURE ON THE PRECIPITATION OF AS ₂ S ₃ FROM AS ₂ O ₃ -NA ₂ S SOLUTION	58
FIGURE 5.5 PSD RESULT FOR EFFECT OF HYDROCHLORIC ACID FLOW RATE ON THE PRECIPITATION OF AS ₂ S ₃ FROM AS ₂ O ₃ -NA ₂ S SOLUTION	59
FIGURE 5.6 PSD RESULT FOR AS ₂ S ₃ SAMPLES OBTAINED BY VARYING AGING TIME	61
FIGURE 5.7 PREDICTED (OLI SOFTWARE) AND EXPERIMENTAL SOLUBILITY OF AS ₂ S ₃ IN NA ₂ S SOLUTIONS.....	62
FIGURE 5.8 RIETVELD REFINEMENT PLOT OF SAMPLE “SYNTHETIC SODIUM ARSENATE” (BLUE LINE - OBSERVED INTENSITY AT EACH STEP; RED LINE - CALCULATED PATTERN; SOLID GREY LINE BELOW - DIFFERENCE BETWEEN OBSERVED AND CALCULATED INTENSITIES; VERTICAL BARS - POSITIONS OF ALL BRAGG REFLECTIONS). COLOURED LINES ARE INDIVIDUAL DIFFRACTION PATTERNS OF ALL PHASES	65
FIGURE 5.9 RIETVELD REFINEMENT PLOT OF SAMPLE “SYNTHETIC PRODUCT #3” (BLUE LINE - OBSERVED INTENSITY AT EACH STEP; RED LINE - CALCULATED PATTERN; SOLID GREY LINE BELOW - DIFFERENCE BETWEEN OBSERVED AND CALCULATED INTENSITIES; VERTICAL BARS - POSITIONS OF ALL BRAGG REFLECTIONS). COLOURED LINES ARE INDIVIDUAL DIFFRACTION PATTERNS OF ALL PHASES	66
FIGURE 5.10 RIETVELD REFINEMENT PLOT OF SAMPLE “SYNTHETIC SODIUM THIO-ARSENATE, PRODUCT #4” (BLUE LINE - OBSERVED INTENSITY AT EACH STEP; RED LINE - CALCULATED PATTERN; SOLID GREY LINE	

BELOW - DIFFERENCE BETWEEN OBSERVED AND CALCULATED INTENSITIES; VERTICAL BARS - POSITIONS OF ALL BRAGG REFLECTIONS). COLOURED LINES ARE INDIVIDUAL DIFFRACTION PATTERNS OF ALL PHASES. ...68

FIGURE 5.11 SOLUBILITY OF SYNTHETIC PRODUCT #2 IN SODIUM HYDROXIDE AND SULFIDE SOLUTIONS EXPOSED TO AMBIENT AIR71

FIGURE 5.12 SOLUBILITY OF SYNTHETIC PRODUCT #3 IN SODIUM HYDROXIDE AND SULFIDE SOLUTIONS EXPOSED TO AMBIENT AIR72

FIGURE 5.13 SOLUBILITY OF PRODUCT #4 (SODIUM THIO-ARSENATE ($\text{Na}_3\text{AsS}_4 \cdot 8\text{H}_2\text{O}$)) IN SODIUM HYDROXIDE AND SULFIDE SOLUTION EXPOSED TO AMBIENT AIR73

FIGURE 5.14 SOLUBILITY OF PRODUCT #4 (SODIUM THIOARSENATE ($\text{Na}_3\text{AsS}_4 \cdot 8\text{H}_2\text{O}$)) IN SODIUM HYDROXIDE AND SULFIDE SOLUTION IN ARGON ATMOSPHERE74

FIGURE 5.15 SOLUBILITY OF SODIUM THIO-ARSENATE (PRODUCT #4, $\text{Na}_3\text{AsS}_4 \cdot 8\text{H}_2\text{O}$) IN CONSTANT SODIUM HYDROXIDE (2.5 M) AND VARYING HYDROSULFIDE CONCENTRATION (0 ~ 1.0 M) SOLUTIONS IN ARGON ATMOSPHERE.....76

FIGURE 5.16 THE SOLUBILITY OF SODIUM THIO-ARSENATE IN CONSTANT HYDROXIDE AT 20 °C (2.5 M NaOH) AND VARYING HYDROSULFIDE SOLUTION COMPARED WITH THAT OBTAINED BY TONGAMP ET AL. (2010) AT 30 °C77

FIGURE B-1 EDX ANALYSIS OF SYNTHETIC AMORPHOUS ARSENIC TRI-SULFIDE102

FIGURE B-2 EDX ANALYSIS OF SYNTHETIC SODIUM ARSENATE102

FIGURE B-3 EDX ANALYSIS OF SYNTHETIC CRYSTALLINE COMPLEX #1103

FIGURE B-4 EDX ANALYSIS OF SYNTHETIC CRYSTALLINE COMPLEX #2.....103

FIGURE B-5 EDX ANALYSIS OF SYNTHETIC CRYSTALLINE COMPLEX #3.....104

FIGURE B-6 EDX ANALYSIS OF SYNTHETIC CRYSTALLINE #4 (SODIUM THIO-ARSENATE)104

FIGURE C-1 RIETVELD REFINEMENT PLOT OF SAMPLE “**AS PRECIPITATE FROM ENARGITE LEACHING WITH $\text{Na}_2\text{S}:\text{ENARGITE} \sim 0.130$** ” (BLUE LINE - OBSERVED INTENSITY AT EACH STEP; RED LINE - CALCULATED PATTERN; SOLID GREY LINE BELOW - DIFFERENCE BETWEEN OBSERVED AND CALCULATED INTENSITIES; VERTICAL BARS - POSITIONS OF ALL BRAGG REFLECTIONS). COLOURED LINES ARE INDIVIDUAL DIFFRACTION PATTERNS OF ALL PHASES.....106

FIGURE C-2 RIETVELD REFINEMENT PLOT OF SAMPLE “**AS PRECIPITATE FROM ENARGITE LEACHING WITH $\text{Na}_2\text{S}:\text{ENARGITE} \sim 0.324$** ” (BLUE LINE - OBSERVED INTENSITY AT EACH STEP; RED LINE - CALCULATED PATTERN; SOLID GREY LINE BELOW - DIFFERENCE BETWEEN OBSERVED AND CALCULATED INTENSITIES;

VERTICAL BARS - POSITIONS OF ALL BRAGG REFLECTIONS). COLOURED LINES ARE INDIVIDUAL DIFFRACTION PATTERNS OF ALL PHASES.....107

FIGURE C-3 RIETVELD REFINEMENT PLOT OF SAMPLE “**AS PRECIPITATE FROM ENARGITE LEACHING WITH**

Na₂S:ENARGITE ~ 0.648” (BLUE LINE - OBSERVED INTENSITY AT EACH STEP; RED LINE - CALCULATED PATTERN; SOLID GREY LINE BELOW - DIFFERENCE BETWEEN OBSERVED AND CALCULATED INTENSITIES;

VERTICAL BARS - POSITIONS OF ALL BRAGG REFLECTIONS). COLOURED LINES ARE INDIVIDUAL DIFFRACTION PATTERNS OF ALL PHASES.....108

Acknowledgments

This thesis would not have been possible without the generous financial support of Newmont Mining Corporation and the Natural Sciences and Engineering Research Council of Canada.

Also, I'd like to thank everyone who generously offered very kind help during the research, especially my supervisor Dr. Edouard Asselin and instructor Dr. Berend Wassink. And without my parents' supports, it'll be much more difficult to finish this work in two years.

Chapter 1 Introduction

Enargite (Cu_3AsS_4) usually associates with copper sulfide minerals, such as chalcopyrite (CuFeS_2), which is the main mineral source for copper. El Indio in Chile, Lepanto in the Philippines, and Chelopech in Bulgaria are three examples of such copper deposits (Filippou et al. 2007) (refer to Tables 1.1 and 1.2 for arsenic mineralization and a regional distribution of arsenical ores).

Table 1.1 Major arsenic minerals occurring in nature (WTO Arsenic Compounds, 2001)

Mineral	Composition	Occurrence
Native arsenic	As	Hydrothermal Veins
Proustite	Ag_3AsS_3	Generally one of the late Ag minerals in the sequence of primary deposition
Rammelsbergite	NiAs_2	Commonly in mesothermal vein deposits
Safflorite	$(\text{Co,Fe})\text{As}_2$	Generally in mesothermal vein deposits
Seligmannite	PbCuAsS_3	Occurs in hydrothermal veins
Smaltite	CoAs_2	-
Niccolite	NiAs	Vein deposits and norites
Realgar	AsS	Vein deposits, often associated with orpiment, clays and limestones, also deposits from hot springs
Orpiment	As_2S_3	Hydrothermal veins, hot springs, volcanic sublimation product
Cobaltite	CoAsS	High-temperature deposits, metamorphic rocks
Arsenopyrite	FeAsS	The most abundant As mineral, dominantly mineral veins
Tennantite	$(\text{Cu,Fe})_{12}\text{As}_4\text{S}_{13}$	Hydrothermal veins
Enargite	Cu_3AsS_4	Hydrothermal veins
Arsenolite	As_2O_3	Secondary mineral formed by oxidation of arsenopyrite, native arsenic and other As minerals
Claudetite	As_2O_3	Secondary mineral formed by oxidation of realgar, arsenopyrite and other As minerals
Scorodite	$\text{FeAsO}_4 \cdot 2\text{H}_2\text{O}$	Secondary mineral

Table 1.1 Major arsenic minerals occurring in nature (WTO Arsenic Compounds, 2001) continued

Mineral	Composition	Occurrence
Annabergite	$(\text{Ni,Co})_3(\text{AsO}_4)_2 \cdot 8\text{H}_2\text{O}$	Secondary mineral
Hoernesite	$\text{Mg}_3(\text{AsO}_4)_2 \cdot 8\text{H}_2\text{O}$	Secondary mineral, smelter wastes
Haematolite	$(\text{Mn,Mg})_4\text{Al}(\text{AsO}_4)(\text{OH})_8$	-
Conichalcite	$\text{CaCu}(\text{AsO}_4)(\text{OH})$	Secondary mineral
Adamite	$\text{Zn}_2(\text{OH})(\text{AsO}_4)$	Secondary mineral
Domeykite	Cu_3As	Found in vein and replacement deposits formed at moderate temperatures
Loellingite	FeAs_2	Found in mesothermal vein deposits
Pharmacosiderite	$\text{Fe}_3(\text{AsO}_4)_2(\text{OH})_3 \cdot 5\text{H}_2\text{O}$	Oxidation product of arsenopyrite and other As minerals

Table 1.2 Arsenic deposits of the world (WTO Arsenic Compounds, 2001)

Type of deposits	As mineral(s)	Average As conc. (mg kg⁻¹)	Location
Enargite-bearing copper-zinc-lead deposits	Enargite	1000 (0.1%)	United States, Argentina, Chile, Peru, Mexico, Republic of the Philippines, Spain, Yugoslavia, USSR
Arsenical pyrite copper deposits	Arsenopyrite, tennantite	40,000 (4%)	United States, Sweden, Federal Republic of Germany, Japan, France, USSR
Native silver and nickel-cobalt arsenide bearing deposits	Smaltite, domeykite, safflorite, rammelsbergite, cobaltite, niccolite, loellingite, arsenopyrite, et al	25,000 (2.5%)	Canada, Norway, Germany, Democratic Republic, Czechoslovakia
Arsenical gold deposits	Arsenopyrite, loellingite	<5000 (0.5%)	United States, Brazil, Canada, Republic of South Africa, Australia, USSR

Table 1.2 Arsenic deposits of the world (WTO Arsenic Compounds, 2001) continued

Type of deposits	As mineral(s)	Average As conc. (mg kg ⁻¹)	Location
Arsenic sulfide and arsenic sulfide gold deposits	Realgar, orpiment	2000 (0.2%)	United States, People's Republic of China
Arsenical tin deposits	Arsenopyrite	2000 (0.2%)	United States, Bolivia, Australia, Indonesia, Malaysia, Republic of South Africa
Arsenical quartz, silver and lead-zinc deposits	Arsenopyrite	6000 (0.6%)	United States, Canada, et al

Since arsenic is toxic (massive poisoning and multiple cancer cases in the past), increasing environmental concern has arisen for the disposal of arsenic compounds by environmental protection organizations all over the world. Related environmental regulations are starting to limit the application of roasting, smelting and converting of high-arsenic content copper sulfide concentrates, due to the generation of As₂O₃ or As₂S₃ dusts. After chronic exposure to arsenic dusts in the air, effects on several human organs/systems (neurological effects and cardiovascular effects) are found to start at an arsenic concentration of 50 µg/m³ (See Table 1.3). Thus, arsenic receives a high penalty charge from smelters, which is typically 2.5 to 3.0 USD for every 0.1% over 0.1% ~ 0.2% arsenic in the concentrate (Peacey et al. 2010). The conventional processing options for copper-arsenic concentrates are therefore increasingly difficult to justify.

Table 1.3 Summary of toxic effects in humans after occupational inhalation exposure to inorganic arsenic compounds (European Commission 2001)

Health endpoints	Effect	Lowest observed effect level (concentration)
Respiratory effects	Irritation of upper respiratory tract in workers exposed to arsenic dusts	0.1-1 mg As/m ³
Neurological effects	After inhalation of inorganic arsenicals, peripheral neuropathy in workers	0.05 mg As/m ³
Gastrointestinal effects	Nausea and anorexia in one worker (but not in another) exposed to arsenic trioxide dust; no other studies with quantitative exposure data available	0.11 mg As/m ³
Cardiovascular effects	Smelter workers exposed to arsenic trioxide dusts have a higher incidence of Raynaud's disease and increased constriction of blood vessels in response to cold	0.05-0.5 mg As/m ³
Skin effects	Hyperkeratosis and hyperpigmentation are common in people exposed by the oral route, but have very rarely been reported after inhalation exposure	No data
Haematological effects	Anaemia is often noted in humans exposed by the oral route, but has not been observed after inhalation exposure	No data

One option to make a clean concentrate (i.e. with low arsenic) for sale to a smelter is to leach enargite in sodium sulfide solution at 95 °C~105 °C, with pH adjustment above 13 with sodium hydroxide: the so-called Alkaline Sulfide Leach (ASL) (Balaz et al. 2000, Delfini et al. 2003, Curreli et al. 2003, Tongamp et al. 2009). After leaching of enargite, a chalcocite-type (Cu₂S) residue and soluble arsenic complexes in leach solution are produced, and thus copper and arsenic are successfully separated. The solid copper-containing residue

can be forwarded for further processing to a smelter and a white arsenic-containing crystal is precipitated (or crystallized) as the leach solution is cooled. Indeed, Nadkarni and Kusik (1988) showed that most of the soluble sodium thio-arsenate (presumed to be Na_3AsS_4 in their work) can be precipitated by cooling the leach solution from leach temperature to room temperature. With its low cost and easy implementation, cooling and precipitation appears to be one of the best options for arsenic separation from the leach liquor. However, quantitative x-ray diffraction of the white arsenic-containing precipitate, which separates from the enargite leaching solution upon cooling, shows that the complexes do not have the exact stoichiometry of sodium thio-arsenate (Na_3AsS_4) – see Chapter 5.

Since the stoichiometry of the arsenic-bearing precipitates is highly variable (Parada Torres 2011) and appears to vary based on the prevailing leach conditions, it is more useful from a fundamental perspective to determine how much arsenic can be separated by cooling solutions of sodium thio-arsenate. In effect, the solubility of stoichiometric sodium thio-arsenate should be determined. However, throughout the relevant literature there is very little, if any, report on the solubility of Na_3AsS_4 .

It is very difficult to find Na_3AsS_4 or any other similar chemical (e.g. hydrate) for purchase. Thus it must be synthesized. Arsenic trioxide and arsenic tri-sulfide are the main reactants that can be used to synthesize sodium thio-arsenate complexes, thus their solubility in alkaline sulphide solutions are also of interest. As an example, sodium thio-arsenate is a light yellow acicular crystal, which grows over a period of 8-10 hours. A slight change in arsenic concentration might destroy the growth of the pure crystal. Hence, the concentration of arsenic tri-sulfide is a key parameter for sodium thio-arsenate synthesis.

The arsenic tri-sulfide ordered from chemical supply companies (e.g. Alfa Aesar) is an amorphous product synthesized at very high temperature and it is likely polymerized. Its solubility in sodium sulfide solutions is too low to complete the sodium thio-arsenate synthesis process. Thus, a new method to synthesize arsenic tri-sulfide in aqueous system is also required.

This thesis is organized as follows:

- Chapter 2 presents a review of the literature relevant to treating arsenic-bearing minerals including a discussion on the alkaline sulfide leach and relevant arsenic chemistry.
- Chapter 3 presents the objectives of the research
- Chapter 4 presents the experimental methods used to synthesize arsenic precipitates and then to measure their solubility
- Chapter 5 presents the results of the work and discusses their importance
- Chapters 6 and 7 present the conclusions from the study and the proposed future work

Chapter 2 Literature Review

2.1 Copper arsenic minerals

Arsenic is a ubiquitous element that comprises about 0.00005% of the earth's crust and ranks 20th in abundance (Gulledge et al. 1973). It has always had connections to- and uses in medicine, agriculture, livestock, electronics and various other industries including metallurgy (Nriagu and Azcue 1990).

There have been several arsenic poisoning episodes reported around the world. The arsenic contamination incident in well water on the south-west coast of Taiwan (1961 ~ 1985) is well known: chronic arsenicism was observed in 40,421 people from 37 villages, which resulted in 7418 cases of hyperpigmentation, 2868 of keratosis, 360 of blackfoot disease, and some cases of cancer (liver, lung, skin, prostate, bladder, kidney (Chen et al. 1988, Tsai et al. 1998, Guo et al. 1997, Bates et al. 1992, Lu et al. 1975). See Table 2.1 for the most commonly found arsenic compounds in air that were investigated by the European Commission in 2001.

Arsenic toxicity is a function of physical state (gas, solution, or powder), the rate of absorption into cells, the rate of elimination, the nature of chemical substituents in the toxic compound and various other factors. The toxicity of arsenical complexes decreases in the following order, arsines (AsH_3) > inorganic As (III) > arsenoxides (organic As (III)) > inorganic As (V) > arsonium compounds > native As (Whitacre and Pearse 1972, Hindmarsh and McCurdy 1986). Thus, it is generally concluded that the soluble inorganic arsenicals are more toxic than the organic ones, and that inorganic As (III) is more toxic than inorganic As (V) (Maeda 1994). Under oxidizing conditions, arsenates (inorganic As (V)) are the stable species and can be strongly sorbed onto clays, iron and manganese oxides/hydroxides as well

as various organic matters. Under reducing conditions, arsenites (inorganic As (III)) are the predominant species, which are more toxic, soluble, and mobile than arsenates (inorganic As (V)) (Reichert and Trelles 1921). Ferric arsenate is the least soluble and least toxic form of arsenic for disposal in the environment (Harris 2000).

Table 2.1 the most commonly found (or anticipated) arsenic compounds in air (European Commission 2001)

Name	Chemical Formula	State of Oxidation	Physical Condition	Melting point	Solubility in water
Arsenic trioxide, As oxide	$As_2O_3, (AsO_3)^{3-}$	+3	Solid (gaseous)	312.3 °C	37 g/l (20 °C)
Arsenic pentoxide	$As_2O_5, (AsO_3)^-, / (AsO_4)^{3-} / (As_2O_7)^{4-}$	+5	Solid	Decomposes at 315 °C	1500 g/l (16 °C)
Arsenic Acid	H_3AsO_4	+5	Solid	35.5 °C	3020 g/l (12.5 °C)
Monomethylarsonic acid (MMA)	$(CH_3)AsO(OH)_2$	+5	Solid	161 °C	Soluble
Dimethylarsinic acid (DMA)	$(CH_3)_2AsO(OH)$	+5	Solid	195~196 °C	660 g/l (25 °C)
Other trivalent As compounds	$AsCl_3$	+3	Liquid	131 °C	Soluble
	As_2S_3	+3	Solid	320 °C	Insoluble
Realgar	As_4S_4	0/+3	Solid	307 °C	Insoluble
Other pentavalent As compounds	As_2S_5	+5	Solid	Decomposes at ~500 °C	Insoluble
Arsin	AsH_3	-3	Gaseous	-117 °C	20% (20 °C)
Metallic As	As	0	Solid	817 °C (28 atm)	Insoluble

(a) Due to its high vapor pressure, it can be present in the vapor phase.

(b) The arsenate species are defined by the pH on the medium (liquid or liquid film on a particle).

(c) This arsenic halide is liquid at room temperature, but can be air-dispersed either in liquid or in vapor state.

In metallurgy, arsenic is usually found in sulfide ores, along with copper, nickel, lead, and cobalt (Mandal and Suzuki 2002). The two main copper-arsenic minerals are enargite (Cu_3AsS_4) and tennantite ($\text{Cu}_{12}\text{As}_4\text{S}_{13}$), and enargite, particularly, is the principal mineral in many deep epithermal copper deposits. There also exist in smaller proportions such arsenic-bearing minerals as luzonite (Cu_3AsS_4), lautite (CuAsS), sinnerite ($\text{Cu}_6\text{As}_4\text{S}_9$), domeykite (Cu_3As), and algodonite (Cu_6As) (Filippou et al. 2007, Maske and Skinner 1971).

Table 2.2 the most common Cu-As-Sb-S minerals and their physical properties (Barthelmy 2004)

Name	Ideal composition	Crystal system	Color	Density (g cm^{-3})	Hardness (Mohs)
Enargite	Cu_3AsS_4	Orthorhombic	steel gray/ violet black	4.46	3
Luzonite	Cu_3AsS_4	Tetragonal	gray/pink brown/red	4.48	3.5
Tennantite	$\text{Cu}_{12}\text{As}_4\text{S}_{13}$	Cubic	gray/brown/ cherry red	4.64	3.5-4
Sinnerite	$\text{Cu}_6\text{As}_4\text{S}_9$	Triclinic	steel gray	4.44	5
Lautite	CuAsS	Orthorhombic	black/steel gray	4.82	3-3.5
Famatinitite	Cu_3SbS_4	Tetragonal	grayish black/ steel black	4.69	3-4
Tetrahedrite	$\text{Cu}_{12}\text{Sb}_4\text{S}_{13}$	Cubic	black/steel gray	4.95	3.5-4

Several copper-arsenic mineral rich deposits have been found all over the world, especially in South America. In Chile, chalcopyrite and pyrite are the primary sulfide ores in the Andean Porphyry Copper deposits, but tennantite and enargite are also present (Pinchiera et al. 1998). For the El Indio deposit, enargite and tennantite presents as major minerals, along with minor quantities of chalcopyrite, arsenopyrite, and tetrahedrite (Smith 1986). Several areas in Mexico are rich in enargite, for example, the Cananea copper deposit has a

high arsenic content, and it is reported that enargite accounts for 80% of the arsenic in its concentrate (Perez-Segura and Zendejas-Mendivil 1991). At the Chelopech mine in Bulgaria, copper-arsenic sulfosalts are the majority of the copper ore body, and 93% of arsenic in the copper-arsenic sulfosalt can be recovered during the flotation process (Baltov et al. 2008). Considerable quantities of copper-arsenic minerals are also found at the Northparkes and (Smith and Bruckard 2007) the Tampakan deposit in the Philippines (Senior et al. 2006), as well as the Gortdrum deposit in the Republic of Ireland (Stuart and Down 1973).

According to Table 2.2, enargite (Cu_3AsS_4) is an orthorhombic cuprous thioarsenate, and luzonite has the same ideal chemical composition but different structure, which is tetragonal dimorph. The inversion temperature from luzonite to enargite is about 280 °C (Maske and Skinner 1971). Filippou reported that another difference in chemical composition between luzonite and enargite is the antimony content. Springer (1969) believed that natural enargite only contains up to 6 wt% Sb, which corresponds to $\text{Cu}_3\text{As}_{0.8}\text{Sb}_{0.2}\text{S}_4$. But for luzonite, much of the arsenic is replaced by antimony, which makes the chemical composition falling between Cu_3AsS_4 and $\text{Cu}_3\text{As}_{0.5}\text{Sb}_{0.5}\text{S}_4$ (Luce et al. 1977). In natural deposits, enargite usually co-exists with pyrite (FeS_2), luzonite, tennantite, and some other copper sulfides which are predominant at deeper levels (Filippou et al. 2007).

Tennantite ($\text{Cu}_{12}\text{As}_4\text{S}_{13}$) is the second most common copper-arsenic mineral, but it has a more complex composition than enargite. Generally, there are two explanations about the composition of tennantite. One explains that tennantite is a cubic cuprous-cupric thioarsenite. The other says that tennantite is the end member of a solid solution series, where arsenic and antimony replace each other in the mineral structure $\text{Cu}_{12+x}(\text{As,Sb})_{4+y}\text{S}_{13}$, where $0 \leq x \leq 1.99$ and $-0.02 \leq y \leq 0.37$ (Skinner et al. 1972, Luce et al. 1977).

2.2 Metallurgical processing of enargite

Conventional pyrometallurgical processing (Figure 2.1) is applied for more than 70% of the world's copper production, most of which originates from chalcopyrite concentrates containing small amounts of enargite (Safarzadeh et al. 2012). However, with the depletion of conventional copper ores, the copper industry is clearly interested in the development and utilization of copper-arsenic deposits, such as those generating concentrates high in enargite and tennantite. However, the deportment and stabilization of arsenic in a benign form that meets all the environmental regulations tends to be a major challenge for industrial processes.

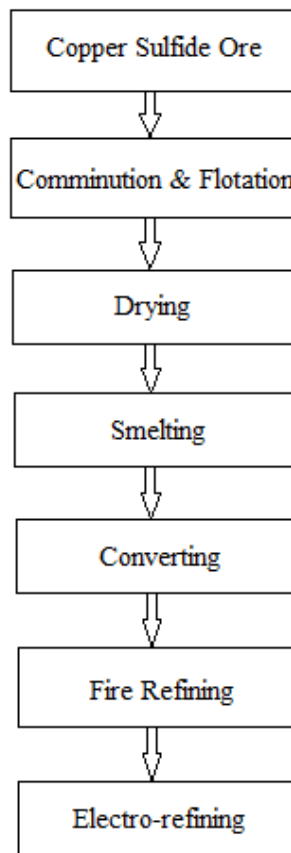


FIGURE 2.1 CONVENTIONAL PROCESSING OF PRIMARY COPPER SULFIDE ORES (SAFARZADEH ET AL. 2012)

The hydrometallurgical route (See Figure 2.2) for low-grade copper oxide ores consists of heap leaching, solvent extraction (or ion exchange) and electrowinning. This route has been well-developed for almost 50 years, especially in South America, and approximately 25% of copper is produced through this process (See Figure 2.2). However, this route is generally not amenable to the processing of enargite or tennantite (See Figure 2.3) although the Newmont Mining Corporation appears to be using a heap bio-leach for an enargite-bearing ore at Yanacocha.

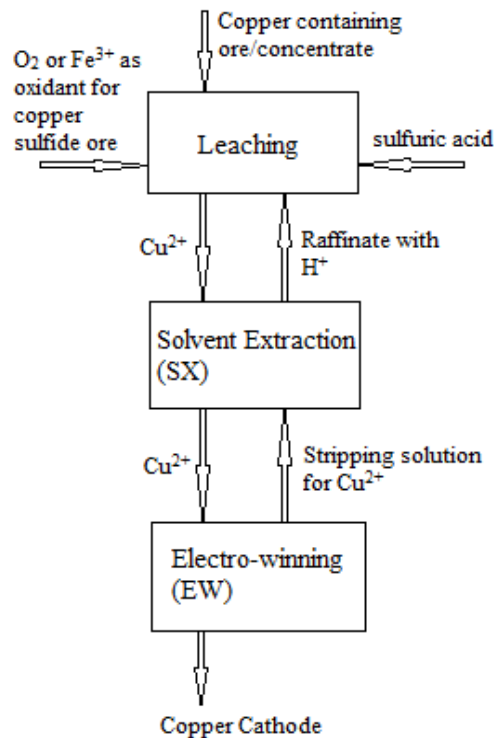


FIGURE 2.2 A CLASSIC HYDROMETALLURGICAL ROUTE FOR COPPER PRODUCTION FROM OXIDE ORES

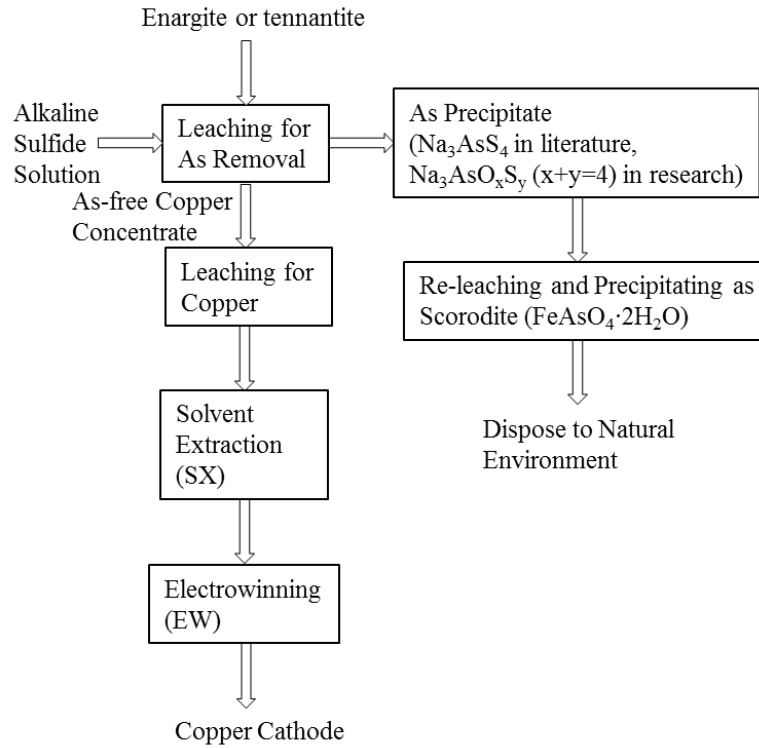


FIGURE 2.3 A HYDROMETALLURGICAL ROUTE FOR ENARGITE OR TENNANTITE

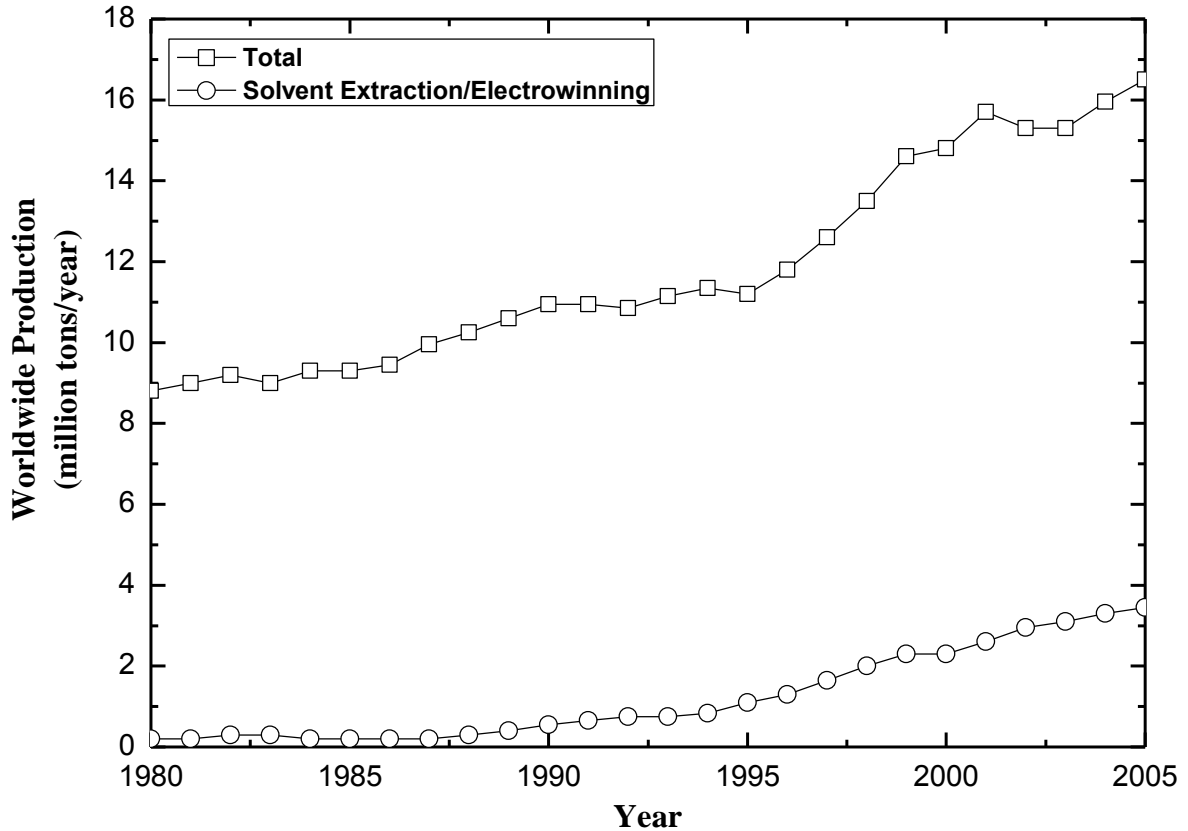
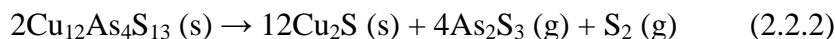
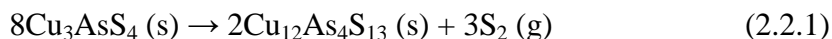


FIGURE 2.4 A COMPARISON OF WORLDWIDE COPPER PRODUCTION BY COMBINED METHODS (TOTAL) AND SOLVENT EXTRACTION/ELECTRO-WINNING (SX/EW) BETWEEN 1980 AND 2005 (REPLOTTED FROM MOATS 2005)

2.2.1 Pyrometallurgical treatment

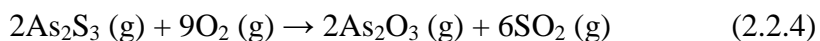
Due to the relatively low melting point of copper-arsenic-sulfur phases, enargite can be smelted at around 640 ~ 690 °C (Muller and Blachnik 2002). Under relatively high SO₂ partial pressure and relatively low O₂ partial pressure at 550~700 °C, enargite transforms into tennantite, and subsequently into digenite (Cu₉S₅), chalcocite (Cu₂S), and nonstoichiometric chalcocite (Cu_{1.96}S) (Padilla et al. 1997, 1999, 2001). This series of reactions is shown as follows:



Overall reaction:



Various laboratory and pilot studies (Secco et al. 1988, Holmstrom 1989, Padilla et al. 1999, 2001) show that reaction 2.2.3 can only occur at an appreciable rate above 600 °C. According to Secco et al. (1998), the arsenic sulfide products (As₂S₃ and AsS) melt before volatilization at 600 °C. Therefore, roasting proceeds at 650 °C for a considerable time to avoid the formation of sticky products. To separate arsenic from Cu as much as possible, 720 °C is required, and the oxygen concentration in the roaster must be less than 0.3% v/v to maintain the efficiency of arsenic elimination (Filippou et al. 2007). The arsenic sulfide gases coming out from roasting can be burnt with excess air at 750 °C to produce gaseous arsenic trioxide and sulfur dioxide:



The oxidized gases are cooled down to 390 °C and then to 120 °C. And most of gaseous As₂O₃ desublimates as “gray arsenic trioxide” at 120 °C, which is captured in bag-house filters. At El Indio (Smith 1986, Smith and Paredes 1988), a similar industrial route (see Figure 2.5) was used and the crude arsenic trioxide captured in bag filters contained 97~97.5% As₂O₃ and about 1.0% Sb. It was packaged and sold until 2002, due to the lack of a market for such an arsenic product (Safarzadeh et al. 2012).

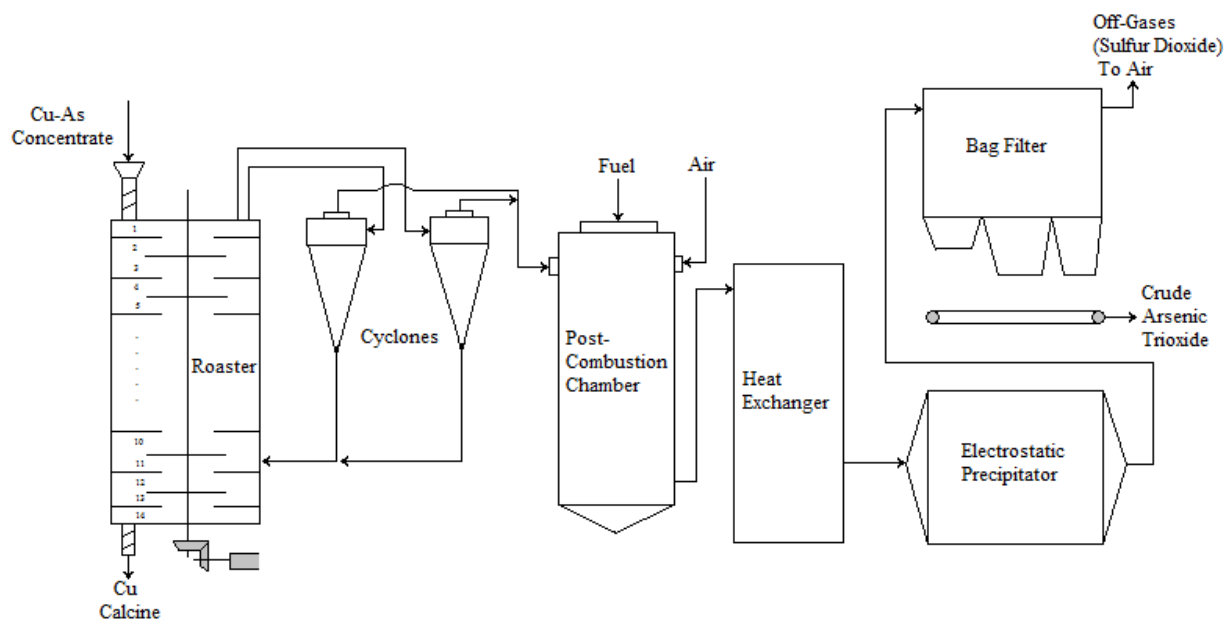


FIGURE 2.5 A SIMPLIFIED FLOWSHEET OF THE EL INDIO ENARGITE ROASTER DRAWN WITH DATA
BY SMITH 1986

Since the arsenic-bearing gases released during mineral processing cannot go directly into the atmosphere, facilities to capture, separate, oxidize, and stabilize the gases are needed. However, the cost for these facilities makes the pyrometallurgical process quite expensive. Furthermore, the considerable amount of SO₂ and toxic metals in fugitive gas emissions from smelters present an ongoing challenge. At present, the maximum allowable arsenic content in copper concentrates for smelting is set at 0.5%, and this is expected to decrease to 0.3% in future (Baxter et al. 2010).

Industrial ore processing of arsenic-bearing sulfides, ideally results in the final disposal of arsenic as scorodite (FeAsO₄ · 2H₂O) due to its long term stability. However, in certain jurisdictions, and for various reasons such as disposal site characteristics (humidity or

rain fall), crystallinity, the presence of oxygen, sulfides and complexing agents, other arsenic mineralizations have historically been sent to tails (Riveros et al. 2001).

2.2.2 Alkaline sulfide leaching of enargite

Enargite is a refractory mineral, compared to the other common copper rich minerals, because it is hard to dissolve in most aqueous media. Based on Figure 2.6 and 2.7 (Filippou et al. 2007), enargite is thermodynamically stable in acid solution (please note that the highly toxic arsine gas, AsH_3 , does not appear on Figures 2.6 or 2.7 despite its thermodynamic stability under reducing conditions). Enargite also does not dissolve easily in alkaline solution. In fact, enargite is the last in the order by which copper sulfides dissolve in ammonia solutions (Kuhn 1974):

Chalcocite > covellite > bornite > chalcopyrite > enargite

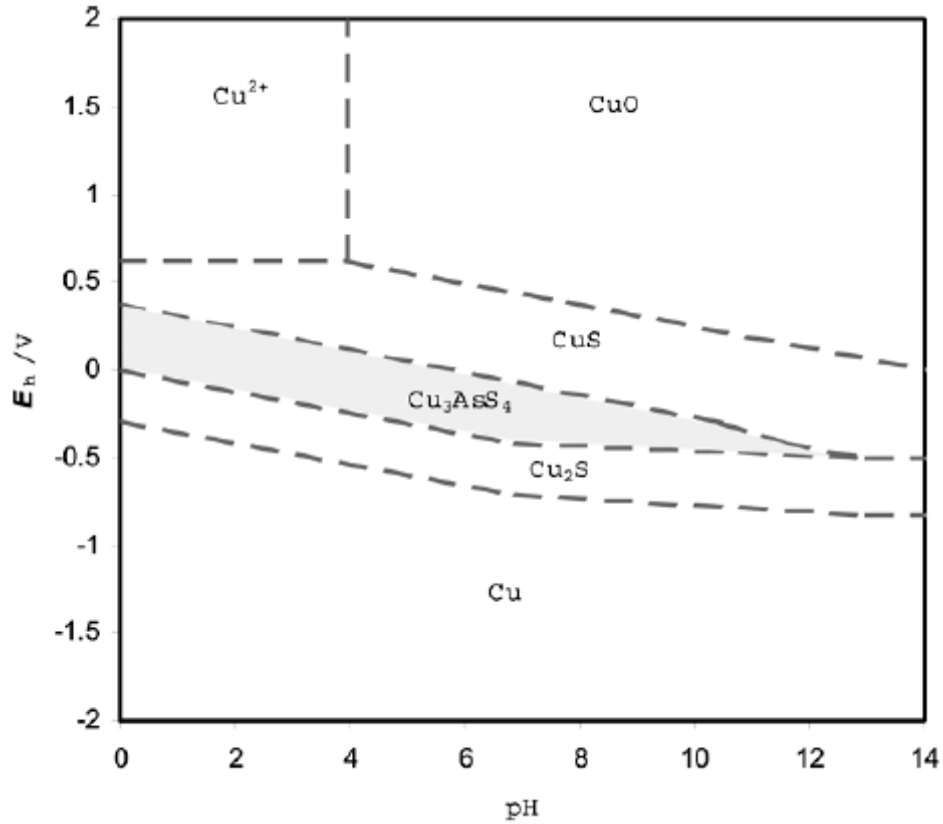


FIGURE 2.6 SIMPLIFIED EH-PH DIAGRAM FOR THE CU-AS-S-H₂O SYSTEM WITH 1 MOL/L DISSOLVED SPECIES AT 25 °C AND 1 ATM (FILIPPOU ET AL. 2007)

Considerable research has focused on the processing of enargite concentrates by hydrometallurgical methods, either for the preparation of a copper-sulfur concentrate that can then be smelted (Mihajlovic 2007) or for the direct extraction of copper from enargite concentrates (Baxter et al. 2010).

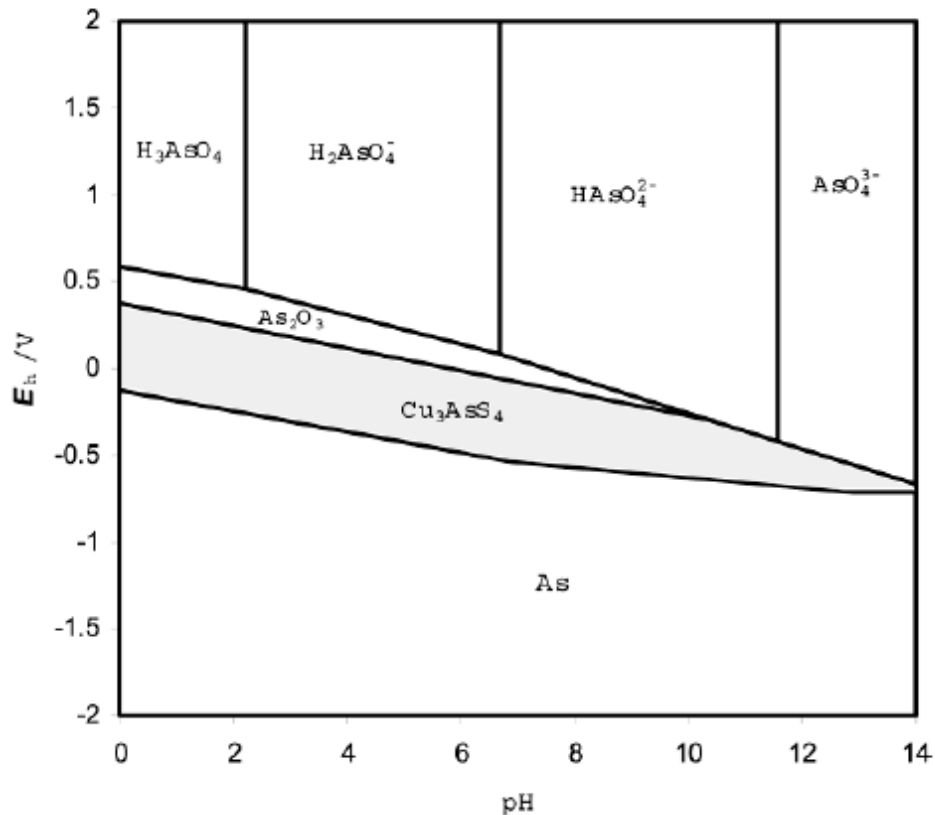


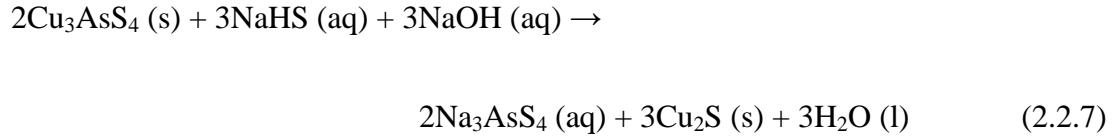
FIGURE 2.7 SIMPLIFIED EH-PH DIAGRAM FOR THE CU-S-AS-H₂O SYSTEM WITH 1 MOL/L DISSOLVED SPECIES AT 25 °C AND 1 ATM (FILIPPOU ET AL. 2007)

Alkaline sulfide leaching, also referred to as the “Sunshine Process”, consists of dissolution of the arsenic (as well as antimony, mercury, gold and tin) from the enargite source mineral in an alkaline sodium sulfide solution (pH > 13) at 95 ~ 105 °C. The residue from this process is a copper sulfide, which, in theory is amenable for shipment and eventual smelting. The general reaction formula for this process is given here:



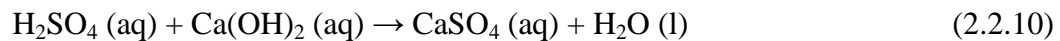
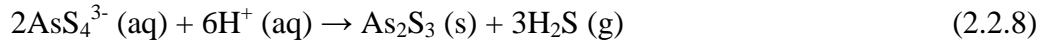
It has also been proposed that NaHS and NaOH can be used effectively to leach enargite as shown in reaction 2.2.7. The rationale given to justify this reaction is that

sufficient caustic is required to ensure that S^{2-} is predominant. However, several studies have indicated that the pKa for the HS^-/S^{2-} equilibrium actually lies near pH 18, and there is significant evidence that both OH^- and HS^- play an active role in the dissolution of enargite (Wilkomirsky et al. 1998).



2.2.3 Arsenic removal and precipitate analysis

After alkaline sulfide leaching, there are generally two ways to eliminate arsenic from the arsenic-pregnant solution: acidification and crystallization. Arsenic tri-sulfides will be precipitated by acidification (2.2.8) (Parada Torres 2011). For further processing, arsenic sulfides can be oxidized with oxygen (or by other means) to form hydrogen arsenate (2.2.9). Scorodite (insoluble ferric arsenate) would be the final disposal form obtained via this method through the addition of ferric sulfate (2.2.11) with proper pH control (2.2.10):



The hydrogen ions in (2.2.8) can originate from sulfuric acid, sulfurous acid or carbonic acid etc. For example, Holmes (1973) provides a two-step acidification via SO_2 , wherein gold complexes (pH~10) and arsenic tri- or penta-sulfides (pH~3, 4) can be precipitated separately.

Crystallization of sodium thio-arsenate occurs via cooling of process liquors. Nadkarni et al. (1975) presented several routes for handling the arsenic crystals after they have been crystallized and these are presented in Figures 2.8 and 2.9. The removal of arsenic by cooling provides a chance to reduce costs as reagents are theoretically not consumed. As is removed from the circuit in Figure 2.8 as the pentasulfide after reaction with sulfuric acid.

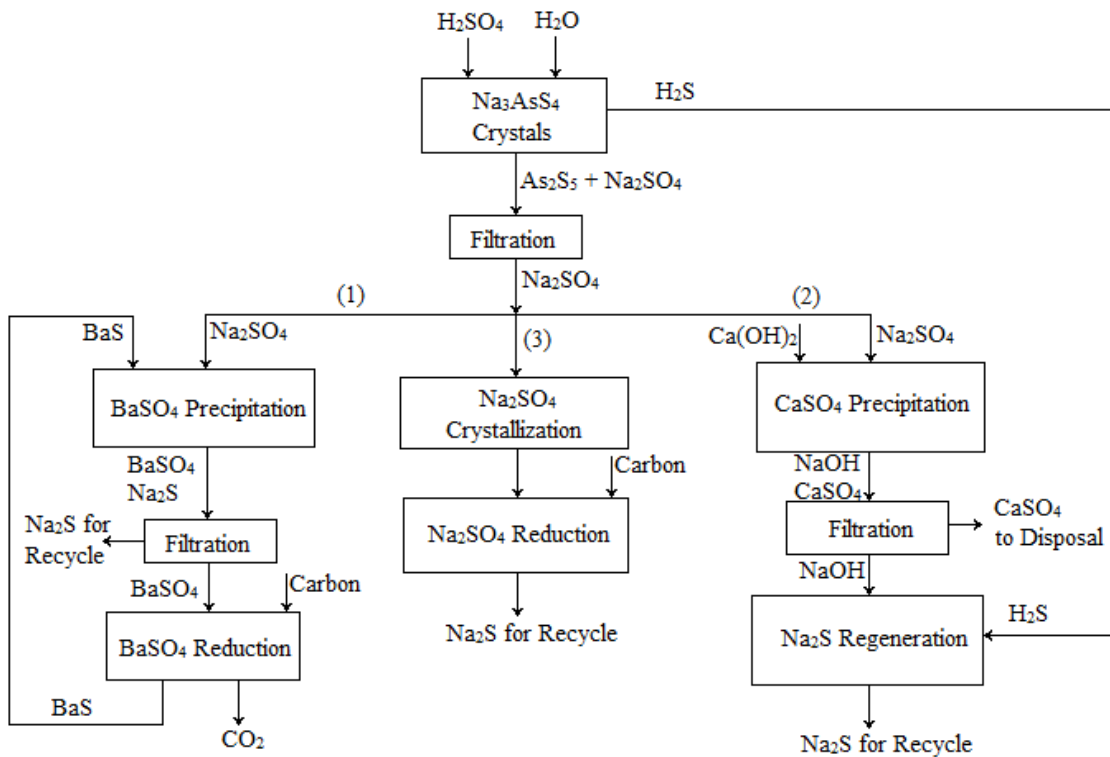


FIGURE 2.8 AN ARSENIC DISPOSAL OPTION 1 BY ADDING H_2SO_4 (NADKARNI ET AL. 1975)

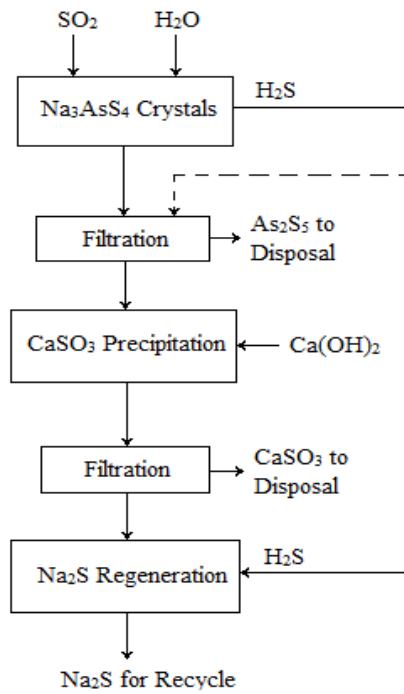
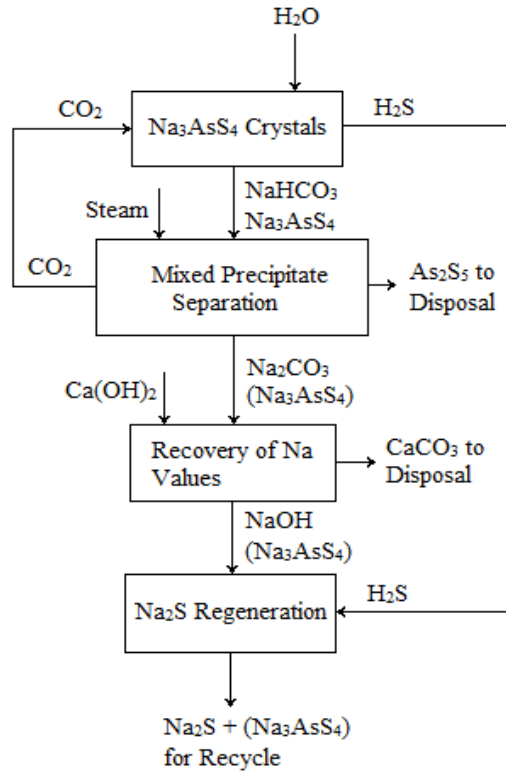


FIGURE 2.9 ARSENIC DISPOSAL OPTIONS 2 AND 3 BY ADDING CO₂ AND SO₂ (NADKARNI ET AL. 1975)

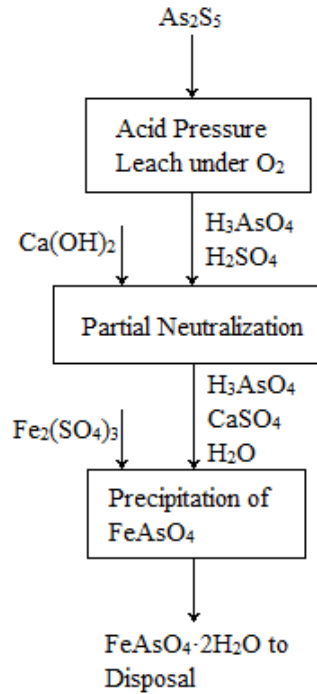
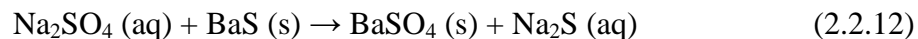


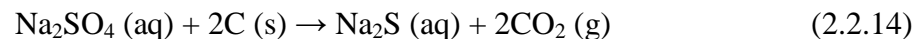
FIGURE 2.10 FINAL ARSENIC ROUTE BY SCORODITE PRECIPITATE (NADKARNI ET AL. 1975)

It is interesting to note that in Figure 2.8 there are three different proposed ways to regenerate the Na_2S solution required for further leaching.

(1). Using barium sulfide

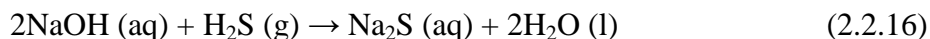


(2). Using carbon



(3). Using calcium sulfate





2.2.4 Sodium thio-arsenate solubility

The solubility of sodium thioarsenate in ASL solutions is very important for arsenic removal and process design. However, there is a lack of experimental data on the solubility of sodium thio-arsenate in ASL solutions in general. In particular, there is very little data as to the solubility at elevated temperatures, which would indicate maximum solution loading of arsenic during leaching. The only available data appears to be presented by Nadkarni and Kusik in 1988 (cf. Figure 2.11) and it reports solubility of arsenic in sodium sulfide solutions from ~20 to 45 °C. Further, it should be noted that Nadkarni and Kusik's work did not confirm that Na_3AsS_4 was the precipitated arsenic species. The only study that appears to positively identify the arsenic precipitate from cooled ASL solutions appears to be that of Tongamp et al. (2010a, 2010b) where Na_3AsS_4 was identified by XRD and ICP (to verify total As content) after precipitation from leached orpiment and oxidation with elemental S at ~30 °C and from solutions containing 2.5 M NaOH and ~3-4.5 M HS^- .

The solubility curve of sodium thio-arsenate and thio-stibnite from Nadkarni and Kusik (1988) as shown in Figure 2.11 is quite steep and is adequate for cooling and crystallizing the arsenic species from solution.

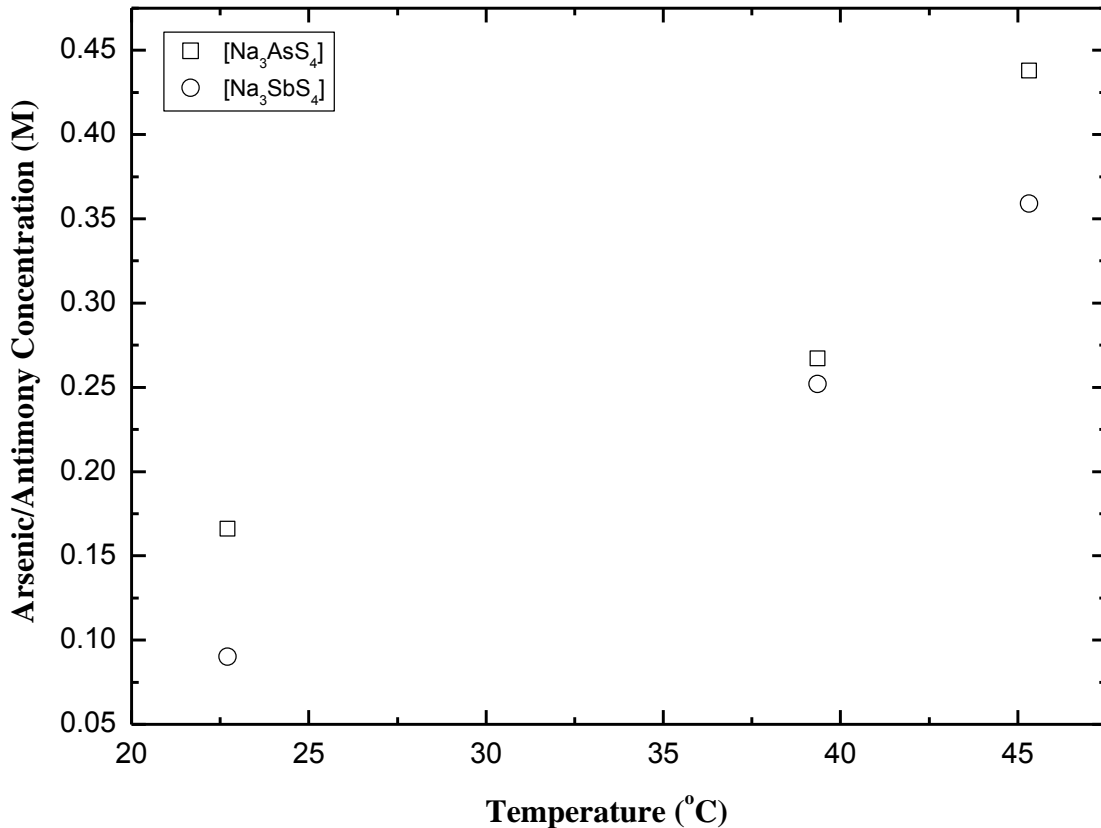


FIGURE 2.11 SOLUBILITY OF SODIUM THIOARSENATE AND STIBNITE IN AQUEOUS SODIUM SULFIDE (2.2~2.4M)
(REPLOTTED FROM NADKARNI AND KUSIK, 1988)

2.3 Synthesis of amorphous As₂S₃

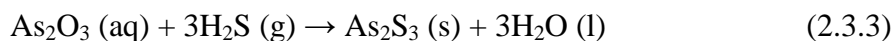
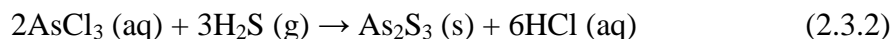
Orpiment, chemical formula As₂S₃, is a common monoclinic arsenic sulfide mineral and may be used as a precursor for the synthesis of sodium thio-arsenate. Natural orpiment is an orange to yellow mineral that can be found worldwide, and occurs as a sublimation product in volcanic fumaroles, low temperature hydrothermal veins, hot springs and as a byproduct of the decay of other arsenic minerals. Synthesized orpiment occurs both in crystalline and amorphous forms, which feature polymeric structures consisting of trigonal pyramidal arsenic (III) centers linked by sulfide centers. The sulfide centers are two-fold coordinated to two arsenic atoms. In crystalline form, orpiment adopts a ruffled sheet

structure (Wells 1984). The bonding between the sheets consists of Van der Waals forces. Amorphous As_2S_3 does not possess a layered structure but is more highly cross-linked (Wells 1984).

Amorphous As_2S_3 may be obtained via fusion of elemental sulfur and elemental arsenic at $390\text{ }^\circ\text{C}$, which gives a polymeric As_2S_3 with the adamantine geometry. Rapid cooling of the reaction melt ensures the disordered arrangement of the bonds, resulting in the glass. The reaction can be shown as following reaction 2.3.1:



Amorphous As_2S_3 also can be formed by hydrogen sulfide purging through an arsenic tri-chloride solution (reaction 2.3.2). Weissberg et al. (1966) precipitated amorphous As_2S_3 from a slightly acidic aqueous solution of As_2O_3 by slowly bubbling bottled H_2S through the solution (reaction 2.3.3).



2.4 Synthesis of sodium thio-arsenate

As mentioned earlier, sodium thio-arsenate is a likely arsenic-containing complex that forms during enargite leaching but very little research has studied sodium thio-arsenate synthesis. Tongamp et al. (2010a, 2010b) added arsenic trisulfide to alkaline leaching solution after enargite leaching, which was continuously recycled until the arsenic concentration reached over 35 g/L . The solution was then treated in a precipitation process

where elemental sulfur and antimony were added to precipitate 50 ~ 60% of the dissolved arsenic as Na_3AsS_4 . The filtrate was recirculated to the enargite leaching process. This process is shown in Figure 2.12:

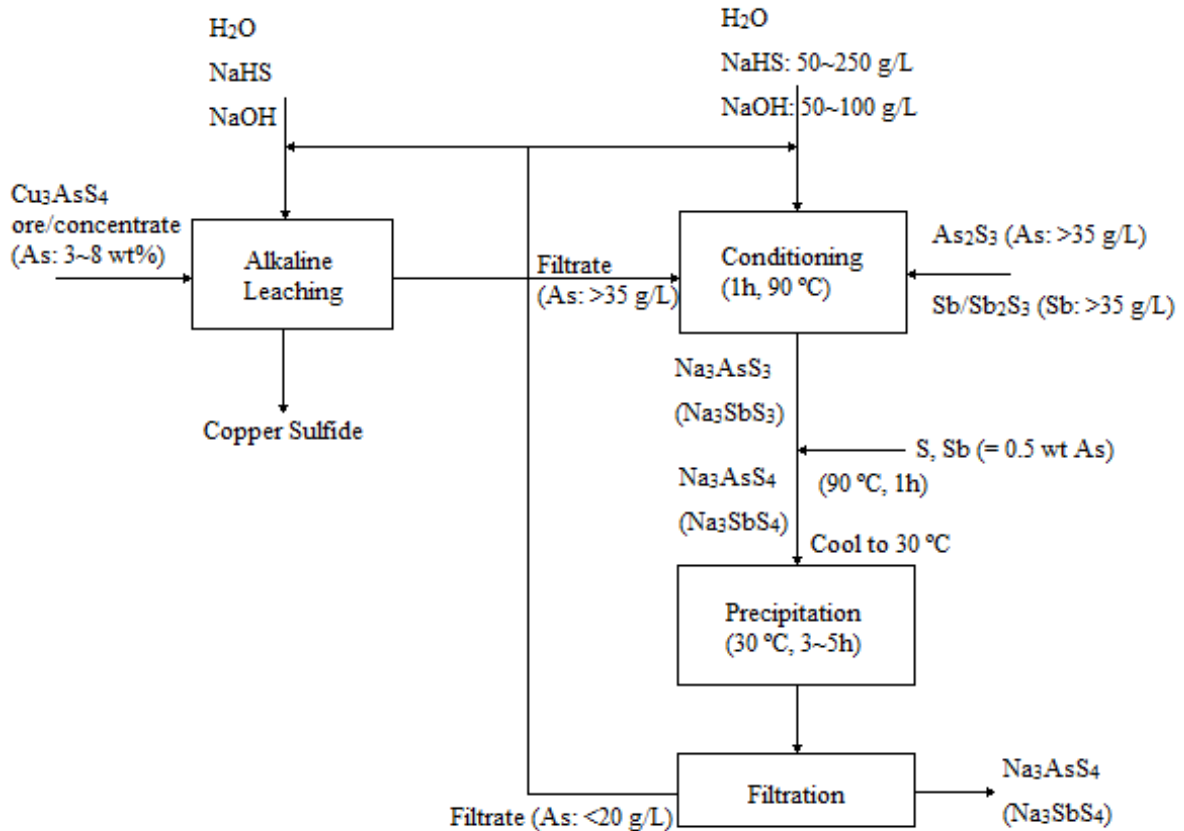
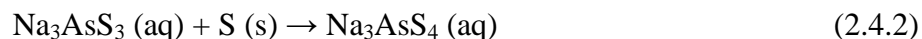
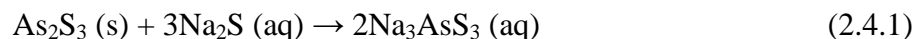


FIGURE 2.12 SCHEMATIC ILLUSTRATION OF THE Cu_3AsS_4 - NaHS - NaOH LEACHING AND Na_3AsS_4 PRECIPITATION PROCESS FOR ARSENIC REMOVAL AND CIRCULATION OF WASTE WATER TO LEACHING AND PRECIPITATION STAGES FOR RE-USE (TONGAMP ET AL. 2010A, 2010B)

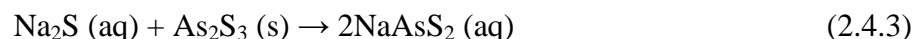
A practical method for sodium thio-arsenate synthesis can be achieved from Tongamp's study. As_2S_3 dissolves in high concentrations of Na_2S (50 ~ 250 g/L) and NaOH (50 ~ 100

g/L) solution at 90 °C, and Na₃AsS₄ can be precipitated with the addition of elemental sulfur as an oxidant followed by cooling to 30 °C. These reactions are shown as follows:

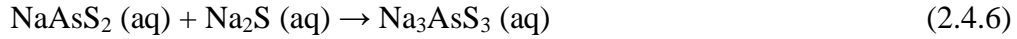
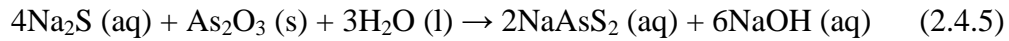


Orpiment dissolution increases linearly from acidic to alkaline conditions (Lengke et al. 2009, Lengke and Tempel, 2002), and a series of thio-arsenate species can be formed. Orpiment dissolution is controlled by weak van der Waals bonding, which further weakens at alkaline pH when hydroxide adsorption occurs at the surface of the orpiment (Mamedov and Mikhailov 1997, Floroiu et al. 2004). In sulfide deficient solutions, model calculations and laboratory studies show that arsenite (AsO₃³⁻) is the dominant aqueous species with 70 ~ 90% of total arsenic at pH 2 ~ 8 (Eary 1992, Floroiu et al. 2004). However, in anoxic, sulfide-rich solutions, the formation of thio-arsenite (AsO_{3-x}S_x³⁻) species has been supported by Helz et al. (1995, 2008). Free sulfide ions are suggested to react with orpiment to form and release thio-arsenite.

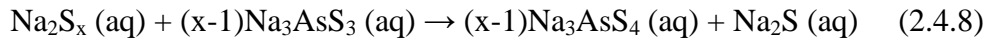
A similar chemical method is provided by Anderson and Twidwell in 2008. As mentioned in their work, a mixture of sodium sulfide and sodium hydroxide is a unique hydrometallurgical system that is very selective for tin, gold, antimony, arsenic and mercury. Thus, when the system is applied to an arsenic containing material like orpiment, a solution of sodium thio-arsenite is formed. The series of chemical reactions is illustrated as:



And arsenic trioxide can also be a reactant to form thio-arsenite. The reactions are:

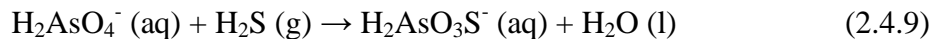


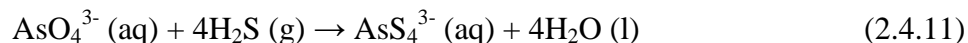
A certain amount of elemental sulfur reacted with sodium sulfide will form polysulfides, which have sufficient oxidizing power to form the arsenate. This can be explained as follows:



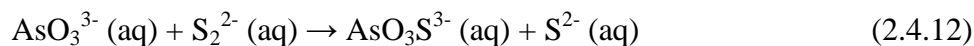
A more specific study by Suess and Planer-Friedrich (2012) shows that thio-arsenates can form as dominant species in the leaching of orpiment (As_2S_3) and arsenopyrite (FeAsS), and the mobility of arsenic needs to be considered in studies, especially at neutral to alkaline pH. Under acidic conditions, no thio-arsenates formed in orpiment dissolution. Under neutral to alkaline conditions, mono-, di-, trithioarsenate species accounted for up to 50% of total arsenic in orpiment leaching solution. Furthermore, X-ray Absorption Spectroscopy based analysis showed that thio-arsenites are necessary precursor species for thio-arsenate formation, which are formed through the oxidation of thio-arsenite at highly alkaline conditions in the presence of trace amounts of oxygen (Planer-Friedrich et al. 2010).

Another way to form thio-arsenate species is presented by Rochette et al. (2000). The species of thio-arsenate (AsO_3S^- , AsO_2S_2^- , and AsOS_3^-) can be formed by controlling the amount of hydrogen sulfide gas, which is purged to react with arsenate.





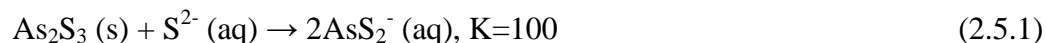
Zhang (2004) also showed that monothio-arsenate ($\text{AsO}_3\text{S}^{3-}$) and dithio-arsenate ($\text{AsO}_2\text{S}_2^{3-}$) can be formed by the recombination of arsenite and disulfide:



2.5 Solubility of amorphous As_2S_3

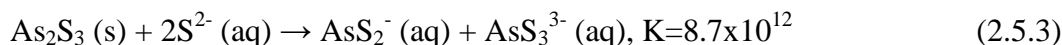
Arsenic is commonly present in sulfide ores, concentrates, and tailings, and As_2S_3 is an important As-S complex during hydrometallurgical processing. To synthesize sodium arsenic oxy-sulfide complexes, a determination of amorphous As_2S_3 solubility in sulfide-rich solutions is needed. Due to the difference in structure, amorphous As_2S_3 may be expected to be more soluble than orpiment (Eary 1992).

The solubility of orpiment in water was determined to be 2.1×10^{-6} mol/L at 16 ~ 18 °C by Biltz (1907), and 3.6×10^{-6} mol/L at 0 °C by Holtje (1929). Ringbom (1953) used the 0 °C solubility data (Holtje 1929) to obtain an equilibrium constant for the following reaction (2.5.1):

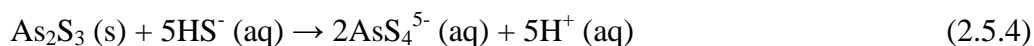


Wunschendorf (1929) determined the mole ratios of $\text{As}_2\text{S}_3/\text{Na}_2\text{S}$ in 1.0 mol/L Na_2S solutions saturated with As_2S_3 , ranging from 0.990 at 18 °C to 1.009 at 100 °C. Babko and

Lisetskaya (1956) studied the equilibria involved in the system of thiosalts with Sn, Sb, and As, by determining the solubility and pH of various buffered solutions which were saturated with SnS₂, Sb₂S₃, and As₂S₃ at 20 °C. The reactions for As₂S₃ dissolution in these solutions was concluded to be:



Srivastava and Ghosh (1957) studied the dissolution of As₂S₃ and As₂S₅ by determining the solubility, conductivity, and potential in dilute aqueous solutions of constant H₂S and variable NaOH concentrations at room temperature. The mechanism of As₂S₃ dissolution with HS⁻ ions was:



Weissberg et al. (1966) measured the solubility of orpiment in Na₂S-H₂O solutions under conditions ranging from 0.55 to 3.43 wt% Na₂S, temperatures from 25 to 200 °C, and pressures from 100 to 1500 bar. Orpiment solubility increases linearly with increasing Na₂S concentration, and decreases non-linearly with increasing pressure. Temperature below 120 °C shows slight effect on the orpiment solubility. And the orpiment solubility grows at an increasing rate as the temperature goes above 120 °C.

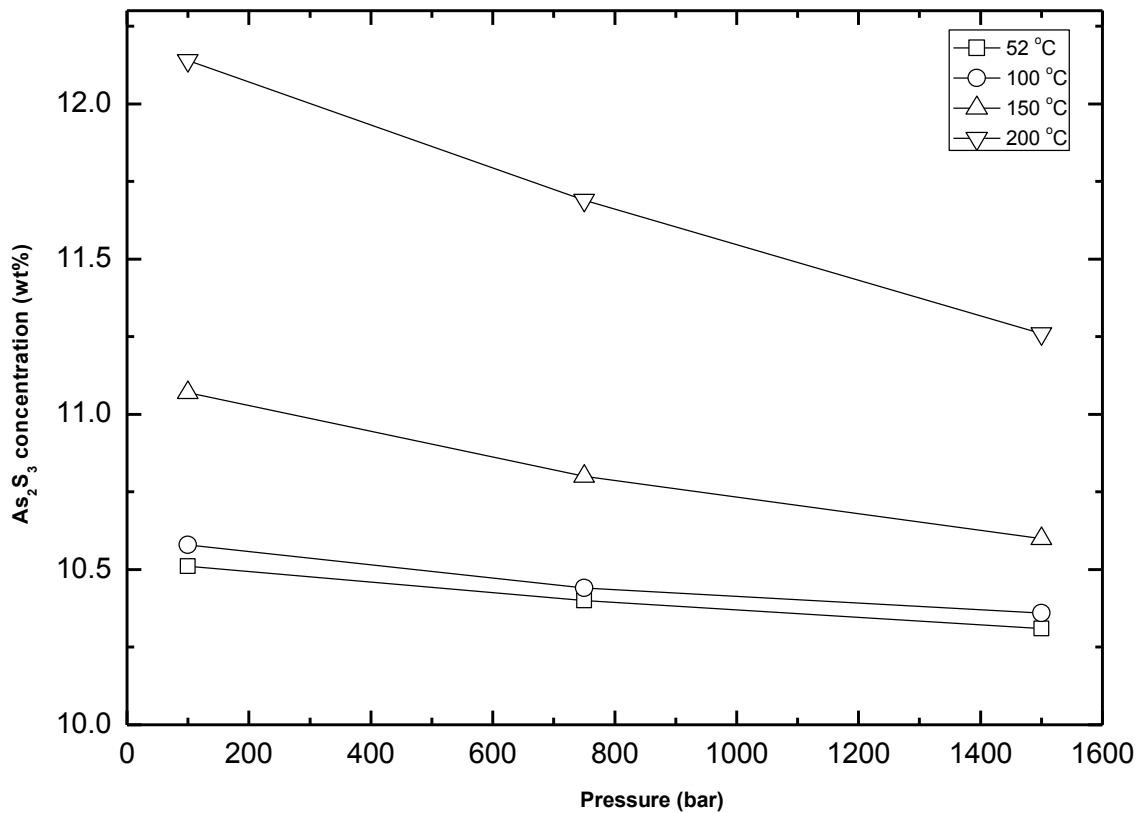


FIGURE 2.13 THE SOLUBILITY OF ORPIMENT IN 3.43 WT % Na_2S SOLUTIONS AT 52, 100, 150 AND 200 °C, AS A FUNCTION OF PRESSURE (REPLOTTED FROM WEISSBERG ET AL. 1966)

Webster (1990) determined the solubility of synthetic, crystalline As_2S_3 in O_2 -free, dilute and sulfide-bearing solutions at temperature of 25 and 90 °C. The predominant dissolved arsenic species were H_3AsO_3 and $H_2As_3S_6^-$ at pH 2 ~ 6.

Chapter 3 Objectives

Based on the literature review it is clear that the solubility of As in ASL solutions requires further study. To generate data relevant to ASL systems, the present work is based on the following objectives:

1. To do a preliminary study on arsenic trioxide solubility in sodium sulfide and sodium hydroxide solutions for the synthesis of amorphous As_2S_3 and sodium arsenic oxy-sulfide complexes.
2. To determine the solubility of synthetic amorphous As_2S_3 in sodium sulfide solutions.
3. To synthesize a series of sodium thio-arsenate complex.
4. To determine the solubility of sodium thio-arsenate in alkaline sulfide solutions.
5. To characterize the arsenic precipitates that result from enargite leaching in alkaline sulfide solutions.

Chapter 4 Experimental Procedures

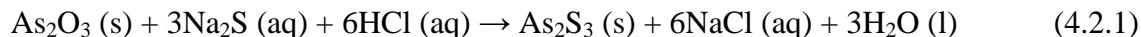
4.1 Preliminary solubility study on arsenic trioxide

Four groups of tests were done with the intention of exploring arsenic dissolution behavior in sodium sulfide and sodium hydroxide solution as well as to establish procedures for synthesis of arsenic tri-sulfide and sodium arsenic oxy-sulfide complexes. Individual experiments at constant temperature (20 °C, 40 °C, 60 °C, 80 °C, 95 °C) were done, each over 48 hours, with magnetic stirring. 300 ml of sodium sulfide and sodium hydroxide solutions with 0.5 M concentration were prepared in a 500 ml jacketed cell. The temperature was maintained by water circulation through the cell jacket from a Cole-Parmer temperature controller/water bath. Over 48 hours, a constant amount of arsenic trioxide was added every 20 ~ 30 minutes until complete dissolution of arsenic trioxide was observed by visual inspection. Addition of arsenic trioxide stopped when no further dissolution was observed. Two different conditions were studied separately: with oxygen addition and without oxygen oxidation. For the oxygen-free solubility tests, argon gas was purged through the solution for more than fifteen minutes before arsenic trioxide addition.

4.2 Synthesis of amorphous As₂S₃

Arsenic tri-sulfide provided by the Alfa-Aldrich Company was first used in the synthesis of sodium arsenic oxy-sulfide complexes, but its low solubility in sodium sulfide and sodium hydroxide solutions was observed in several experiments. This As₂S₃ may have been polymerized at high temperature thus affecting its solubility. Synthesis of amorphous arsenic tri-sulfide was then done in an aqueous system via a new method.

This method is shown in reaction 4.2.1 as follows:



The Delta Gibbs Free Energy (ΔG°) of this reaction (4.2.1) at temperatures ranging from 0 °C to 90 °C was calculated thermodynamically by the HSC software and it is shown in Figure 4.1:

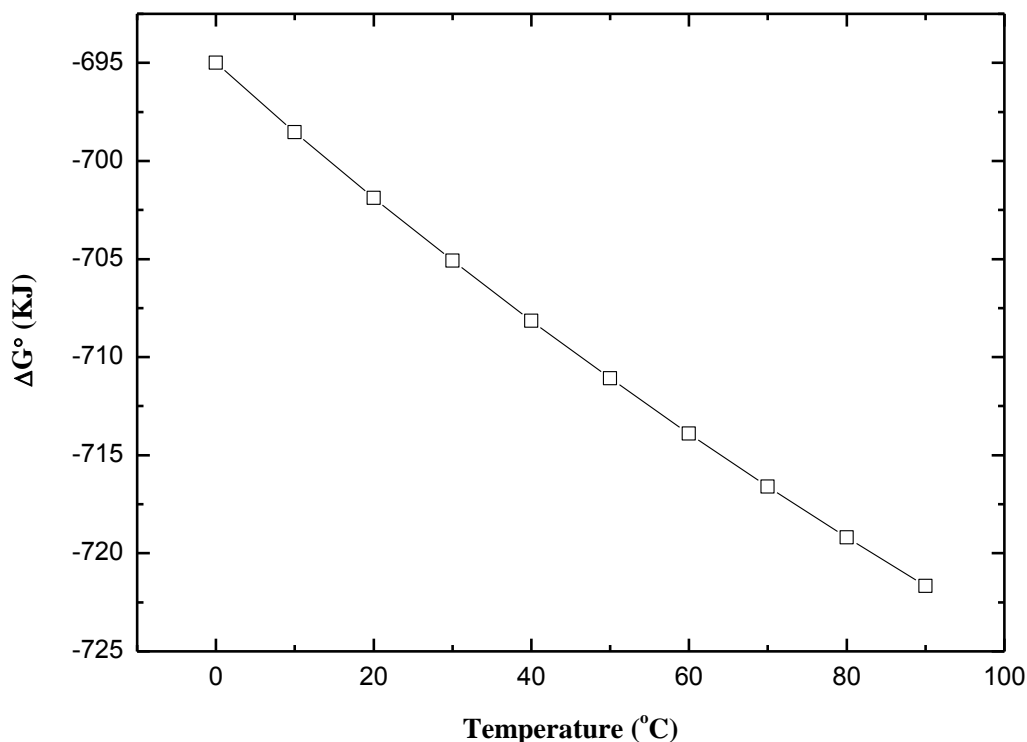


FIGURE 4.1 THE DELTA GIBBS ENERGY OF As_2S_3 SYNTHESIS REACTIONS BY HSC

As predicted by HSC, the formation of arsenic tri-sulfide in reaction 4.2.1 is very favorable. And as temperature increases, the reaction should proceed more favorably. Furthermore, the predicted solubility of As_2S_3 (by OLI software simulation) in acidic (HCl) and alkaline (Na_2S) solutions through the pH range 0~12 shows that As_2S_3 is highly soluble in the alkaline sulfide system. OLI software simulation uses a basic electrolyte thermodynamic model - the AQ model, which is based on a true speciation model, a predictive equation of state (Helgeson EOS), an activity coefficient model, and convergence

heuristics. The model is based upon published experimental data. The model uses data regression wherever possible and estimation and extrapolation where required. Also it provides general simulation capability giving accurate prediction for almost any water chemistry mixture over a very wide range. Figure 4.2 demonstrates that As_2S_3 is barely soluble in HCl and at low pH. OLI was not able to calculate the solubility above pH 12.

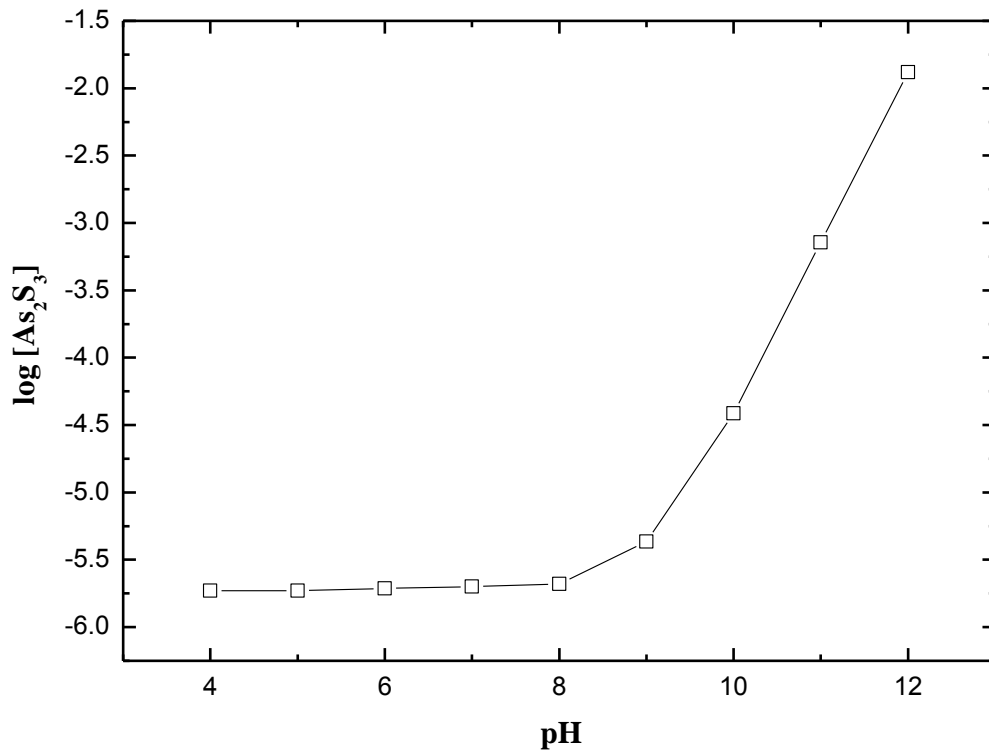


FIGURE 4.2 As_2S_3 SOLUBILITY PREDICTED BY OLI AT PH RANGE 0~12 AT 25 °C

Based on these data, the synthesis of As_2S_3 could occur through the use of the following experimental setup.

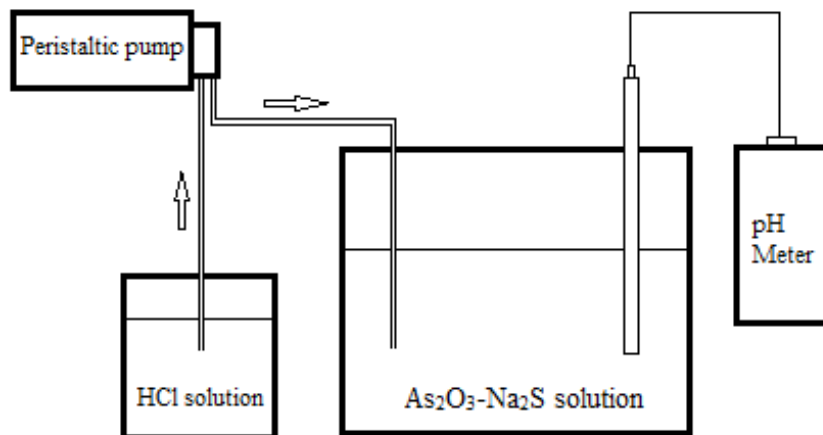


FIGURE 4.3 EXPERIMENT SETUP FOR As_2S_3 SYNTHESIS

Arsenic trioxide powder was dissolved in sodium sulfide solution at different concentrations at different temperatures, and HCl solution was pumped slowly into the reactor. The inflow of hydrochloric acid solution stopped when pH dropped below 5, at which point virtually all of the arsenic was precipitated as yellow As_2S_3 . The yellow precipitate was kept in solution for varying aging times to allow for particle growth.

4.2.1 Concentration effect

Since the effect of the concentrations of sodium sulfide and hydrochloric acid solutions plays a large role in the synthesis of As_2S_3 , optimized concentrations of these reagents were first determined. 0.1 M, 0.2 M, 0.3 M sodium sulfide solution and 1 M, 2 M, 3 M hydrochloric acid were tested with different combinations as shown in Table 4.1.

Table 4.1 Conditions of As_2S_3 synthesis concentration tests

Experiment No.	Temperature (°C)	[Na_2S] (M)	[HCl] (M)	Flow rate (ml/min)	Aging time (hr)
1	50	0.1	1	3.2	16
2	50	0.1	2	3.2	16
3	50	0.1	3	3.2	16

Table 4.1 Conditions of As_2S_3 synthesis concentration tests continued

Experiment No.	Temperature (°C)	[Na_2S] (M)	[HCl] (M)	Flow rate (ml/min)	Aging time (hr)
4	50	0.2	1	3.2	16
5	50	0.2	2	3.2	16
6	50	0.2	3	3.2	16
7	50	0.3	1	3.2	16
8	50	0.3	2	3.2	16
9	50	0.3	3	3.2	16



FIGURE 4.4 SYNTHETIC ARSENIC TRI-SULFIDE POWDER

The synthetic yellow precipitates were vacuum filtered, and dried in an oven overnight (below 100 °C). After drying the solid was dissolved and ground with a mortar and pestle in DI water to remove any residual NaCl and HCl, and then filtered again. The solid

was again dried overnight (below 100 °C) and ground again with a mortar and pestle into finer powder. The yellow powder samples (Figure 4.4) were analyzed by EDX (Hitachi Model S3000N VPSEM) and the PSD was measured by Malvern Mastersizer 2000 Laser Diffraction Particle Size Analyser.

4.2.2 Temperature effect

The As₂S₃ synthesis experiments were operated at different temperature (25 °C, 40 °C, 60 °C, and 80 °C) with the same procedure as described above, and the optimized concentrations of sodium sulfide and hydrochloric acid (as determined above) were applied. The detailed experimental conditions for the effect of temperature are presented in Table 4.2.

Table 4.2 Conditions of As₂S₃ synthesis temperature tests

Experiment No.	Temperature (°C)	[Na₂S] (M)	[HCl] (M)	Flow rate (ml/min)	Aging time (hr)
10	25	0.1	1	3.2	2
11	40	0.1	1	3.2	2
12	60	0.1	1	3.2	2
13	80	0.1	1	3.2	2

4.2.3 Effect of hydrochloric acid addition rate

The rate of HCl solution addition was also studied, and the experimental parameters are presented in Table 4.3.

Table 4.3 Conditions of As₂S₃ synthesis flow rate tests

Experiment No.	Temperature (°C)	[Na₂S] (M)	[HCl] (M)	Flow rate (ml/min)	Aging time (hr)
14	50	0.1	1	3.2	2
15	50	0.1	1	5.9	2

4.2.4 Aging time effect

The main impact of different aging times was expected to be on particle size. 2, 8 and 48 hours aging times were applied in experiment detailed in Table 4.4.

Table 4.4 Conditions of As_2S_3 synthesis aging time tests

Experiment No.	Temperature (°C)	[Na_2S] (M)	[HCl] (M)	Flow rate (ml/min)	Aging time (hr)
16	50	0.1	1	3.2	2
17	50	0.1	1	3.2	8
18	50	0.1	1	3.2	48

4.3 Solubility of amorphous As_2S_3 in sodium sulfide solution

To prepare for sodium thioarsenate synthesis, the solubility of amorphous arsenic trisulfide in sodium sulfide solutions was determined by a series of experiments. Similar to the previous arsenic trioxide solubility tests, fifteen experiments were run at constant temperature (20 °C, 40 °C, 60 °C, 80 °C, 95 °C) at three different concentrations (1 wt% or 0.13 M, 2 wt% or 0.26 M, and 3 wt% or 0.39 M) of sodium sulfide solution. Over 48 hours, the 50 ml sodium sulfide solution was stirred, and a constant amount of synthetic arsenic trisulfide powder was periodically added until dissolution stopped as determined by visual inspection.

4.4 Synthesis of sodium thio-arsenate

4.4.1 Synthesis of precursor sodium arsenate by hydrogen peroxide oxidation of As (III)

White sodium arsenate crystals (Figure 4.5) were first produced by dissolving 30 g arsenic trioxide in 250 ml sodium hydroxide solution (4 M), followed by oxidation with 300 ml hydrogen peroxide (3 M) at 50 °C. Since the solubility of sodium arsenate decreases dramatically with decreasing temperature, sodium arsenate crystals precipitated as the solution was cooled. The reactions are as follows:

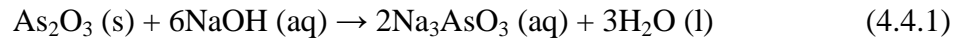
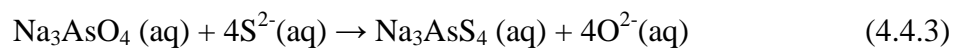


FIGURE 4.5 SYNTHETIC SODIUM ARSENATE

Different sulfide sources were then used (solid sodium sulfide, pre-dissolved sodium sulfide, hydrogen sulfide gas) throughout the sodium thio-arsenate synthesis attempts. The anticipated sodium thio-arsenate production reaction was (the original concentration of sodium arsenate was 3.2 M):



4.4.1.1 Synthesis of sodium thio-arsenate from sodium arsenate and sodium sulfide solution

32.5 g As_2O_3 was dissolved in 0.5 L of sodium hydroxide solution (6 M) at room temperature, and hydrogen peroxide (0.5 mol) was added for the oxidation of As (III) to As (V). 2 L of concentrated sodium sulfide solution (2 M) was then pumped in to the mixture and stirred overnight. A white acicular crystal was found to precipitate (Figure 4.6). After filtration, washing and drying, the crystalline product (#1) was analyzed by Energy Dispersive X-Ray Spectroscopy (EDX).



FIGURE 4.6 CRYSTALLINE PRECIPITATE #1 SYNTHESIZED BY ADDITION OF SODIUM SULFIDE SOLUTION TO SODIUM ARSENATE SOLUTION

4.4.1.2 Synthesis of sodium thio-arsenate from sodium arsenate and solid sodium sulfide

The $\text{As}_2\text{O}_3\text{-H}_2\text{O}_2\text{-NaOH}$ solution was prepared as before, but 960 g or 4 mol solid sodium sulfide nona-hydrate ($\text{Na}_2\text{S}\cdot 9\text{H}_2\text{O}$) was added to the sodium arsenate solution with

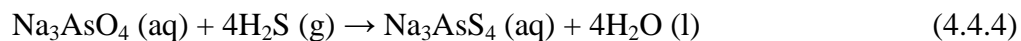
overnight stirring (As:S ratio ~ 0.25). A white crystal was precipitated (Figure 4.7). After filtration, washing and drying, the crystalline product (#2) was analyzed by EDX.



FIGURE 4.7 CRYSTALLINE PRECIPITATE #2 SYNTHESIZED BY ADDITION OF SOLID SODIUM SULFIDE TO SODIUM ARSENATE SOLUTION

4.4.1.3 Synthesis of sodium thio-arsenate from sodium arsenate and hydrogen sulfide gas

Different amounts (10 g, 20 g, 100 g, and 300 g) of synthetic sodium arsenate were added to sodium sulfide solutions (2 M) separately at room temperature. A pH meter was used during the hydrogen sulfide gas sparging process (see setup in Figure 4.8). The temperature of the solution was increased to 70 °C to ensure that the entire sodium arsenate solid was dissolved. Hydrogen sulfide gas was then slowly sparged through the Na₃AsO₄-Na₂S solution (with stirring) at a rate of approximately 30 bubbles per minute until the pH stopped changing, which meant the reaction had reached equilibrium.



Following that, the solution was naturally cooled to room temperature. Only the sodium sulfide solution with 300 g of added sodium arsenate resulted in the precipitation of a crystal (Figure 4.9). After filtration, washing and drying, the crystalline product #3 was analyzed by EDX.

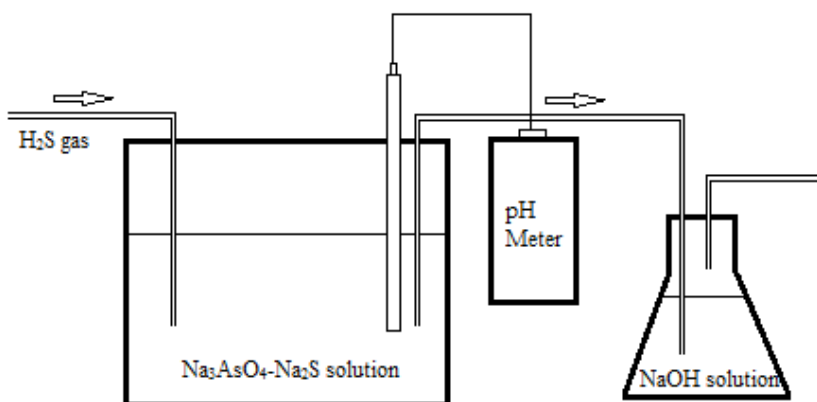


FIGURE 4.8 EXPERIMENTAL SETUP FOR SYNTHESIS OF SODIUM ARSENIC OXY-SULFIDE COMPLEXES BY H₂S



FIGURE 4.9 CRYSTALLINE PRECIPITATE #3 SYNTHESIZED BY H₂S GAS ADDITION TO SODIUM ARSENATE SOLUTION

4.4.2 Synthesis of sodium thio-arsenate by reaction of arsenic tri-sulfide with elemental sulfur

To eliminate the oxygen content of the product, synthetic arsenic tri-sulfide can be used in the synthesis of sodium thio-arsenate by reaction with elemental sulfur. The yellow As₂S₃ powder (50 g) was dissolved in concentrated sodium sulfide solution (200 ml at 3 M) at 60 °C, and various amounts of elemental sulfur were added until the complete dissolution of As₂S₃. The solution was cooled down naturally from 60 °C to room temperature until the solution became homogeneous and the color became dark yellow. The anticipated reactions were as follows:

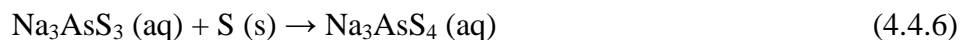
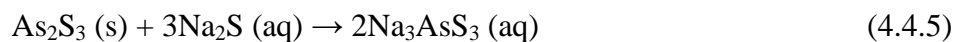


FIGURE 4.10 CRYSTALLINE PRECIPITATE #4 SYNTHESIZED BY REACTION OF ELEMENTAL SULFUR (12.8 G) WITH ARSENIC TRISULFIDE (50 G) IN 200 ML AT 3M SODIUM SULFIDE



FIGURE 4.11 CRYSTALLINE PRECIPITATE #4 SYNTHESIZED BY REACTION OF ELEMENTAL SULFUR WITH ARSENIC TRISULFIDE AFTER FILTRATION

As temperature decreased, an acicular crystal was precipitated (Figure 4.10). The resulting synthetic crystal #4 (Figure 4.11) was analyzed by EDX and Quantitative X-Ray Diffraction (QXRD).

4.5 Solubility of synthetic sodium arsenic oxy-sulfide complexes and sodium thio-arsenate

The solubility of synthetic crystals #2, #3 and #4 was measured separately in three different leach solution (Table 4.5) at 20 °C, 40 °C, 60 °C, 80 °C and 95 °C.

Table 4.5 Three different leach solutions for solubility tests

Experiment No.	[NaOH] (M)	[Na ₂ S] (M)
1	2.5	1.0
2	2.5	0.5
3	1.0	1.0

To limit the formation of polysulfide species, argon gas was sparged during the solubility experiments to avoid oxidation by ambient oxygen. Some experiments were performed at constant sodium hydroxide concentration where the concentration of the hydrosulfide ion was varied from 0 M to 1.0 M (Table 4.6). For these experiments, the solubility of synthetic sodium thioarsenate crystals was again studied in an argon atmosphere from 20 °C to 95 °C.

Table 4.6 Three conditions for varying hydrosulfide and constant NaOH

Experiment No.	[NaOH] (M)	[NaHS] (M)
1	2.5	0
2	2.5	0.5
3	2.5	1.0

4.6 Solubility accuracy calibration test

Since the dissolution of synthetic complexes in sodium sulfide and hydroxide solutions is very quick and obvious to the naked eye, the saturation point was determined by visual inspection. Nonetheless, to calibrate the accuracy of this saturation point, as determined by visual inspection, two more solubility tests were performed. For the 2.5 M NaOH & 1.0 M Na₂S solution at 20 °C in an argon atmosphere and for the 2.5 M NaOH & 0.5 M NaHS solution at 60 °C in argon, the following procedure was done:

- 0.1 ml of the saturated solution was taken at the point of visual saturation, diluted 500 times, and the solution was analyzed for arsenic by ICP
- The mixture (now containing two phases) was then allowed to reach equilibrium over at least 12 hours. 0.1 mL of the solution phase was then again taken, diluted and sent for ICP analysis.
- These two ICP analyses were compared to ascertain the accuracy of the visual inspection method.

4.7 Precipitation from an enargite leaching test

An enargite sample (Figure 4.12, Tables 4.7 and 4.8) was leached in mixed sodium hydroxide (2.5 M) and sodium sulfide solution (0.5 M) at 95 °C for 24 hours, after which time the leaching solution was rapidly vacuum filtered at high temperature in less than ten minutes.



FIGURE 4.12 ENARGITE MINERAL SAMPLES

Table 4.7 Elemental analysis of the enargite sample

Element	Content (wt %)
Cu	28.30
Fe	15.03
As	9.44
Sb	0.40
Bi	0.26
Ag	0.04
Zn	2.55
Ni	0.00
Al	0.00
Ca	0.05
Pb	1.25

Table 4.8 Quantitative phase analysis of the enargite sample

Mineral	Formula	Content (wt %)
Enargite	Cu_3AsS_4	44.1
Tennantite	$(\text{Cu, Ag, Fe, Zn})_{12}\text{As}_4\text{S}_{13}$	4.6
Luzonite	$\text{Cu}_3(\text{As, Sb})\text{S}_4$	2.3
Pyrite	FeS_2	34.6
Chalcopyrite	CuFeS_2	6.5
Sphalerite	$(\text{Zn, Fe})\text{S}$	4.2
Galena	PbS	1.2
Quartz	SiO_2	2.5

Large yellow needle-like crystalline precipitates appeared after the leach solution had cooled overnight (cf. Figure 4.13 and Figure 4.14). To determine the As content in the crystal, 1 gram of the crystal was dissolved in 1 liter of DI water and sent for ICP. The As content in the crystals as determined by ICP was ~ 0.38 wt%. This number is not accurate as a large

amount of water was likely still associated with the crystals. Nevertheless, since very low arsenic was found in the crystals, most of the arsenic was left in the leach solution.

In order to further understand why the arsenic did not precipitate upon cooling, another arsenic precipitation test was done by separating the leach solution (without crystals) into two equal volumes (referred to as solution a. and b.). One half of the mass of precipitated low As crystals was put into solution a., while nothing was added to solution b. Both solutions were then heated to 90 °C with stirring. Sulfur was then added to both solutions at an As:S ratio of 1 and the mixture was equilibrated for 2 hours. The solutions were then cooled, but no crystalline precipitate was found. Finally, 0.1 ml of solutions a. and b. was sampled, diluted 1000 times and sent for ICP analysis.



FIGURE 4.13 CRYSTAL PRECIPITATED FROM PREGNANT ASL SOLUTION AFTER ENARGITE LEACHING



FIGURE 4.14 SIZE OF CRYSTALLITES OBTAINED UPON COOLING OF ASL PREGNANT LEACH SOLUTION

Chapter 5 Results and Discussion

5.1 Solubility of As_2O_3 in Na_2S and NaOH solution

In the absence of oxygen, the solubility of arsenic in 0.5 M sodium sulfide is constant at ~1.0 M from 20 °C to 80 °C. At 95 °C, the solution turns to black when the arsenic concentration reaches 0.75 M. In the presence of oxygen, arsenic solubility is constant from 20 °C to 40 °C, and then increases linearly from 0.8 M at 40 °C to 2.0 M at 95 °C (cf. Figure 5.1)

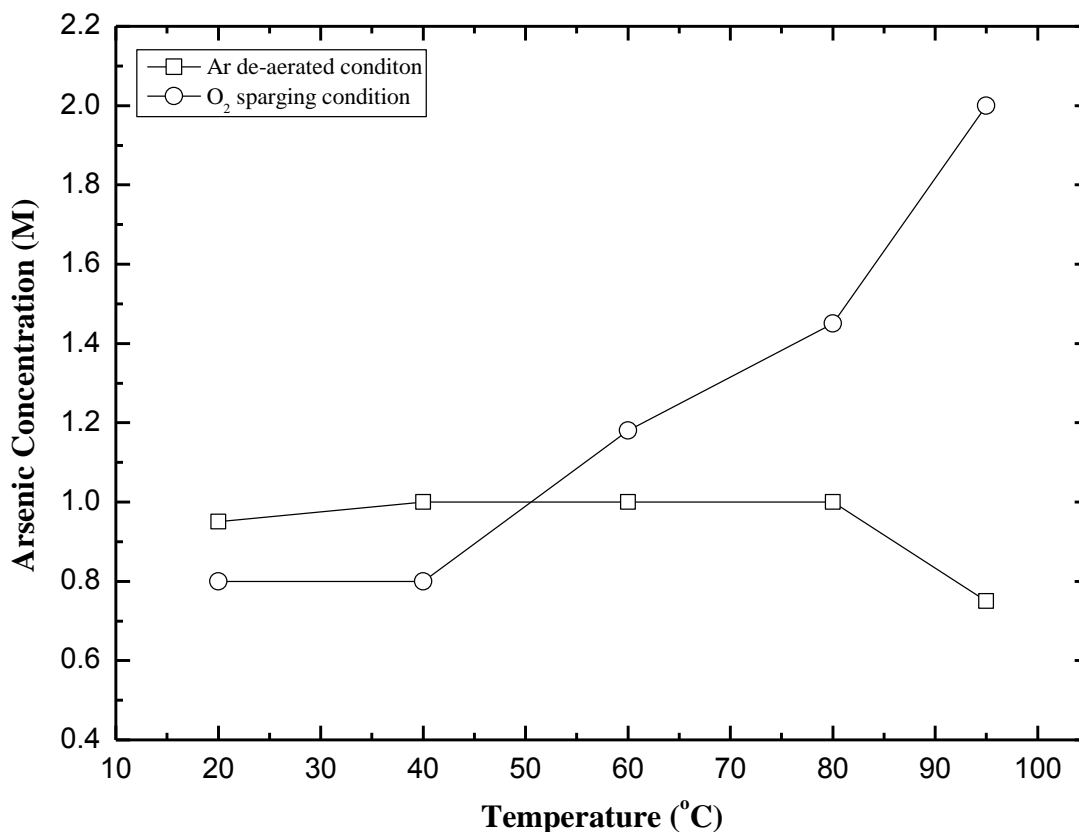
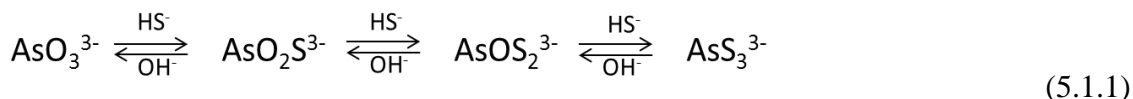


FIGURE 5.1 SOLUBILITY OF As_2O_3 IN 0.5 M SODIUM SULFIDE SOLUTIONS

When dissolved in sodium sulfide solution, arsenic exists as AsO_3^{3-} , $\text{AsO}_2\text{S}^{3-}$, AsOS_2^{3-} , and AsS_3^{3-} . According to Kim (2000), the kinetics of As (III) to As (V) oxidation at low

temperatures are slow. For example, it takes 2 ~ 5 days for pure oxygen and 4 ~ 9 days for air to oxidize more than 50% of the As (III) in groundwater to As (V). Thus, the function of oxygen may be to push As species transformation from AsS_3^{3-} to AsO_3^{3-} . This can be shown as follows:



The solubility curves presented in Figure 5.1 likely represent the solubility of a mixture of arsenic (III) oxy-sulfide ions. Oxygen sparging may result in oxygen reduction and the formation of hydroxyl through reaction 5.1.2:



The accompanying anodic reaction could be sulphide oxidation. Thus the equilibrium in 5.1.1 would be pushed to the left, and the solubility of this mixture with more oxygen increases dramatically with increasing temperature, possibly indicating that the As (III) oxy-anions are more soluble than the As (III) oxy-sulfide ions. On the other hand, without oxygen from outside the system, the solubility stays stable from 25 to 80 °C, and decreases from 1 M to 0.75 M at elevated temperature.

The solubility of As_2O_3 in 0.5 M NaOH (i.e. without sulfide) is presented in Figure 5.2. Without oxygen (or sulfide) present, the arsenic solubility in 0.5 M sodium hydroxide solution increases significantly from 20 °C to 95 °C, especially from 60 °C to 95 °C. It is of note that the de-aerated condition in Figure 5.2 is similar in profile to that of the oxygen saturated conditions in Figure 5.1. The arsenic solubility in the presence of oxygen but absence of sulfide also appears to be similar. These findings further corroborate the idea that

added oxygen does not significantly contribute to oxidation of As (III) during the experiments presented herein but, rather, it shifts the speciation from As (III) sulfides to As (III) oxy-anions.

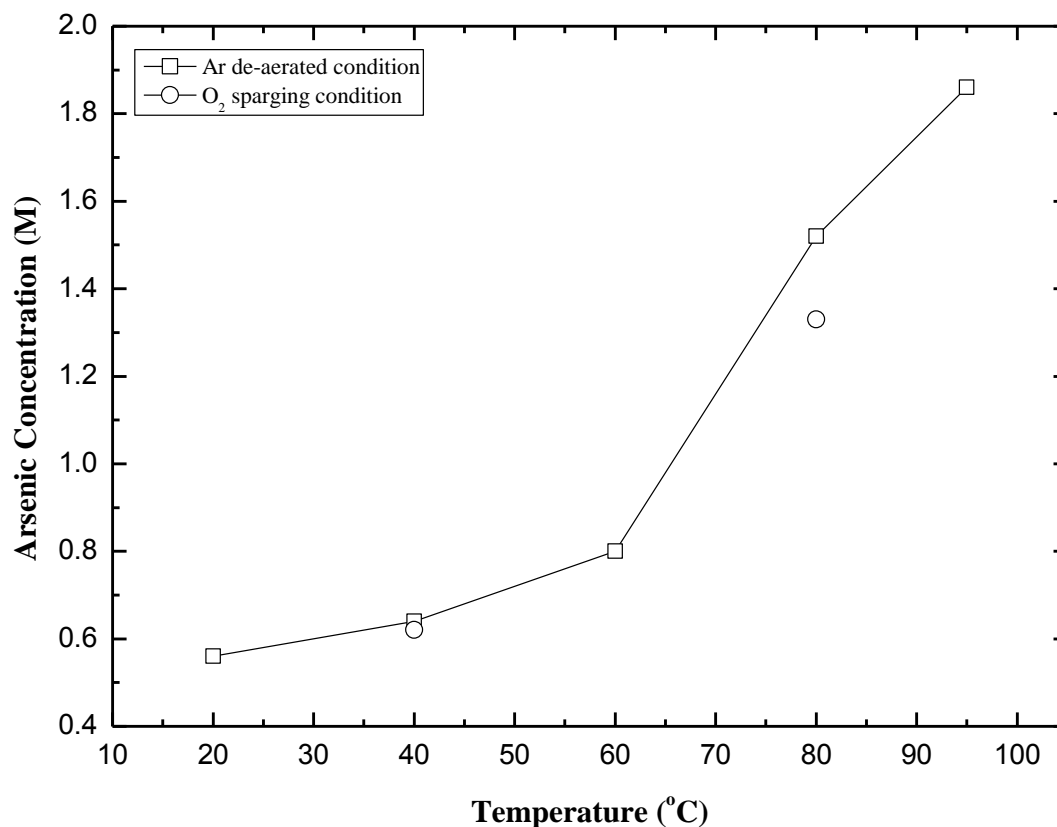
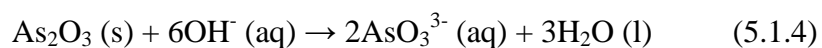
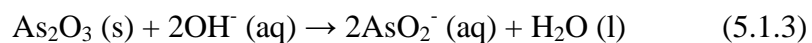


FIGURE 5.2 SOLUBILITY OF As_2O_3 IN 0.5 M SODIUM HYDROXIDE SOLUTIONS

For both conditions in Figure 5.2, arsenites (AsO_3^{3-}) exist in the solutions, according to reactions 5.1.2 and 5.1.3 (Zheng Y.J. et al., 2008).



However, it should be noted that the solubility of As quickly ($T > 20\text{ }^{\circ}\text{C}$) exceeded the added hydroxide in Figure 5.2 indicating that reactions 5.1.3 and 5.1.4 may no longer be valid at higher temperature. As observed from Figure 5.2, the solubility of As_2O_3 in NaOH with oxidation at $80\text{ }^{\circ}\text{C}$ is slightly lower than the solubility of As_2O_3 without oxidation. This may be because high temperatures have a positive effect on the oxidation of As (III) with oxygen (Wang et al. 2000).

5.2 Characterization of synthesized amorphous As_2S_3

Since the solubility of arsenic trioxide is relatively high, white arsenic trioxide is dissolved very quickly in sodium sulfide solution. When dilute hydrochloric acid solution (1 M, 2 M, and 3 M) was slowly pumped into the $\text{As}_2\text{O}_3\text{-Na}_2\text{S}$ solution an interesting phenomenon was observed: as soon as the hydrochloric acid solution droplet touched the $\text{As}_2\text{O}_3\text{-Na}_2\text{S}$ solution, a yellow precipitate formed at the droplet surface, which then quickly disappeared as the acid and alkaline solution mixed. The yellow precipitate re-appeared at the bottom of the cell as bulk pH was lowered and it was found to be arsenic tri-sulfide (As_2S_3) after characterization. The reason for its disappearance after its first precipitation at the HCl solution droplet surface is due to arsenic tri-sulfide's high solubility in sodium sulfide solution and its low solubility in hydrochloric acid solution.

To optimize the conditions of arsenic tri-sulfide synthesis, different concentrations of sodium sulfide and hydrochloric acid solution, temperature, flow rate of hydrochloric acid solution, and aging time were applied. The products were compared according to their EDX spectra and PSD results.

5.2.1 Effect of reagent concentrations

For different concentrations of sodium sulfide (0.1 M, 0.2 M, and 0.3 M) and hydrochloric acid (1 M, 2 M, 3 M), the characterization results are as follows:

Table 5.1 EDX result for effect of concentration

Experiment #	Temperature (°C)	[Na ₂ S] (M)	[HCl] (M)	Flow rate (ml/min)	Aging time (h)	EDX Result	
						As wt%	S wt%
1	50	0.1	1	3.2	16	61.8	38.2
2	50	0.1	2	3.2	16	61.93	38.07
3	50	0.1	3	3.2	16	67.04	32.96
4	50	0.2	1	3.2	16	59.7	40.3
5	50	0.2	2	3.2	16	69.93	30.07
6	50	0.2	3	3.2	16	67.22	32.78
7	50	0.3	1	3.2	16	61.95	38.05
8	50	0.3	2	3.2	16	65.95	34.05
9	50	0.3	3	3.2	16	63.57	36.43

Theoretically, the EDX result for arsenic tri-sulfide should be close to 61 wt% As and 39 wt% S.

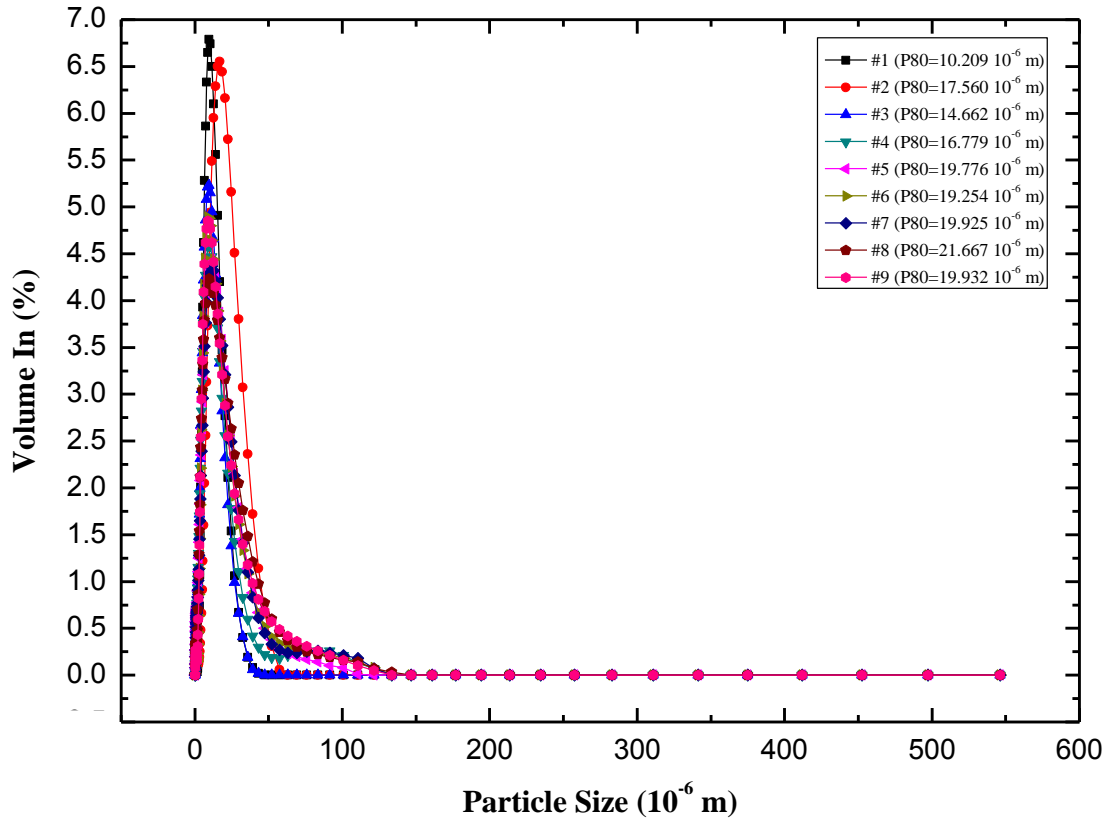


FIGURE 5.3 PSD RESULT FOR EFFECT OF CONCENTRATION ON THE PRECIPITATION OF As_2S_3 FROM $As_2O_3-Na_2S$ SOLUTION

The chemical composition of the samples from experiments #1, #2, #4, #7 is close to the theoretical value. The particle size from experiments #1 and #2 had mean values of approximately 10.21 μm and 17.56 μm . In conclusion, the more diluted solution used for both sodium sulfide and hydrochloric acid solutions, the better the chemical composition and the coarser the particle size distribution. The latter makes solid-solution separation easier.

5.2.2 Effect of temperature

Different Temperatures (25 $^{\circ}C$, 40 $^{\circ}C$, 60 $^{\circ}C$, and 80 $^{\circ}C$) were used, and the EDX results and PSD results are shown in Table 5.2 and Figure 5.4.

Table 5.2 EDX result for effect of temperature

Experiment #	Temperature (°C)	[Na ₂ S] (M)	[HCl] (M)	Flow rate (ml/min)	Equilibrium time (h)	EDX	
						As wt%	S wt%
10	25	0.1	1	3.2	2	56.34	43.66
11	40	0.1	1	3.2	2	59.19	40.81
12	60	0.1	1	3.2	2	59.36	40.64
13	80	0.1	1	3.2	2	59.11	40.89

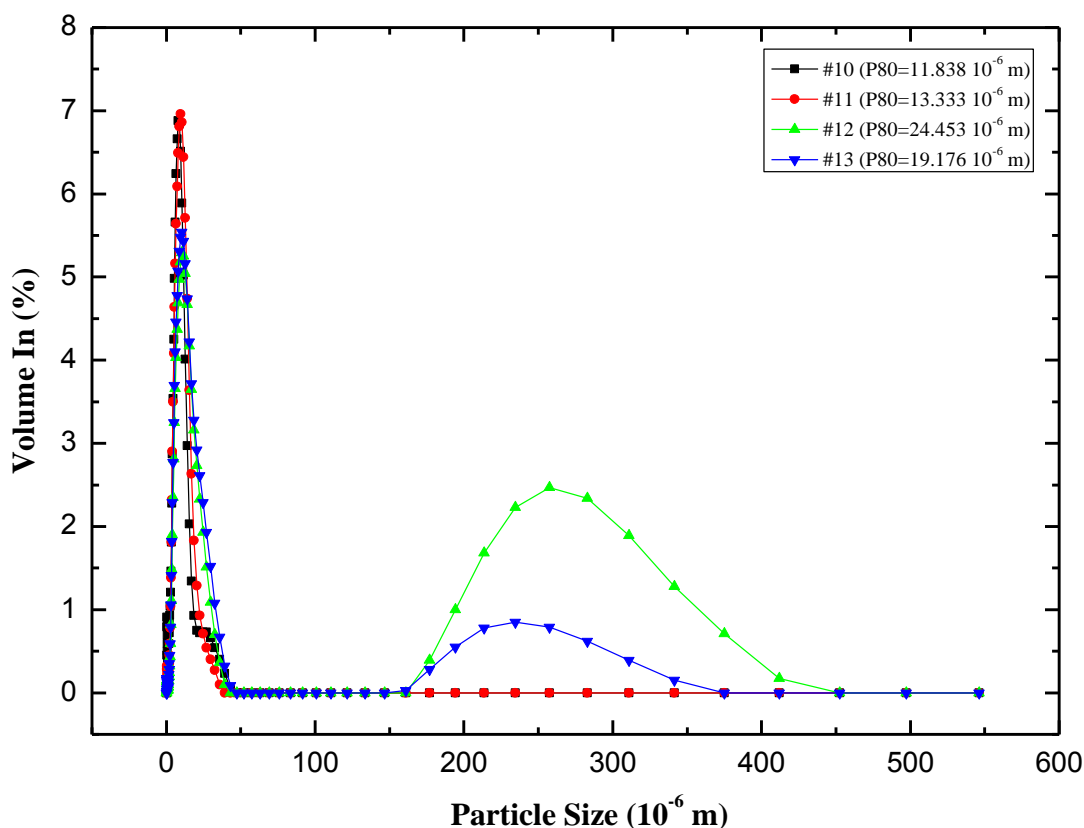


FIGURE 5.4 PSD RESULT FOR EFFECT OF TEMPERATURE ON THE PRECIPITATION OF AS₂S₃ FROM AS₂O₃-NA₂S SOLUTION

Arsenic tri-sulfide samples synthesized from 40 °C to 80 °C have similar chemical compositions. A better particle size distribution for solid-solution separation can be achieved at lower temperature (25 °C ~ 40 °C). At 60 °C and 80 °C, the PSD is bi-modal and a portion of the particles are distributed around 200 μm to 400 μm. Thus, a temperature of around 40 °C to 60 °C would appear to be optimal.

5.2.3 Effect of hydrochloric acid solution flow rate

Two different flow rates of hydrochloric acid solution (3.2 ml/min, 5.9 ml/min) were applied. The EDX and PSD results for these experiments are listed in Table 5.3.

Table 5.3 EDX result for effect of hydrochloric acid flow rate

Experiment #	Temperature (°C)	[Na ₂ S] (M)	[HCl] (M)	Flow rate (ml/min)	Equilibrium time (h)	EDX	
						As wt%	S wt%
14	50	0.1	1	3.2	2	61.44	38.56
15	50	0.1	1	6.4	2	59.35	40.65

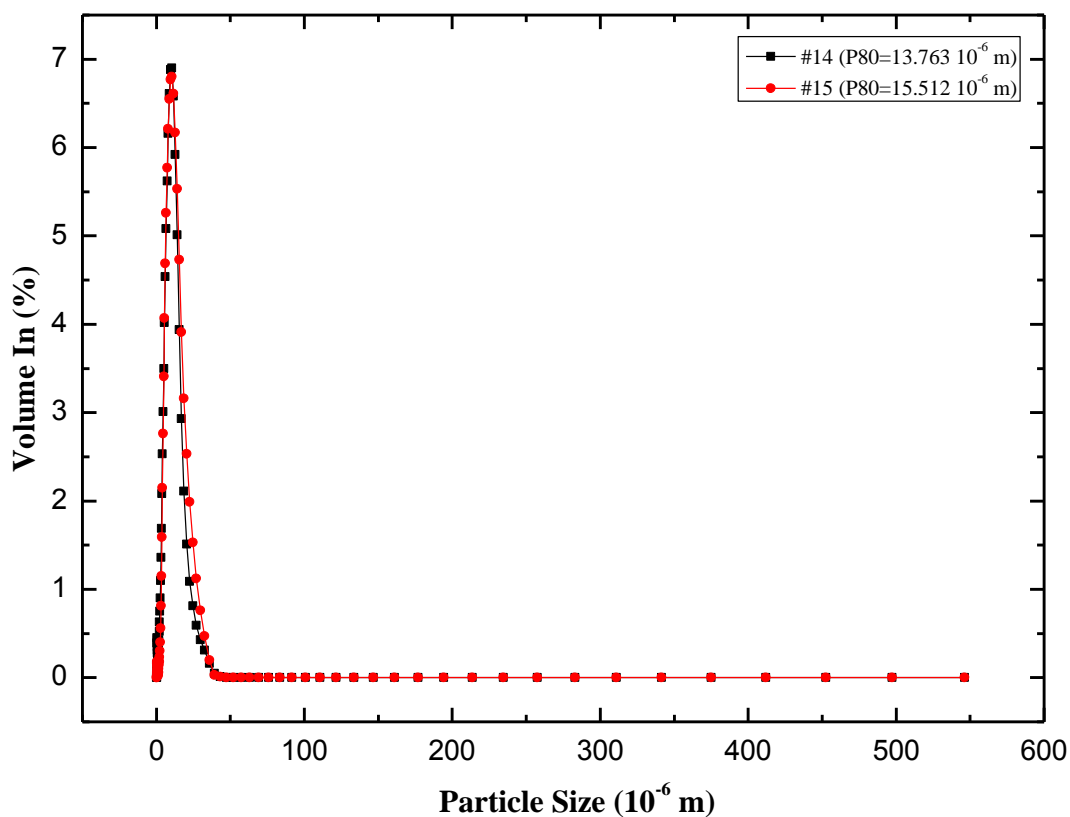


FIGURE 5.5 PSD RESULT FOR EFFECT OF HYDROCHLORIC ACID FLOW RATE ON THE PRECIPITATION OF AS₂S₃ FROM AS₂O₃-NA₂S SOLUTION

The EDX result and PSD result showed similar chemical composition and particle size distribution. Thus, the effect of hydrochloric acid solution addition rate was not significant.

5.2.4 Effect of aging time

The aging time after the reaction was also varied: 2 h, 8 h, and 24 h aging times were applied. The EDX and PSD results are shown in Table 5.4.

Table 5.4 EDX result for effect of aging time

Experiment #	Temperature (°C)	[Na ₂ S] (M)	[HCl] (M)	Flow rate (ml/min)	Equilibrium time (h)	EDX	
						As wt%	S wt%
16	50	0.1	1	3.2	2	59.50	40.50
17	50	0.1	1	3.2	8	52.63	47.37
18	50	0.1	1	3.2	48	58.84	41.16

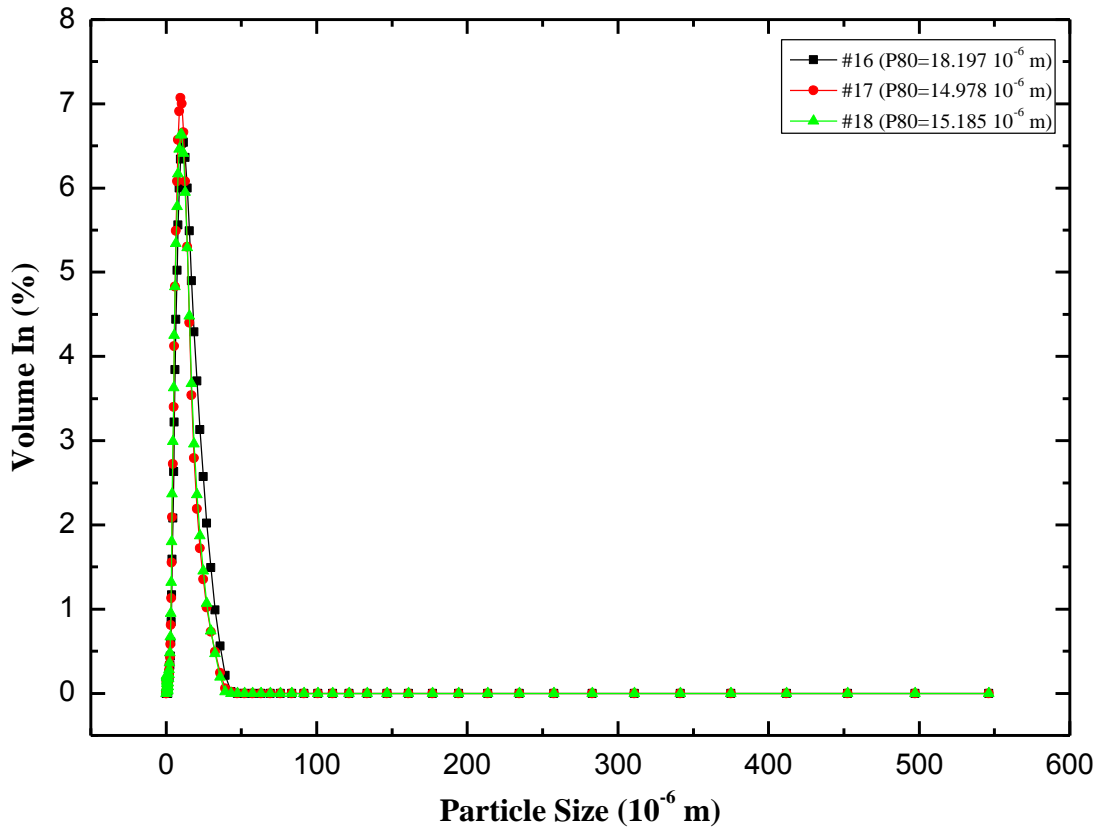


FIGURE 5.6 PSD RESULT FOR As_2S_3 SAMPLES OBTAINED BY VARYING AGING TIME

Experiments #16 and #18 had the closest chemical composition to the theoretical composition of arsenic tri-sulfide. All three experiments had similar PSDs with a concentrated particle distribution around $15 \mu m \sim 18 \mu m$. In conclusion, the aging time should be short (2 hours) or very long (48 hours) so that an ideal result in terms of chemistry can be achieved.

5.3 Solubility of As_2S_3 in Na_2S solution

Figure 5.7 presents the solubility of As_2S_3 in Na_2S solution as predicted by OLI systems software and as measured. According to OLI, arsenic tri-sulfide dissolves linearly

with the concentration of sodium sulfide. Temperature has almost no influence on the solubility.

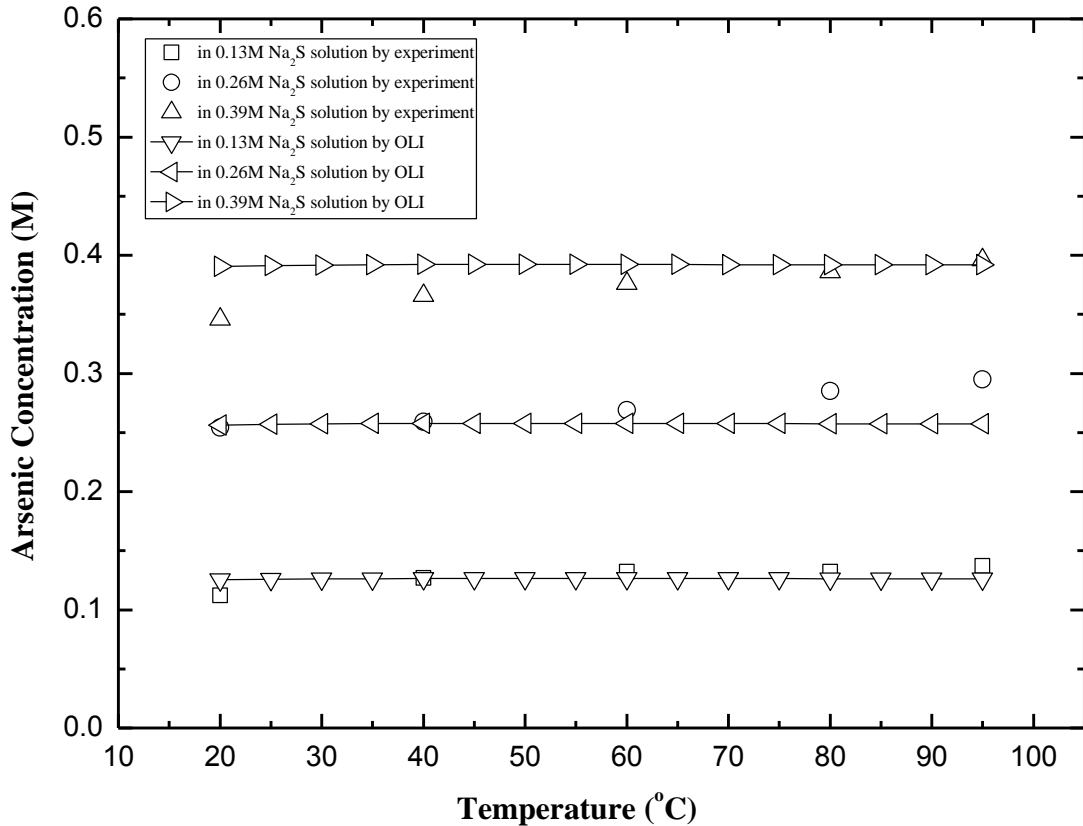


FIGURE 5.7 PREDICTED (OLI SOFTWARE) AND EXPERIMENTAL SOLUBILITY OF As_2S_3 IN Na_2S SOLUTIONS

Generally, experimental data for the solubility of As_2S_3 agrees well with the predicted solubility by the OLI systems software. The solubility of arsenic tri-sulfide is about 0.11 M (1 wt% Na_2S solution), 0.25 M (2 wt% Na_2S solution), and 0.35 M (3 wt% Na_2S solution) at 20 °C, and increases to 0.14 M (1 wt% Na_2S solution), 0.29 M (2 wt% Na_2S solution), and 0.39 M (3 wt% Na_2S solution) at 95 °C. The obvious difference between predicted solubility and experimentally measured solubility is the effect of temperature. Temperature increments did modestly improve the measured solubility of arsenic tri-sulfide. The effect of sodium

sulfide concentration is generally consistent between the model and measurements shown here. The solubility of amorphous As_2S_3 linearly increases with the concentration of sodium sulfide solution.

Referring to the data of Weissberg (1966); the solubility of synthetic crystalline As_2S_3 is 0.4280 M at 52 °C and 0.4309 M at 100 °C in 3.43 wt% Na_2S solution. The solubility of amorphous As_2S_3 can be predicted from our work (using the assumption of a linear relationship between Na_2S concentration and As_2S_3 solubility) as 0.4046 M at 20 °C, 0.4216 M at 40 °C, 0.4335 M at 60 °C, 0.4493 M at 80 °C, and 0.4612 M at 95 °C in 3.43 wt% sodium sulfide solutions. Compared with the Weissberg data presented these values are reasonably close.

5.4 Characterization of synthetic crystalline products

5.4.1 Attempts to synthesize sodium arsenic oxy-sulfide from sodium arsenate precursor

Synthetic sodium arsenate was synthesized first and analyzed by EDX (cf. Table 5.5). This complex was then used for sodium arsenic oxy-sulfide complex synthesis.

Table 5.5 Elemental analysis of synthetic sodium arsenate by EDX

Element	Concentration (wt %)
Oxygen	41.56
Sodium	20.34
Arsenic	38.10

Synthetic crystal #1, #2, and #3 were synthesized by using sodium sulfide solution, solid sodium sulfide, and hydrogen sulfide gas, respectively. They were analyzed by EDX for elemental composition and these data are presented in Table 5.6.

Table 5.6 EDX analysis for synthetic crystal #1, #2, and #3

Sample	Sodium (wt%)	Arsenic (wt%)	Oxygen (wt%)	Sulfur (wt%)
Synthetic crystal #1	20.38	34.10	45.10	0.43
Synthetic crystal #2	27.33	10.67	47.27	14.73
Synthetic crystal #3	23.12	31.27	40.60	5.02

Comparing the EDX results of these three synthetic crystals, sodium sulfide solution is not a good choice for the replacement of oxygen by sulfur in sodium arsenate, because the sulfur content in crystal #1 is very low (0.43 %). However, for crystal #2 and #3, the oxygen in the original sodium arsenate is replaced by sulfur from solid Na₂S or H₂S gas to some extent.

Synthetic sodium arsenate (cf. Table 5.5 and Figure 5.8) and product #3 (cf. Table 5.6 and Figure 5.9) were characterized by QXRD, but an unknown crystalline phase (not in the database) was detected for both samples. For synthetic sodium arsenate, there was only a minor amount of this unknown crystalline phase; but for synthetic product #3, the unknown crystalline phase was the main species. Thus we can only estimate the chemical composition of these synthetic products by EDX for O:S ratio and ICP for arsenic content.

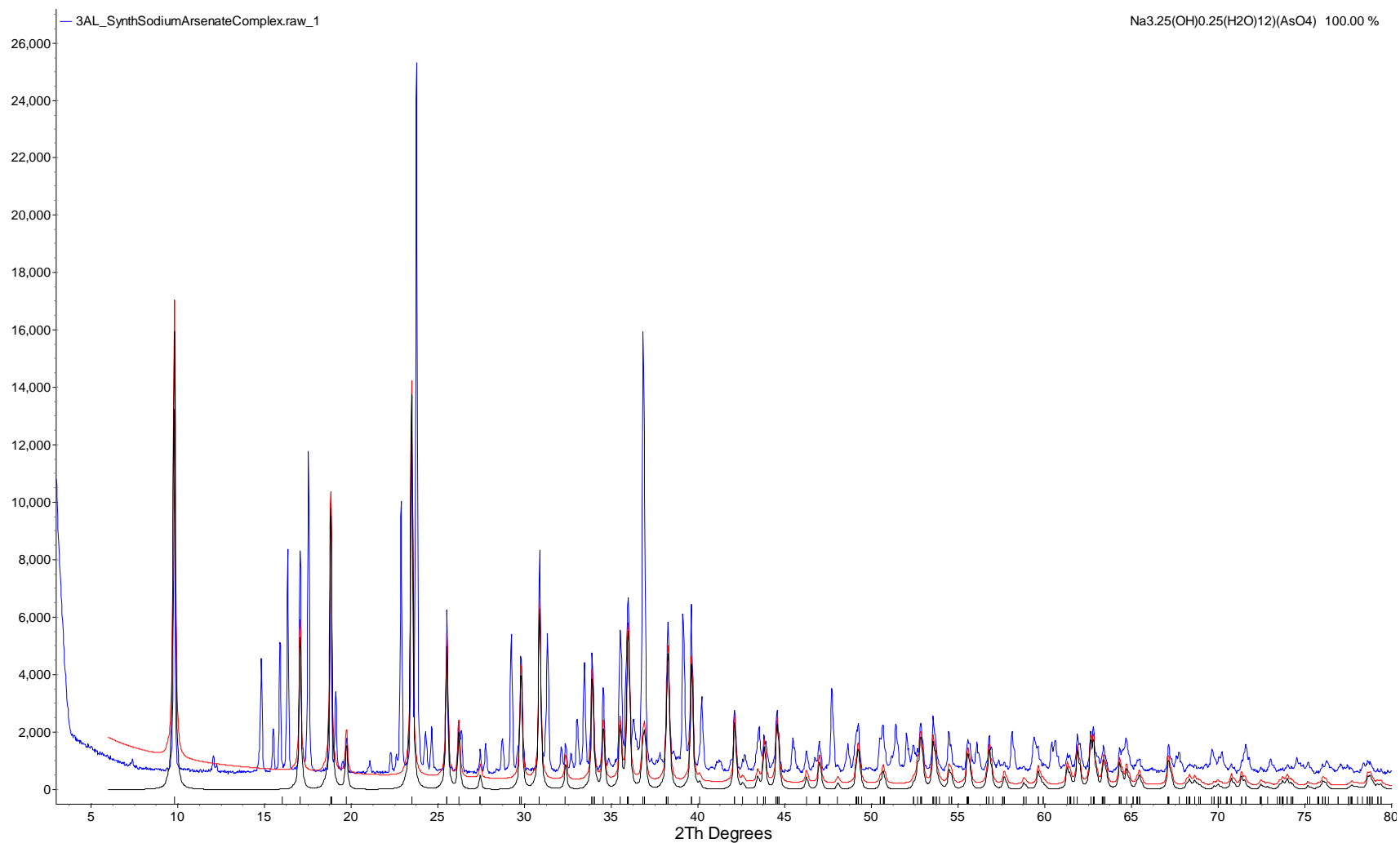


FIGURE 5.8 RIETVELD REFINEMENT PLOT OF SAMPLE “SYNTHETIC SODIUM ARSENATE” (BLUE LINE - OBSERVED INTENSITY AT EACH STEP; RED LINE - CALCULATED PATTERN; SOLID GREY LINE BELOW - DIFFERENCE BETWEEN OBSERVED AND CALCULATED INTENSITIES; VERTICAL BARS - POSITIONS OF ALL BRAGG REFLECTIONS). COLOURED LINES ARE INDIVIDUAL DIFFRACTION PATTERNS OF ALL PHASES

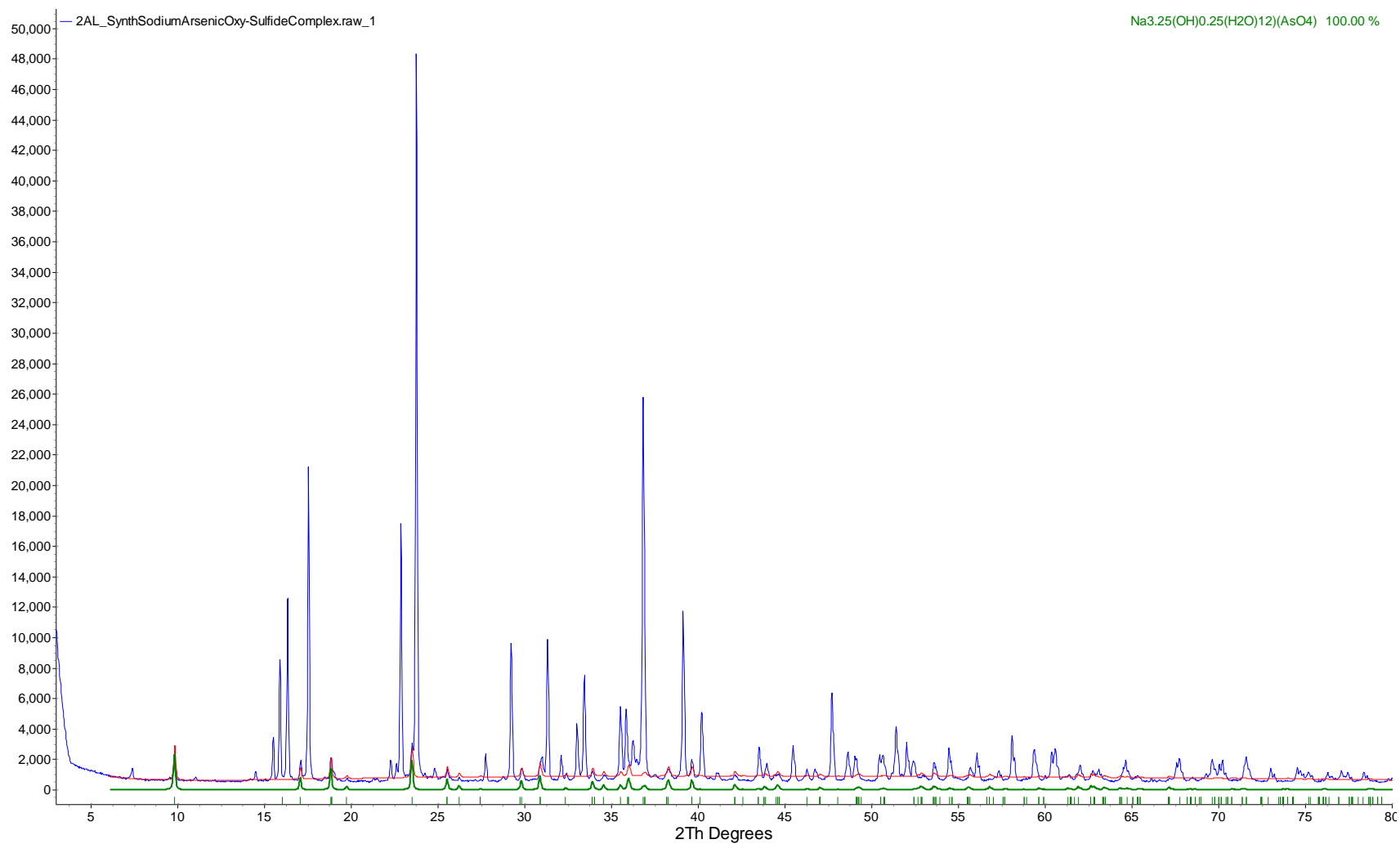


FIGURE 5.9 RIETVELD REFINEMENT PLOT OF SAMPLE “SYNTHETIC PRODUCT #3” (BLUE LINE - OBSERVED INTENSITY AT EACH STEP; RED LINE - CALCULATED PATTERN; SOLID GREY LINE BELOW - DIFFERENCE BETWEEN OBSERVED AND CALCULATED INTENSITIES; VERTICAL BARS - POSITIONS OF ALL BRAGG REFLECTIONS). COLOURED LINES ARE INDIVIDUAL DIFFRACTION PATTERNS OF ALL PHASES

5.4.2 Synthesis of sodium thioarsenate by reaction of As₂S₃ with elemental sulfur

Precipitate #4 showed the highest elemental sulfur content of all the synthetic sodium thioarsenate-type precipitates (cf. Table 5.7). Precipitate #4 was also characterized by QXRD for quantitative phase determination, as shown in Table 5.8 and Figure 5.10. Both Table 5.8 and Figure 5.8 show that a relatively pure crystal of sodium thioarsenate was produced.

Table 5.7 Elemental analysis of synthetic crystalline precipitate #4 by EDX

Element	Concentration (wt %)
Sodium	16.4
Sulfur	48.5
Arsenic	35.1

Table 5.8 QXRD result and crystal parameters of synthetic sodium thio-arsenate

Phase name	Synthetic	Standard parameters
	Na ₃ AsS ₄ · 8H ₂ O	in database
Space group	P121/c1	P121/c1
Cell volume (Å ³)	1506.04(5)	1490.65
Purity (wt%)	100.000	100.000
Crystal density (g/cm ³)	1.765	1.85
Lattice parameters		
a (Å)	8.6927(2)	8.651(3)
b (Å)	12.9878(2)	12.995(4)
c (Å)	13.7126(2)	13.596(5)
Beta (°)	103.393(1)	102.77(7)

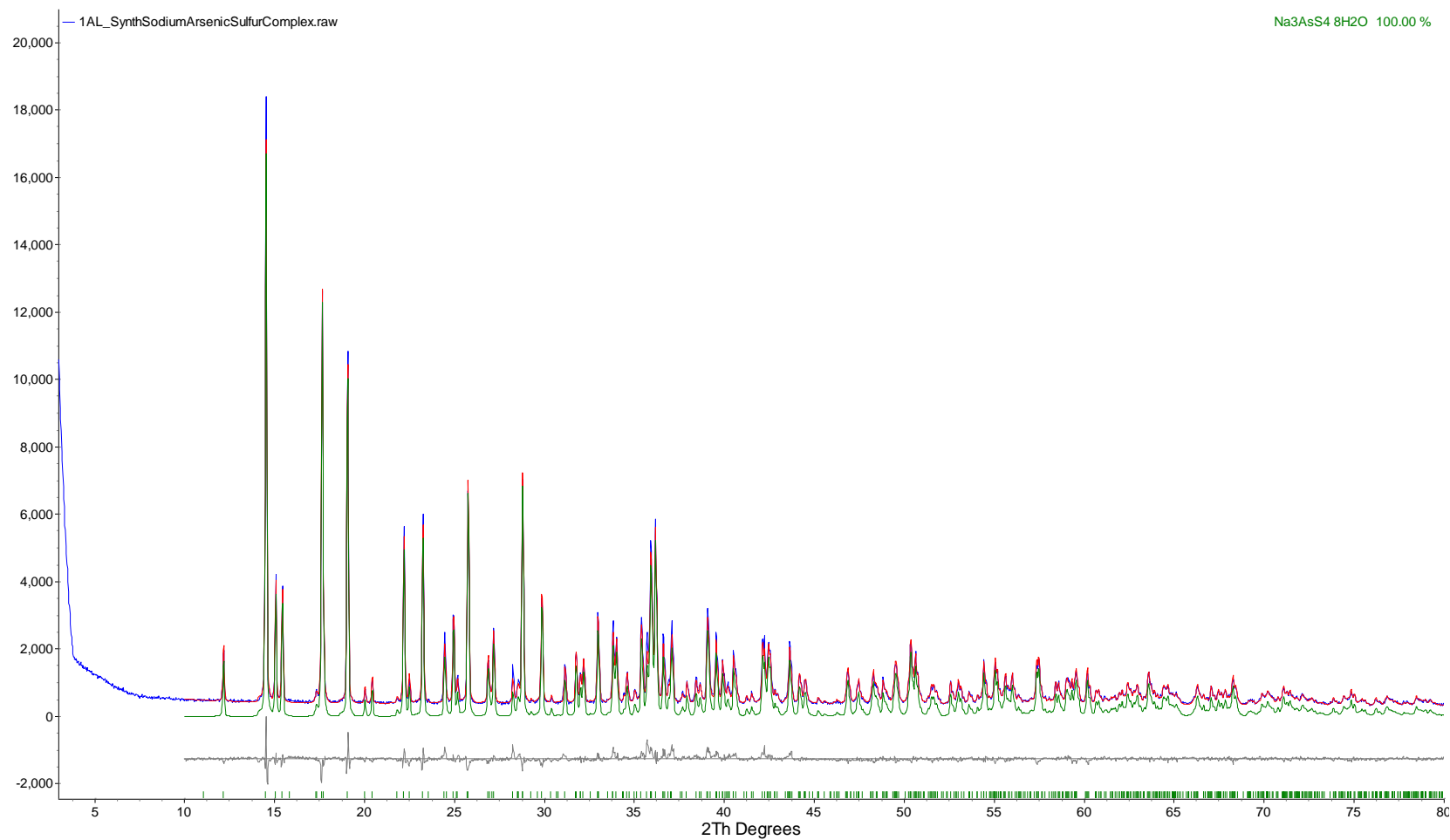


FIGURE 5.10 RIETVELD REFINEMENT PLOT OF SAMPLE “SYNTHETIC SODIUM THIO-ARSENATE, PRODUCT #4” (BLUE LINE - OBSERVED INTENSITY AT EACH STEP; RED LINE - CALCULATED PATTERN; SOLID GREY LINE BELOW - DIFFERENCE BETWEEN OBSERVED AND CALCULATED INTENSITIES; VERTICAL BARS - POSITIONS OF ALL BRAGG REFLECTIONS). COLOURED LINES ARE INDIVIDUAL DIFFRACTION PATTERNS OF ALL PHASES.

5.4.3 Arsenic content determination by ICP analysis

The synthetic precipitates #2, #3, and #4 were analyzed by EDX and QXRD (sodium thio-arsenate), but neither of these methods can give an exact bulk arsenic concentration. Hence, for each synthetic crystalline complex, one gram of the solid was dissolved in one liter of DI water. The average arsenic content was then measured by ICP-OES (detection range for ICP analysis: 0.2 ~ 10000.0 mg/L) as shown in Table 5.9:

Table 5.9 ICP analysis for arsenic content in precipitates #2, 3 and 4

Sample	As (mg/L) 2 g of precipitate in 1 L	As (wt%)	
		wt% in the solid by calculation from ICP solution assay	As (wt%) by EDX
Synthetic crystal #2	161.7	8.1	10.7
Synthetic crystal #3	377.8	18.9	31.3
Synthetic crystal #4	367.5	18.4	35.1

The theoretical concentration of As in sodium thio-arsenate octa-hydrate ($\text{Na}_3\text{AsS}_4 \cdot 8\text{H}_2\text{O}$) is 18.03%. Thus, according to QXRD and ICP results, the chemical and structural composition of synthetic sodium thio-arsenate, product #4, is very pure. For synthetic crystals #2 and #3, no valid QXRD spectra were obtained indicating that the precipitates were amorphous. Compared with the As concentration by ICP, the As concentration by EDX is much higher for all three crystals. This is because during EDX analysis crystalline water was likely lost due to evaporation in the vacuum chamber of the microscope. For products #2 and #3, the degree of hydration cannot be determined by drying because they are very stable at room temperature and melt at around 60 ~ 80 °C. Hence, their crystalline water number are estimated as 12.5 (24.3%) and 8.7 (39.5%) according to the As concentration determined by ICP and EDX.

5.5 Solubility of synthesized sodium thio-arsenate products

5.5.1 Sodium arsenate precursor synthesized by oxidation of As (III) with hydrogen peroxide

5.5.1.1 Sodium thio-arsenate synthesized by the addition of sodium sulfide solution to dissolved sodium arsenate precursor (product #1)

Since the content of sulfur and arsenic in precipitate #1 is very low, it was not used for the determination of solubility.

5.5.1.2 Sodium thio-arsenate synthesized by the addition of solid sodium sulfide to dissolved sodium arsenate precursor (product #2)

The solubility of synthetic crystal #2 is presented in Figure 5.9. Since there's no valid QXRD result, water content cannot be determined quantitatively. Instead, the degree of hydration is calculated by comparison of EDX (without crystalline water) and ICP (with crystalline water). There are 24.3 wt% of water in crystal #2 by theoretical calculation, which might be higher than the real water content by compare with crystal #4 (sodium thio-arsenate). Thus, the solubility of synthetic crystal #2 will be slightly lower than the exact solubility data.

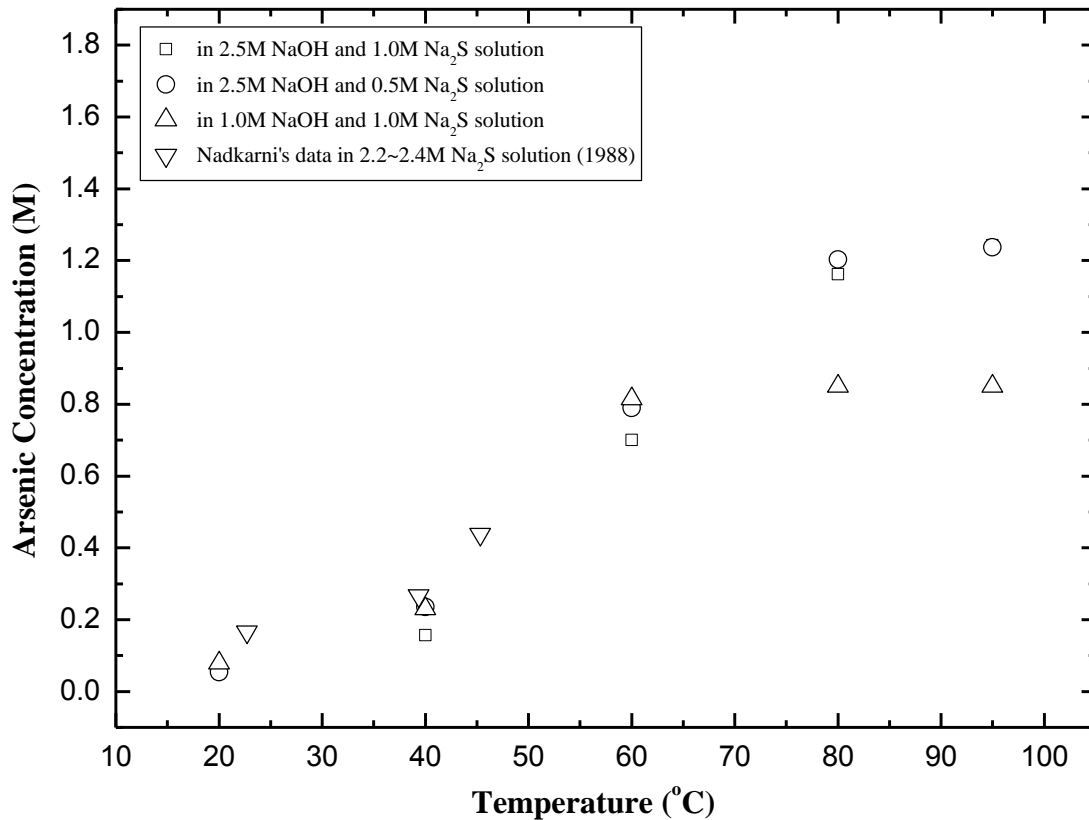


FIGURE 5.11 SOLUBILITY OF SYNTHETIC PRODUCT #2 IN SODIUM HYDROXIDE AND SULFIDE SOLUTIONS EXPOSED TO AMBIENT AIR

Compared with Nadkarni and Kusik's data in 2.2 ~ 2.4 M sodium sulfide solution, the solubility of synthetic crystal #2 is a little lower than that of Na_3AsS_4 by Nadkarni and Kusik (1988) in Na_2S solution. As temperature is increased, the solubility of synthetic crystal #2 increases quickly from 0.05 M (20 °C) up to 1.25 M (95 °C) in 2.5 M NaOH and 0.5 M/1.0 M Na_2S solution. In 1.0 M NaOH and 1.0 M Na_2S solution, the solubility of synthetic crystal #2 is slightly greater than for the other two concentration conditions in the range of 20 °C to 60 °C, and then reaches a saturation point (of ~ 0.85 M As) at 80 °C.

5.5.1.3 Sodium thio-arsenate synthesized by the addition of hydrogen sulfide to dissolved sodium arsenate precursor (product #3)

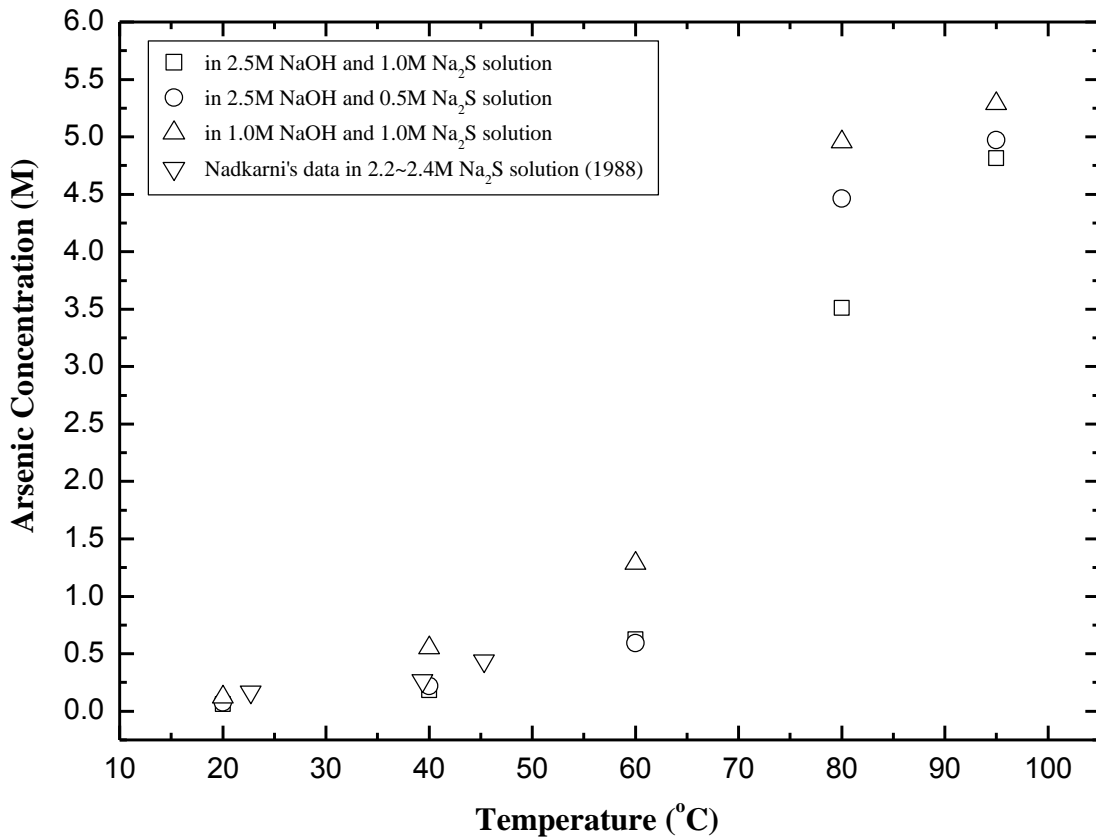


FIGURE 5.12 SOLUBILITY OF SYNTHETIC PRODUCT #3 IN SODIUM HYDROXIDE AND SULFIDE SOLUTIONS EXPOSED TO AMBIENT AIR

The water content in crystal #3 was estimated to be 39.5%. Since this estimate may result in error, it is possible that the actual solubility for As may be slightly higher than the experimental data presented in Figure 5.12.

The solubility of synthetic crystal #3 in 2.5 M NaOH and 0.5 M/1.0 M Na₂S solution fit very well with the solubility of “Na₃AsS₄” reported by Nadkarni and Kusik in 2.2 ~ 2.4 M sodium sulfide solution. Thus, there is a possibility that the sodium thioarsenate mentioned by Nadkarni and Kusik (1988) from enargite leaching in sodium hydroxide (0.25 M) and sulfide (2.2 ~ 2.4 M) solution is in fact a sodium arsenic oxy-sulfide complex, rather than stoichiometric sodium thio-arsenate.

5.5.2 Synthesis of thio-arsenate by oxidation of As (III) with elemental sulfur

5.5.2.1 Solubility of sodium thio-arsenate (product #4) in leach solution under air atmosphere and argon atmosphere

The solubility of sodium thio-arsenate was first measured in air. To assess the degree of polysulfide interference, the same solubility experiments were repeated under argon atmosphere.

The sulfide and hydrosulfide ions may act as reducing agents for As (V), after the dissolution of Na_3AsS_4 in NaOH and Na_2S solution. Since the solubility of As (III) is greater than As (V), the reduction of As (V) to As (III) should be accompanied by an increase in measured solubility.

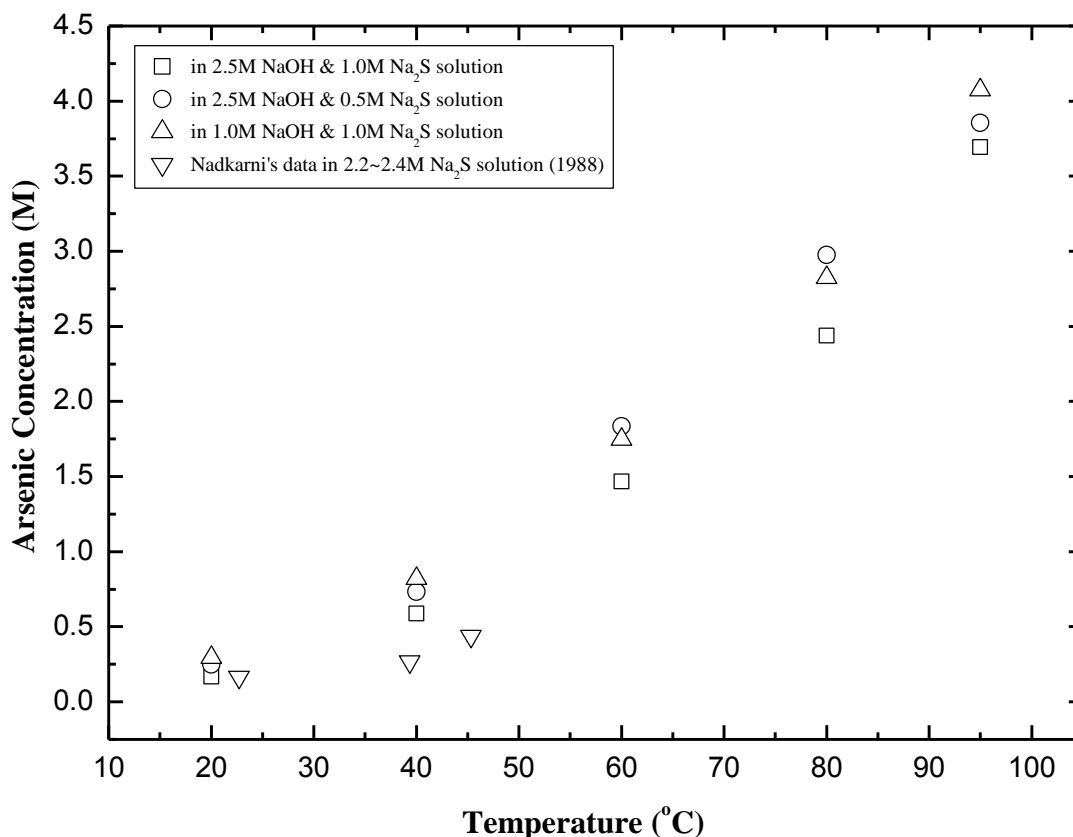


FIGURE 5.13 SOLUBILITY OF PRODUCT #4 (SODIUM THIO-ARSENATE ($\text{Na}_3\text{AsS}_4 \cdot 8\text{H}_2\text{O}$)) IN SODIUM HYDROXIDE AND SULFIDE SOLUTION EXPOSED TO AMBIENT AIR

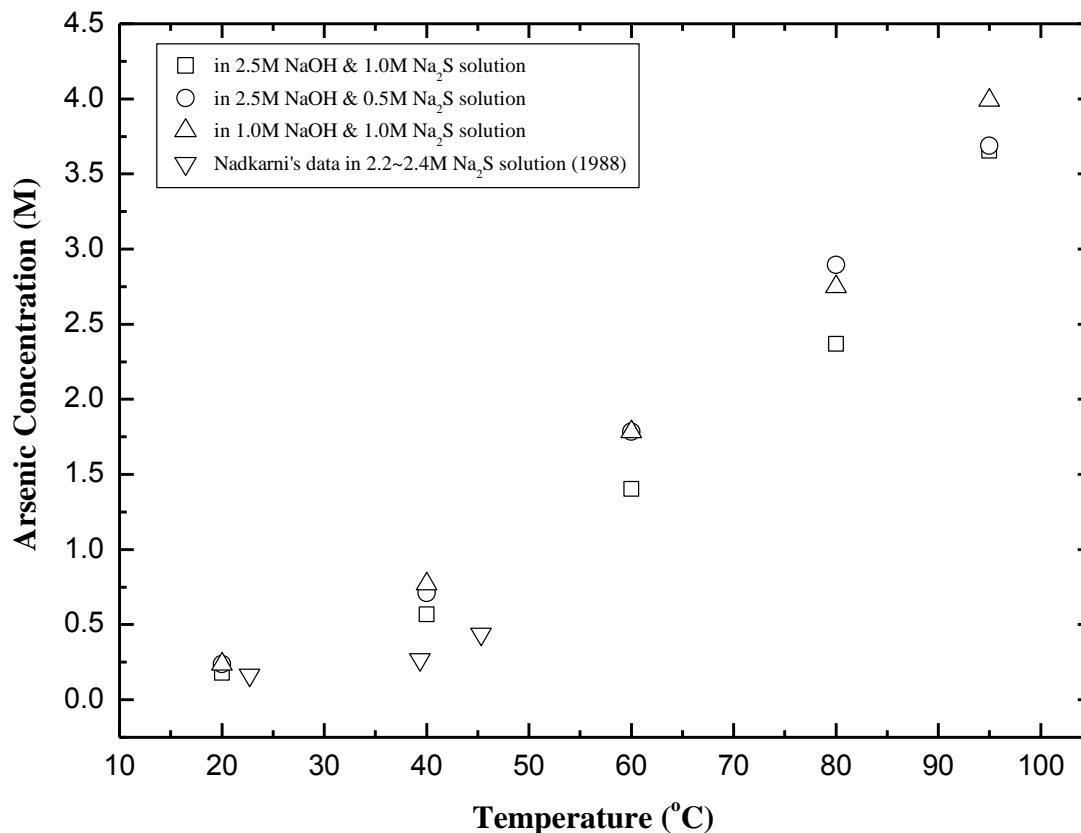


FIGURE 5.14 SOLUBILITY OF PRODUCT #4 (SODIUM THIOARSENATE ($\text{Na}_3\text{AsS}_4 \cdot 8\text{H}_2\text{O}$)) IN SODIUM HYDROXIDE AND SULFIDE SOLUTION IN ARGON ATMOSPHERE

After comparison, the solubility data of synthetic sodium thioarsenate under air and argon atmospheres are very close. Thus, the oxygen in the air does not affect the crystal dissolution much. This may indicate that negligible amounts of sulfide or hydrosulfide were oxidized to elemental sulfur, which means that almost all of arsenic in the solution exists as As (V). Thus the solubility experiments should theoretically be accurate.

Rochette et al. (2000) found that in an acidic environment ($\text{pH} \sim 4$), reduction of As (V) to As (III) by sulfide is a rapid process, with a rate constant of $3.2 \times 10^2 \text{ M/h}$. However, for the conditions used here, the solution pH is well above 13, and S^{2-} and HS^- are highly stable. Thus the oxidation of S^{2-} to S^0 and the attendant increase in measured solubility is likely not a problem for our work.

By comparison, Nadkarni and Kusik's Na_3AsS_4 solubility data is ~ 55 % lower than the experimental data at 40 °C for synthetic $\text{Na}_3\text{AsS}_4 \cdot 8\text{H}_2\text{O}$ (product #4) presented here. According to Figure 5.10 above and the QXRD analyses from enargite leaching tests presented in Table 5.11, a possible explanation for this is that Nadkarni and Kusik is actually reporting the solubility of a mixture of sodium arsenic oxy-sulfide complexes.

The solubility of synthetic sodium thioarsenate (product #4) grows rapidly from around 0.17 M at 20 °C to almost 4.0 M at 95 °C. Hence, based on solubility data, about 93.75% of synthetic sodium thio-arsenate can be separated from solution by cooling, which means that near quantitative arsenic removal from the leach solution can be achieved. However, it was observed through the course of this study that if the arsenic concentration in solution is too high, the solution can become a solid or gel-like material after cooling. According to Tongamp et al., (2010), an initial As concentration of 0.51 ~ 0.79 M can fall to 0.18 ~ 0.26 M through cooling from 90 °C to 30 °C, thus reaching 60% ~ 73% As removal (note that the current study cooled to 20 °C). Thus there should be an ideal high temperature As concentration point where high arsenic removal is obtained but also where gel-formation is avoided.

5.5.2.3 Solubility of synthetic crystal #4 (sodium thio-arsenate) at constant hydroxide (2.5 M/100 g/L) and varying hydrosulfide content (0 M ~ 1.0 M/0 ~ 56 g/L) in argon

To study the solubility of sodium thio-arsenate with increasing hydrosulfide concentration, several experiments were done in solutions with constant sodium hydroxide concentrations (2.5 M) at different temperatures.

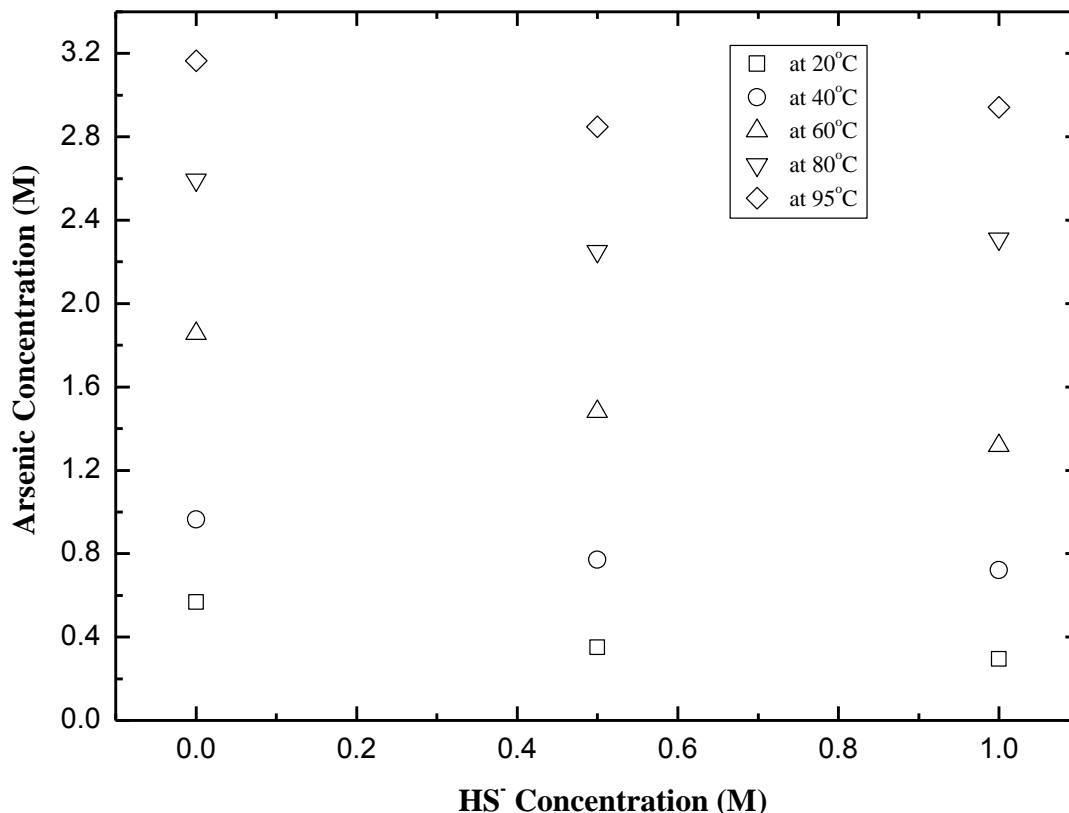


FIGURE 5.15 SOLUBILITY OF SODIUM THIO-ARSENATE (PRODUCT #4, $\text{Na}_3\text{AsS}_4 \cdot 8\text{H}_2\text{O}$) IN CONSTANT SODIUM HYDROXIDE (2.5 M) AND VARYING HYDROSULFIDE CONCENTRATION (0 ~ 1.0 M) SOLUTIONS IN ARGON ATMOSPHERE

As seen from Figure 5.13, there is an obvious decrease in solubility as hydrosulfide concentration is increased, especially at lower temperature 20 ~ 60 °C. By increasing the total solute in the original solution, it is likely that the common ion effect results in lower sodium thio-arsenate solubility. A similar trend was found in the previous solubility experiments for products #3 and #4 ($\text{Na}_3\text{AsS}_4 \cdot 8\text{H}_2\text{O}$) in sodium hydroxide and sulfide solutions. For example, the solubility of products #3 and #4 is higher in 1.0 M NaOH and 1.0 M Na_2S solution than in 2.5 M NaOH and 1.0 M Na_2S solution. To verify this assumption, Tongamp's (2010) experimental data are presented with ours in Figure 5.14. Tongamp's data appears to maintain the trend of lowering solubility as HS^- concentration increases although a plateau does appear to exist around 0.2 M As.

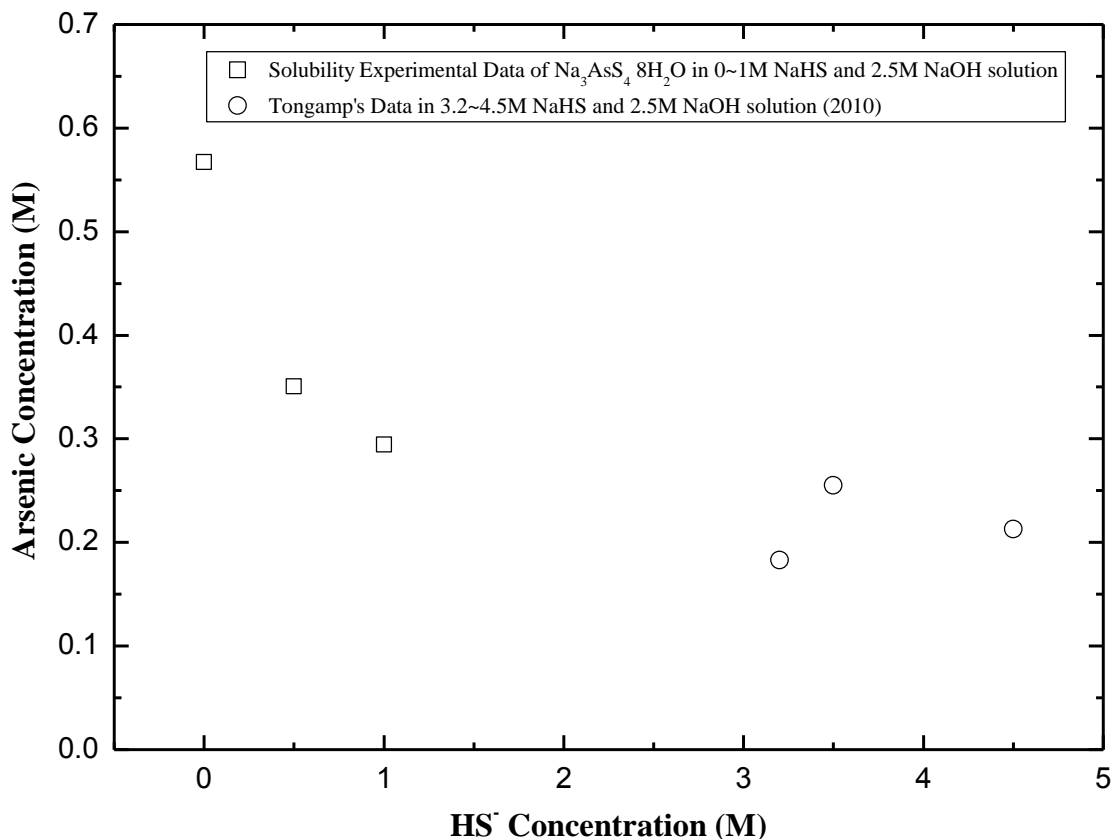


FIGURE 5.16 THE SOLUBILITY OF SODIUM THIO-ARSENATE IN CONSTANT HYDROXIDE AT 20 °C (2.5 M NaOH) AND VARYING HYDROSULFIDE SOLUTION COMPARED WITH THAT OBTAINED BY TONGAMP ET AL. (2010) AT 30 °C

For all three synthetic complexes (#2, #3 and #4), solubility increases with temperature. The main difference observed is the importance of the temperature effect which is, from low to high: crystal #2 < crystal #4 (sodium thio-arsenate) < crystal #3. Compared with Nadkarni and Kusik's solubility data for "Na₃AsS₄", the best agreement with the experimental data presented herein is for the solubility of synthetic crystal #3 (also #2 to some extent) between 20 °C to 45 °C. In contrast, the solubility of relatively pure synthetic sodium thio-arsenate (product #4) is obviously greater than that presented by Nadkarni and Kusik. The QXRD results of the arsenic precipitate obtained after cooling of solution used for enargite leaching (refer to Chapter 5.7), show that the "industrial" precipitate should be a mixture of sodium arsenic oxy-sulfide complexes (Na₃AsO₂S₂, Na₃AsOS₃, and Na₃AsO₃S etc.). Hence, the solubility of synthetic crystal #3, instead of pure sodium thio-arsenate, appears to be a better reference for the solubility of arsenic in ASL solutions.

5.6 Solubility accuracy calibration test

Two solubility tests were done for solubility accuracy calibration, and the two conditions are: in 2.5M NaOH & 1.0M Na₂S at 20 °C under argon atmosphere (experiment a.) and in 2.5M NaOH & 0.5M NaHS at 60 °C under argon atmosphere (experiment b.). When the solution was determined to be saturated according to visual observation, the first solution sample was taken and diluted 500 times in DI water. Then, after equilibration overnight (more than 12 hours), the second sample was taken in the same way. The four solution samples were sent for ICP analysis and the results are shown in Table 5.9.

Table 5.10 Solubility data for accuracy calibration

Experiment	As Conc. determined by visual inspection (M)	As Conc. in 1 st sample by ICP (M)	As Conc. in 2 nd sample by ICP (M)
a	0.178	0.169	0.179
b	1.482	1.275	1.332

According to Table 5.9, the solubility data achieved by visual observation (which involves calculation of dissolved arsenic based on the mass of sample added) and by ICP of solutions both at the time of visual saturation and after overnight exposure are reasonably close. Since the error obtained between the visual saturation method and the 1st sample ICP measurement is actually larger than that obtained when comparing visual inspection with the 2nd sample (overnight saturation), the error in the methodology lies not in the ability to “see” the point of saturation but rather in the ability to generate a completely homogenous head sample or to get reproducible assays.

5.7 Solubility of As in ASL solutions originating from an enargite leaching test

The enargite concentrate was leached in 2.5 M NaOH and 0.5 M Na₂S solution at 95 °C for 24 hours, but very low arsenic content was detected by ICP analysis of the crystallite obtained after cooling of the solution (Table 4.9). This was initially thought to be due to speciation i.e. that the As was preferentially speciated as As (III) instead of As (V). Thus elemental sulfur was added into solution portion a. (with ½ of the crystallites also added to the solution) and solution portion b. (no crystal) at 90 °C with the intention of complete

oxidation of arsenic in the leach solution. However, upon cooling of this “oxidized” solution, still no crystalline precipitate was obtained. The Arsenic concentration determined by ICP analysis of solutions a. and b. is presented in Table 5.10.

Table 5.11 Arsenic concentration of solution a. and b. by ICP

Sample	As conc. (g/L)	As conc. (M)	Volume (L)	As mass (g)
a.	38.5	0.51	0.35	13.48
b.	29.9	0.40	0.35	10.47

According to elemental and phase analyses of the concentrate, the total arsenic in the head sample was 28.32 g. Referring to the ICP results in Table 5.10, the arsenic in the crystals and in the leach solution were 6.02 g $((13.48 - 10.47) \times 2)$ and 20.93 g, respectively. Thus, the arsenic extraction during leaching was approximately 95.16%.

The reason why no precipitate was observed, even after oxidation, may be gleaned from the solubility data presented above. The solubility of synthetic product #4 at room temperature is around 0.25 M As (cf. Figure 5.11 and Table A-14) in 2.5 M NaOH and 0.5 M Na₂S solution. However, much of the sodium hydroxide and sulfide is consumed during leaching, which can increase the arsenic solubility such as in 1.0 M NaOH and 1.0 M Na₂S solution (cf. Figure 5.10 and Table A-12). It seems likely, then, that the 0.4 M As concentration (Table 5.10) was below the solubility limit (which was apparently above 0.51 M As here) for this particular ASL solution. This is corroborated to a certain extent by Tongamp et al. (2010) who mention that it is necessary to increase the arsenic concentration to at least > 35 g/L or 0.47 M in 50 ~ 250 g/L or 0.89 ~ 4.46 M NaHS and 50 ~ 100 g/L or 1.25 ~ 2.5 M NaOH solution before precipitation by cooling.

The nature of the crystallite is also clearly important. The crystallite analyzed in Table 5.10 was found to be too unstable to analyze by QXRD and three other enargite leaching tests performed during this thesis in 3.9 M NaOH and Na₂S concentration varying from 0.34 to 0.86 to 1.72 M, revealed that the predominant crystallized As complex was found to be sodium arsenic oxide sulfide hydrate (Na₃AsO₂S₂ · 11H₂O) (Table 5.11), which represented 89.3%, 83.4%, and 87.1% of the crystalline phases (XRD-detectable) in the

precipitate, respectively. Sodium thio-arsenate was never detected. Hence, we can conclude that the arsenic precipitate that occurs after cooling of ASL solutions is a mixture of sodium arsenic oxy-sulfide complexes ($\text{Na}_3\text{AsO}_2\text{S}_2$, $\text{Na}_3\text{AsO}_3\text{S}$, Na_3AsOS_3 , and perhaps Na_3AsS_4), rather than only sodium thio-arsenate as previously reported in the literature (Nadkarni and Kusik 1988, Anderson et al 2008). It is also important to note that because the leaching system was exposed to an air atmosphere, carbon dioxide was likely involved in some of the reactions as it produced Trona ($\text{Na}_3\text{H}(\text{CO}_3)_2 \cdot 2\text{H}_2\text{O}$) in the precipitate. The leaching reactors in future work should be de-aerated to simulate industrial conditions where the surface to volume ration would be much lower.

Table 5.12 QXRD result for arsenic precipitate from enargite leaching tests (See XRD spectra in Appendix Figure C-1, 2, 3)

Phase	Ideal Formula	#1	#2	#3
		3.9M NaOH & 0.34 M Na_2S solution	3.9M NaOH & 0.86 M Na_2S solution	3.9M NaOH & 1.72 M Na_2S solution
Sodium Arsenic Oxide Sulfide Hydrate	$\text{Na}_3\text{AsO}_2\text{S}_2(\text{H}_2\text{O})_{11}$	89.3%	83.4%	87.1%
Sodium Sulfide Arsenate Hydrate	$\text{Na}_3\text{AsO}_3\text{S}(\text{H}_2\text{O})_7$	4.1%	0.6%	1.0%
Sodium Aluminum Silicate Hydrogen Carbonate Hydrate	$\text{Na}_{7.67}(\text{Al}_6\text{Si}_6\text{O}_{24})(\text{HCO}_3)(\text{CO}_3)_{0.5}(\text{H}_2\text{O})_{4.19}$	2.6%	4.8%	4.2%
Arsenolite	As_2O_3	0.5%	0.7%	0.7%
Trona	$\text{Na}_3\text{H}(\text{CO}_3)_2 \cdot 2\text{H}_2\text{O}$	3.5%	10.5%	6.9%
Total		100.0%	100.0%	99.9%

For the three enargite leaching tests presented in Table 5.11, the arsenic concentration in solution was around 58.5 g/L (0.78 M). Compared with the measured solubility of

products #2, #3, and #4, the As concentration in these ASL solutions (~ 0.78 M) is above the highest arsenic solubility (0.57 M) at room temperature (solubility of As from synthetic $\text{Na}_3\text{AsS}_4 \cdot 8\text{H}_2\text{O}$ in 2.5 M NaOH solution in Table A-21). Thus to precipitate arsenic from ASL solutions, we need to increase the arsenic concentration above the arsenic saturation point at room temperature for the synthetic solutions tested in this work. This finding may be related, as discussed above, to the amount of sodium hydroxide and sulfide that remains unreacted after leaching.

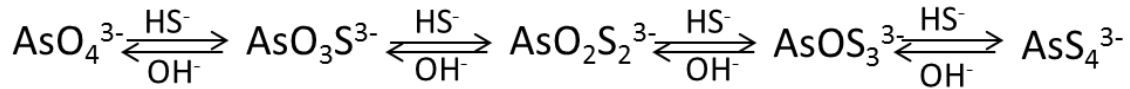
In aggregate, these data indicate that solubility studies of “pure” crystallites in simulated solutions (such as those reported here) can only yield order of magnitude estimates of what one might expect to see in an industrial process. The chemistry of the ASL is so complicated that As solubility almost certainly has to be determined on a case by case basis.

Chapter 6 Conclusion

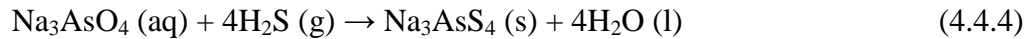
1. The optimum conditions for As_2S_3 synthesis are low concentration of sodium sulfide (0.1 M) and hydrochloric acid (1M), temperatures of $40\text{ }^\circ\text{C} \sim 60\text{ }^\circ\text{C}$, and long aging time.
2. The solubility of synthetic amorphous arsenic tri-sulfide in sodium sulfide solution increases linearly with the concentration of sodium sulfide, but changes only slightly with temperature.
3. A good way to synthesize sodium arsenic oxide sulfide complexes is to add solid sodium sulfide or purge hydrogen sulfide gas into sodium arsenate solution, but it is difficult to control the O:S ratio in the final product.
4. Relatively pure sodium thio-arsenate crystals can be synthesized by dissolving amorphous As_2S_3 in sodium sulfide solution with the addition of elemental sulfur at high temperature ($\sim 70\text{ }^\circ\text{C}$). After slowly cooling the solution, a cluster of faint yellow crystal is formed.
5. In sodium hydroxide and sulfide solutions, the solubility of synthetic sodium thio-arsenate increases dramatically with temperature, and a similar trend was found for the solubility of synthetic sodium arsenic oxide sulfide products. This gives an effective path to separate arsenic from leach solution.
6. There are two ways to enhance the crystallization of the arsenic precipitate: increase the sodium hydroxide and sodium sulfide concentrations or increase the arsenic concentration in leach solution before cooling.
7. According to the QXRD analyses of the arsenic precipitates resulting from cooling of ASL solutions, pure “sodium thio-arsenate” cannot be considered a likely crystallite in industrial processes. The precipitated complexes are comprised of sodium arsenic oxide sulfides ($\text{Na}_3\text{AsO}_2\text{S}_2$, Na_3AsOS_3 , and $\text{Na}_3\text{AsO}_3\text{S}$).
8. The ASL solutions originating from enargite leaching are able to maintain a certain degree of supersaturation over the solubilities measured in this work. However, direct comparison is difficult as each solution appears to generate a different type of crystallite.

Chapter 7 Future Work

A good way to decrease sulfide or hydrosulfide consumption during arsenic precipitation by cooling may be to increase the ratio of NaOH:Na₂S in the leach solution. Ongoing work at UBC has demonstrated that leaching in sub-stoichiometric sulphide solutions is possible. The crystalline arsenic precipitates would then be preferentially present as sodium arsenic oxy-sulfide species with a high O:S ratio. This may save money as in some jurisdictions sulphide is more expensive than hydroxide but this may also help to improve the recirculation of the sulfide source. Thus not only could more sulfides be recirculated, but more arsenic removal could be achieved due to the common ion effect.



This thesis provides some evidence to support the contention that the As oxy-sulfides are more stable than the sulphides. For example, in the case of sodium thioarsenate synthesis by method I, hydrogen sulfide gas was used according to the following anticipated reaction (4.4.4):



Sodium thioarsenate formation should have been more favorable in this case than when adding Na₂S as the sulphide source. However, EDX results showed that after complete reaction, the O:S ratio in the final product was still as high as 8:1. Moreover, in the three enargite leaching tests presented in Table 5.11 it was observed that the lowest molar O:S ratio was 1:1 (in Na₃AsO₂S₂(H₂O)₁₁) and that the product with a 3:1 O:S ratio (Na₃AsO₃S(H₂O)₇) was most prevalent as the OH⁻:S²⁻ ratio was highest. It seems reasonable, therefore, to suggest that a more systematic investigation of the process mass balance (leaching and crystallization) for low sulphide, high hydroxide, leaching be undertaken.

References

- Achimovičová M., Baláž M. and Sánchez M., 1998. Alkaline leaching of arsenic and antimony from enargite. *Acta Metallurgica Slovaca*, 4, 33 – 37.
- Anderson C. G., Twidwell L.G., 2008. Antimony, arsenic, gold, mercury and tin separation, recovery and fixation by alkaline sulfide hydrometallurgy. The Southern African Institute of Mining and Metallurgy: Lead and Zinc, 121-132.
- ATSDR, Agency for Toxic Substances and Disease Registry; Toxicological Profile for Arsenic. Update, 1998. U.S. Department of Health, Public Health Service, Atlanta.
- Babko A. K., Lisetskaya G.A., 1956. Equilibrium in reactions of formation of thiosalts of tin, antimony and arsenic in solution. *Zh. Neorg. Khim.*, 1, 969-980.
- Baláž, P., 2000. Extraction of antimony and arsenic from sulfidic concentrates. *Acta Montanistica Slovaca*, 3, pp. 265 – 268.
- Baltov I., Hristov N., Evtiminova K., Dontchev I., Kuzev L., 2008. Metallurgical challenges in the recovery of copper and gold from the Chelopech mine, Bulgaria. In: Proc. XXIVth International Minerals Processing Congress, 1785-1792.
- Bates M.N., Smith A.H., Hopenhayn-Rich C., *Am. J. Epidemiol.* 135 (1992) 462.
- Baxter K., Scriba H., and Vega I., 2010. Treatment of high-arsenic copper-gold concentrates- An options review. Proceedings of Copper 2010, Copper 2010, Hamburg, Germany, 1783-1802.
- Biltz W., 1907. Einige Versuche über ultramikroskopische Löslichkeits Bestimmung. *Z. Phys. Chem.*, 58, 288-292.
- Blom S., Lagerkvist B. and Linderholm H., 1985. Arsenic exposure to smelter workers: clinical and neurophysiological studies. *Scand. J. Work Environ. Health*, 11, 265-269.
- Chen C. J., Kuo T.L., Wu M.M., *Lancet* 1 (1988) 414.
- Church Holmes W., Coltrinari E.L., 1973. Process for removal of arsenic from sulfidic ore.
- Coltrinari E.L., 1977. Sodium sulfide leach process.
- Curreli, L., Garbarino, C., Ghiani, M., and Orrù, G., 2009. Arsenic leaching from a gold bearing enargite flotation concentrate. *Hydrometallurgy*, 96, pp. 258 – 263.
- Delfini, M., Ferrini, M., Manni, A., Massacci, P., and Piga, L., 2003. Arsenic leaching by Na₂S to decontaminate tailings coming from colemanite processing. *Minerals Engineering*, 16, pp. 45 – 50.
- Eary L. E., 1992. The solubility of amorphous As₂S₃ from 25 to 90 °C. *Geochim. Cosmochim. Acta*, 56, 2267-2280.

Filippou D., St-Germain P., Grammatikopoulos T.. Mineral Processing & Extractive Metall. Rev., 28 (2007) 247-298.

Floroiu R. M., Davis A.P., Torrents A., 2004. Kinetics and Mechanism of $As_2S_3(am)$ dissolution under N_2 . Environ. Sci. Technol., 42, 81-85.

Gulledge J. H., O'Connor J.T., J. AWWA (1973) 548.

Guo H.R., Chiang H.S., Hu H., Lipsitz S.R., Monson R.R., Epidemiology 8 (1997) 545.

Harris G. B., 2000. The removal and stabilization of arsenic from aqueous process solutions: past, present and future. Minor Elements: 3-20.

Helz G. R., Tossell J.A., Charnock J.M., Patrick R.A.D., Vaughan D.J., Garner D.C., 1995. Oligomerization in As (III) sulfide solutions: Theoretical constraints and spectroscopic evidence. Geochim. Cosmochim. Acta, 59, 4591-4604.

Helz G. R., Tossell J.A., 2008. Thermodynamic model for arsenic speciation in sulfidic waters; a novel use of ab initio computations. Geochim. Cosmochim. Acta, 72, 4457-4468.

Hindmarsh J. T., McCurdy R.F., Crit. Rev. Clin. Lab. Sci. 23 (1986) 315.

Holmes W C. Process for removal of arsenic from sulfo-ore: U.S. Patent 3,709,680. 1973.

Holmström A °, 1989. Removal of arsenic from gold-rich concentrates by roasting. Scandinavian Journal of Metallurgy, 18, 12–30.

Holtje R. V., 1929. Über die Löslichkeit von Arsentrisulfid und Arsenpentasulfid (in German). Z. Anorg. Chem., 181, 395-407.

Ide C. W. and Bowler R.G., Bucknell H.M. et al., 1988. Arsenic and old glass. J. Soc. Occup. Med., 38, 85-88.

Kim M. J. and Nriagu J., 2000. Oxidation of arsenite in groundwater using ozone and oxygen. The Science of the Total Environment, 247, 71-79.

Kuhn T. S. 1974. Second thoughts on paradigms. The structure of scientific theories, 459-482.

Lagerkvist B. J. and Zetterlund B., 1994. Assessment of exposure to arsenic among smelter workers: a five-year follow-up. Am. J. Ind. Med., 25, 477-488.

Lagerkvist B., Linderholm H. and Nordberg G.F., 1986. Vasospastic tendency and Raynaud's phenomenon in smelter workers exposed to arsenic. Environ. Res., 39, 465-474.

Lagerkvist B., Linderholm H. and Nordberg G.F., 1988. Arsenic and Raynaud's phenomenon: vasospastic tendency and excretion of arsenic in smelter workers before and after the summer vacation. Int. Arch. Occup. Environ. Health, 60, 361-364.

Lengke M. F., Tempel R.N., 2002. Arsenic sulfide oxidation at acid pH values. *Trans. Soc. Mining, Metall. Explor.*, 312, 116-119.

Lengke M. F., Tempel R.N., 2002. Reaction rates of natural orpiment oxidation at 25-40 °C and pH 6.8-8.2 and comparison with amorphous As₂S₃ oxidation. *Geochim. Cosmochim. Acta*, 66, 3281-3291.

Lengke M. F., Sanpawanitchakit C., Tempel R.N., 2009. The oxidation and dissolution of arsenic-bearing sulfides. *Can. Mineral.*, 47, 593-613.

Long G., Peng Y., Bradshaw D., 2012. A review of copper-arsenic mineral removal from copper concentrates. *Mineral Engineering*, 36-38, 179-186.

Luce F. D., Tuttle C.L. and Skinner B.J., 1977. Studies of sulfosalts of copper: V. Phases and phase relations in the system Cu-Sb-As-S between 350 °C and 500 °C. *Economic Geology*, 72, 271-289.

Lu F. J., Yang C.K., Lin K.H., Formosan J.. *Med. Assoc.* 79 (1975) 596.

Maeda S., Biotransformation of arsenic in the freshwater environment, in: Nriagu J.O. (Ed.), *Arsenic in the Environment Part I, Cycling and Characterization*, Wiley, New York, 1994, pp. 155–187.

Mamedov S. B., Mikhailov M.D., 1997. Dissolution kinetics of glassy and crystalline As₂S₃ in aqueous sodium sulfide and hydroxide. *J. Non-Cryst. Solids*, 221, 181-186.

Mandal B K, Suzuki K T. Arsenic round the world: a review. *Talanta*, 2002, 58(1): 201-235.

Maske S. and Skinner B.J., 1971. Studies of the sulfosalts of copper. I. Phases and phase relations in the system Cu-As-S. *Economic Geology*, 66, 901-918.

Mihajlovic I. et al. 2007. A potential method for arsenic removal from copper concentrates. *Minerals Engineering*, 20, 26-33.

Moats M. and Free M., 2007. A bright future for copper electrowinning. *JOM*, 59 (10), 34-36.

Mu ¨ller A., and Blachnik R., 2002. Reactivity of the system copper–arsenic-sulphur. I. The formation of Cu₃AsS₄, enargite. *Thermochimica Acta*, 387, 153–171.

Nadkarni , R. M. and Kusik , C. L. , 1988. Hydrometallurgical removal of arsenic from copper concentrates. In *Arsenic Metallurgy: Fundamentals and Applications* , (R. G. Reddy , J. L. Hendrix , and P. B. Queneau , Eds.), Warrendale , PA : The Metallurgical Society , pp. 263 – 286.

Nadkarni R. M., Kusik C.L., Meissner H.P., 1975. Method for removing arsenic and antimony from copper ore concentrates.

Nriagu J. O., Azcue J.M., in: Nriagu J.O. (Ed.), *Arsenic in the Environment. Part 1: Cycling and Characterization*, John Wiley and Sons, Inc, New York, 1990, 1-15.

Padilla R., Fan Y., Sanchez M., and Wilkomirsky I., 1997. Arsenic volatilization from enargite concentrate. In *EPD Congress 1997*, (Mishra B., Ed), Warrendale, PA: The Minerals, Metals and Materials Society, 73-83.

Padilla R., Fan Y., and Wilkomirsky I., 1999. Thermal decomposition of enargite. In *EPD Congress 1999*, (Mishra B., Ed), Warrendale, PA: The Minerals, Metals and Materials Society, 341-351.

Padilla R., Fan Y., and Wilkomirsky I., 2001. Decomposition of enargite in nitrogen atmosphere. *Canadian Metallurgical Quarterly*, 40, 335-342.

Parada Torres F. A., 2011. The alkaline sodium sulphide leaching of enargite.

Peacey, J. G., Gupta, M. Z., and Ford, K. J. R., 2010. Review of process options to treat enargite. In *Copper 2010*, Hamburg, Germany, vol. 3, pp. 1035–1050.

Perez-Segura E., Zendejas-Mendivil S., 1991. Arsenic in ore and concentrates of the Cananea copper deposit. *Transactions of the AIME* 290, 1922-1929.

Perry K., Bowler R.G., Bucknell H.M. et al., 1948. Studies in the incidence of cancer in a factory handling inorganic compounds of arsenic. II. Clinical and environmental investigations. *B. J. Ind. Med.*, 5, 6-15.

Pinchiera M., Kelm U., Helle S. and Alvarez J., 1998. Copper losses as fine particles in Chilean porphyry copper ores. *Latin American Perspectives*, Chapter 4, Mineral Processing and Technology, SME, 171-178.

Planer-Friedrich B, Suess E, Scheinost A C, et al. Arsenic speciation in sulfidic waters: Reconciling contradictory spectroscopic and chromatographic evidence. *Analytical chemistry*, 2010, 82(24): 10228-10235.

Reichert F., Trelles R.A., *An. Asoc. Quim. Argent.* 9 (1921) 89.

Ringbom A., 1953. Solubilities of sulfides. Preliminary report to the Int. Union of Pure and Applied Chem., Comm. On Physico-Chem. Data of Analytical Interest.

Riveros P.A., Dutrizac J.E., Spencer P., 2001. Arsenic disposal practices in the metallurgical industry. *Canadian Metallurgical Quarterly*, 40 (4) (2001), pp. 395–420.

Rochette E. A., Bostick B.C., Li G.C., Fendorf S., 2000. Kinetics of arsenate reduction by dissolved sulfide. *Environ. Sci. Technol.*, 34, 4714-4720.

Safarzadeh M S, Moats M S, Miller J D. Recent trends in the processing of enargite concentrates. *Mineral Processing and Extractive Metallurgy Review*, 2012.

Secco A. C., Riveros G.A., and Luraschi A.A., 1988. Thermal decomposition of enargite and phase relations in the system copper-arsenic-sulfur. In *Copper* 87,

Pyrometallurgy of Copper, (Diaz C., Landolt C., and Luraschi A., Eds.), Santiago, Chile: Universidad de Chile, 4, 225-238.

Senior G. D., Guy P.J., Bruckard W.J., 2006. The selective flotation of enargite from other copper minerals – a single mineral study in relation to beneficiation of the Tampakan deposit in the Philippines. *International Journal of Mineral Processing*, 81, 15-26.

Skinner B. J., Luce F.D. and Makovicky E., 1972. Studies of sulfosalts of copper. III. Phases and phase relations in the system Cu-Sb-S. *Economic Geology*, 67, 924-938.

Smith E. H., 1986. Metallurgy and mineral processing plant at St. Joes El Indio mine in Chile. *Mining Engineering, SME-AIME Transactions*, 971-979.

Smith L. K., Bruckard W.K., 2007. The separation of arsenic from copper in a Northparkes copper-gold ore using controlled-potential flotation. *International Journal of Mineral Processing*, 84, 15-24.

Smith E. H., Paredes E., 1988. How St. Joe Gold's El Indio mine has become a major producer of high quality crude arsenic trioxide. In *Arsenic Metallurgy: Fundamentals and Applications*, (Reddy R.G., Hendrix J.L., and Queneau P.B., Eds), Warrendale, PA: The Metallurgical Society, 145-160.

Springer G. 1969. Compositional variations in enargite and luzonite. *Mineralium Deposita*, 4(1): 72-74.

Srivastava M. H.N., Ghosh S., 1957. Dissolution studies of arsenic sulfides. *Proc. Nat. Acad. Sci. India*, A26, Pt.E. 250-255.

Stuart M., Down R.F., 1973. Mercury removal from copper concentrate. In: *Proc. AIME Annual Meeting*, 73-B-26.

Suess E, Planer-Friedrich B. Thioarsenate formation upon dissolution of orpiment and arsenopyrite. *Chemosphere*, 2012.

Tongamp , W. , Takasaki , Y. , and Shibayama , A. , 2009. Arsenic removal from copper ores and concentrates through alkaline leaching in NaHS media. *Hydrometallurgy* , 98, pp. 213 – 218.

Tongamp , W. , Takasaki , Y. , and Shibayama , A. , 2010a. Selective leaching of arsenic from enargite in NaHS-NaOH media. *Hydrometallurgy* , 101, pp. 64 – 68.

Tongamp , W. , Takasaki , Y. , and Shibayama , A. , 2010b. Selective leaching of arsenic from copper ores and concentrates containing enargite in NaHS media. In *Copper 2010*, Hamburg, Germany, vol. 7, pp. 2883–2896.

Tsai S. M., Wang T.N., Ko Y.C., *Toxicol J. Environ. Health A* 55 (1998) 389.

United Nations Synthesis Report on Arsenic in Drinking Water, 2001.

Wang Q., Nishimura T., Umetsu Y., 2000. Oxidative precipitation of Arsenic removal in effluent treatment. *Minor Elements*: 39-52.

Webster J. G., 1990. The solubility of As_2S_3 and speciation of As in dilute and sulfide-bearing fluids at 25 and 90 °C. *Geochimica et Cosmochimica Acta*, 54, 1009-1017.

Weissberg B. G., Dickson F.W., Tunell G., 1966. Solubility of orpiment (As_2S_3) in Na_2S-H_2O at 50-200 °C and 100-1500 bars, with geological applications. *Geochimica et Cosmochimica Acta*, 30, 815-827.

Wells A. F., 1984. *Structural Inorganic Chemistry*, Oxford: Clarendon Press. ISBN 0-19-855370-6.

Whitacre R. W., Pearse C.S., *Arsenic and the Environment*, Mineral Industries Bulletin, Colorado, School of Mines, 1972, p. 1.

Wilkomirsky I., Parada F., Ulloa A., et al. 1998. Dearsenifying of copper and gold-copper concentrates in double wall pilot fluid bed reactor//Sánchez M. A., Vergara F., Castro S. H. *Proceedings of the IV International Conference on Clean Technologies for the Mining Industry*. Concepción, Chile: Concepción University Press, 2, 613-621.

Wunschendorf M. H., 1929. Recherches sur les thioarsenites (sulfoarsenites): II Composés du sodium et de l'ammonium. *Bull. Soc. Chim. Fr.*, 45, 897-902.

Zhang S., 2004. Oxidation of refractory gold concentrates and simultaneous dissolution of gold in aerated alkaline solutions. *Applied Chemistry*. Murdoch University, Perth, Australia, 333.

Zheng Y.J. et al., 2008. Industrial experiment of copper electrolyte purification by copper arsenite. *J. Cent. South Univ. Technol.*, 15, 204-208.

Appendix

Part A. Tables of solubility data by experiment and OLI systems software for amorphous As₂S₃ and synthetic crystals

A.1 Solubility data of orpiment in literature and amorphous As₂S₃ by experiment and OLI systems software

Table A-1 Orpiment solubility in solutions to which no sulfide has been added (Webster 1990)

At 25 °C

pH	mS _{kt} (x 10 ⁵)	I _{part} *	As (mg/kg)
1.40	1.7	0.444	0.82
1.42	1.8	0.444	0.89
1.55	0.9	0.400	0.46
2.14	1.3	0.040	0.64
2.23	1.5	0.040	0.76
2.58	1.0	0.011	0.50
2.58	1.3	0.011	0.64
3.02	0.9	0.004	0.44
3.07	1.1	0.004	0.54
3.84	2.4	0.001	1.2
4.28	2.4	0.000	1.2
5.16	6.1	0.000	3.0
5.98	2.9	0.000	1.4
6.06	5.7	0.000	2.9
6.28	6.0	0.000	3.0
6.45	6.1	0.050	3.0
7.16	81	0.000	41

At 90 °C

pH	mS (x 10 ⁴)	I _{part}	As (mg/kg)
1.16	3.3	0.200	17
1.27	3.6	0.200	18
2.61	2.8	0.006	14
2.61	2.0	0.006	9.4
3.00	3.0	0.002	15
3.46	5.4	0.010	27

At 90 °C continued

pH	mS (x 10⁴)	I_{part}	As (mg/kg)
3.60	3.5	0.020	17
3.84	4.2	0.100	21
4.02	3.5	0.200	17
4.29	3.4	0.000	17
4.29	3.0	0.000	15
5.11	4.7	0.000	24
5.11	3.8	0.000	19
5.18	3.9	0.000	20
5.93	5.8	0.000	30
5.93	2.7	0.000	14
6.09	8.9	0.010	44
6.27	7.2	0.000	36
6.85	11	0.000	52

Table A-2 Orpiment solubility in solutions to which sulfide has been added (Webster 1990)

At 25 °C

pH	mS_{kt}	I_{part}	As (mg/kg)
1.45	0.0016	0.392	0.64
2.21	0.0294	0.036	0.009
2.23	0.0282	0.036	0.02
3.05	0.0320	0.005	0.04
3.36	0.0168	0.011	0.28
4.25	0.0239	0.000	2.3
4.35	0.0170	0.000	0.71
4.50	0.0170	0.000	0.84
4.51	0.0133	0.001	1.1
4.82	0.0212	0.001	2.1
5.56	0.0283	0.002	16
5.59	0.0228	0.000	20
6.46	0.0180	0.026	110
6.64	0.0197	0.079	620
6.75	0.0180	0.057	280

At 90 °C

pH	mS_{kt}	I_{part}	As (mg/kg)
1.57	0.0168	0.066	0.06
1.64	0.0184	0.066	0.07
2.05	0.0255	0.022	0.08
2.07	0.0218	0.020	0.05
2.08	0.0194	0.020	0.03
2.10	0.0206	0.020	0.08
2.54	0.0225	0.006	0.30
2.57	0.0188	0.006	0.36
3.07	0.0214	0.002	0.76
3.07	0.0214	0.002	0.88
3.70	0.0184	0.006	0.97
3.70	0.0185	0.006	3.9
4.12	0.0294	0.000	1.8
4.23	0.0184	0.000	4.6
4.23	0.0184	0.000	3.4
4.27	0.0192	0.000	4.1
4.30	0.0171	0.000	1.2
4.41	0.0192	0.000	6.3
4.55	0.0087	0.000	6.6
4.56	0.0087	0.000	4.3
4.58	0.0172	0.000	6.6
4.76	0.0026	0.000	4.5
4.77	0.0039	0.000	6.4
5.10	0.0350	0.000	170
5.18	0.0039	0.000	5.2
5.21	0.0178	0.002	35
5.21	0.0178	0.002	35
5.23	0.0204	0.000	69
5.25	0.0310	0.000	50
5.38	0.0221	0.001	54
5.46	0.0158	0.002	23
5.57	0.0158	0.002	24
5.64	0.0339	0.000	30
5.75	0.0338	0.000	24

At 90 °C continued

pH	mS_{kt}	I_{part}	As (mg/kg)
5.99	0.0196	0.001	69
6.07	0.0242	0.001	130
6.07	0.0242	0.001	120
6.10	0.0240	0.001	120
6.22	0.0011	0.020	55
6.27	0.0195	0.020	64
6.31	0.0015	0.100	77
6.35	0.0011	0.200	56
6.59	0.0231	0.028	250
6.59	0.0246	0.028	330
6.75	0.0308	0.100	440
6.87	0.0315	0.036	700
6.88	0.0367	0.040	900
6.97	0.0285	0.036	550
7.00	0.0340	0.080	710
7.05	0.0319	0.040	660
7.10	0.0591	0.055	1400
7.11	0.0055	0.100	210
7.24	0.0051	0.050	150
7.26	0.0567	0.072	720
7.28	0.1328	0.144	1000
7.31	0.0588	0.072	850

Table A-3 Solubility prediction of As₂S₃ in 1 wt% of 1 L Na₂S solution

Temperature (°C)	Mole of As₂S₃ (mol)	Concentration of As₂S₃ (M)
20	0.125339	0.125339
25	0.125837	0.125837
30	0.126152	0.126152
35	0.126349	0.126349
40	0.126467	0.126467
45	0.12653	0.12653
50	0.126554	0.126554

Table A-3 Solubility prediction of As_2S_3 in 1 wt% of 1 L Na_2S solution continued

Temperature (°C)	Mole of As_2S_3 (mol)	Concentration of As_2S_3 (M)
55	0.126549	0.126549
60	0.126525	0.126525
65	0.126487	0.126487
70	0.126442	0.126442
75	0.126395	0.126395
80	0.126353	0.126353
85	0.126322	0.126322
90	0.12631	0.12631
95	0.126322	0.126322

Table A-4 Solubility prediction of As_2S_3 in 2 wt% of 1 L Na_2S solution

Temperature (°C)	Mole of As_2S_3 (mol)	Concentration of As_2S_3 (M)
20	0.256194	0.256194
25	0.256847	0.256847
30	0.257254	0.257254
35	0.257506	0.257506
40	0.257655	0.257655
45	0.257732	0.257732
50	0.257757	0.257757
55	0.257745	0.257745
60	0.257707	0.257707
65	0.257651	0.257651
70	0.257585	0.257585
75	0.257516	0.257516
80	0.257453	0.257453
85	0.257404	0.257404
90	0.257377	0.257377
95	0.257381	0.257381

Table A-5 Solubility prediction of As_2S_3 in 3 wt% of 1 L Na_2S solution

Temperature ($^{\circ}\text{C}$)	Mole of As_2S_3 (mol)	Concentration of As_2S_3 (M)
20	0.390506	0.390506
25	0.391252	0.391252
30	0.391714	0.391714
35	0.391997	0.391997
40	0.392163	0.392163
45	0.392246	0.392246
50	0.39227	0.39227
55	0.392251	0.392251
60	0.392201	0.392201
65	0.39213	0.39213
70	0.392046	0.392046
75	0.39196	0.39196
80	0.391878	0.391878
85	0.391811	0.391811
90	0.391768	0.391768
95	0.391759	0.391759

Table A-6 Solubility of As_2S_3 in 1 wt%, 2 wt%, and 3 wt% of 80 ml Na_2S solution

Concentration of Na_2S	Temperature ($^{\circ}\text{C}$)	Weight of As_2S_3 added (g)	Mole of As_2S_3 (mol)	Concentration of As_2S_3 (M)
1 wt% Na_2S Solution	20	2.2	8.94E-3	0.112
	40	2.5	0.010	0.127
	60	2.6	0.011	0.132
	80	2.6	0.011	0.132
	95	2.7	0.011	0.137
2 wt% Na_2S Solution	20	5.0	0.020	0.254
	40	5.1	0.021	0.259
	60	5.3	0.022	0.269
	80	5.6	0.023	0.285
	95	5.8	0.024	0.295
3 wt% Na_2S Solution	20	6.8	0.028	0.346
	40	7.2	0.029	0.366
	60	7.4	0.030	0.376
	80	7.6	0.031	0.386
	95	7.8	0.032	0.396

A.2 Solubility data of synthetic crystal #2, #3, #4 (sodium thio-arsenate) by experiment

A.2.1 Solubility of synthetic crystal #2 in air

For synthetic crystal #2, the experimental solubility data is shown as follows:

1. In 100 ml 2.5 M sodium hydroxide and 1.0 M sodium sulfide solution

Table A-7 Solubility of in 2.5 M NaOH and 1.0 M Na₂S solution

Temperature (°C)	Weight of product #2 added (g)	Mole of Arsenic (mol)	Concentration of Arsenic (Molar)
20	5	5.39E-3	0.053
40	15	0.016	0.156
60	77	0.083	0.700
80	146	0.157	1.162
95	160	0.173	1.243

2. In 100 ml 2.5 M sodium hydroxide and 0.5 M sodium sulfide solution

Table A-8 Solubility of in 2.5 M NaOH and 0.5 M Na₂S solution

Temperature (°C)	Weight of product #2 added (g)	Mole of Arsenic (mol)	Concentration of Arsenic (M)
20	5	5.39E-3	0.053
40	23	0.025	0.235
60	89	0.096	0.789
80	153	0.165	1.203
95	159	0.172	1.237

3. In 100 ml 1.0 M sodium hydroxide and 1.0 M sodium sulfide solution

Table A-9 Solubility of in 1.0 M NaOH and 1.0 M Na₂S solution

Temperature (°C)	Weight of product #2 added (g)	Mole of Arsenic (mol)	Concentration of Arsenic (M)
20	7.5	8.09E-03	0.079
40	22.5	0.024	0.230
60	92.5	0.100	0.815
80	97.5	0.105	0.850
95	97.5	0.105	0.850

A.2.2 Solubility of synthetic crystal #3 in air

For synthetic crystal #3, the experimental solubility data is shown as follows:

1. In 10 ml 2.5 M sodium hydroxide and 1.0 M sodium sulfide solution

Table A-10 Solubility of in 2.5 M NaOH and 1.0 M Na₂S solution

Temperature (°C)	Weight of product #3 added (g)	Mole of Arsenic (mol)	Concentration of Arsenic (M)
20	0.25	6.30E-04	0.062
40	0.75	0.002	0.183
60	2.75	0.007	0.625
80	31	0.078	3.510
95	78	0.196	4.814

2. In 10 ml 2.5 M sodium hydroxide and 0.5 M sodium sulfide solution

Table A-11 Solubility of in 2.5 M NaOH and 0.5 M Na₂S solution

Temperature (°C)	Weight of product #3 added (g)	Mole of Arsenic (mol)	Concentration of Arsenic (M)
20	0.3	7.56E-04	0.075
40	0.9	0.002	0.219
60	2.6	0.007	0.594
80	59	0.149	4.462
95	89.6	0.226	4.972

- In 10 ml 1.0 M sodium hydroxide and 1.0 M sodium sulfide solution

Table A-12 Solubility of in 1.0 M NaOH and 1.0 M Na₂S solution

Temperature (°C)	Weight of product #3 added (g)	Mole of Arsenic (mol)	Concentration of Arsenic (M)
20	0.5	1.26E-03	0.123
40	2.4	0.006	0.552
60	6.4	0.016	1.287
80	88.4	0.223	4.957
95	123.4	0.311	5.291

A.2.3 Solubility of synthetic crystal #4 (sodium thio-arsenate) in air

Since the QXRD result is very ideal (100% purity), the solubility of sodium thio-arsenate (Na₃AsS₄ 8H₂O) should be relatively accurate. For synthetic crystal #4 (sodium thio-arsenate), the experimental solubility data is shown as follows:

- In 20 ml 2.5 M sodium hydroxide and 1.0 M sodium sulfide solution under air atmosphere

Table A-13 Solubility of Na₃AsS₄ 8H₂O in 2.5 M NaOH and 1.0 M Na₂S solution

Temperature (°C)	Weight of Na ₃ AsS ₄ 8H ₂ O added (g)	Mole of Arsenic (mol)	Concentration of Arsenic (M)
20	1.4	3.43E-03	0.168
40	5.2	0.013	0.588
60	14.8	0.036	1.466
80	29.2	0.072	2.439
95	58.2	0.143	3.693

- In 20 ml 2.5 M sodium hydroxide and 0.5 M sodium sulfide solution under air atmosphere

Table A-14 Solubility of $\text{Na}_3\text{AsS}_4 \cdot 8\text{H}_2\text{O}$ in 2.5 M NaOH and 0.5 M Na_2S solution

Temperature (°C)	Weight of $\text{Na}_3\text{AsS}_4 \cdot 8\text{H}_2\text{O}$ added (g)	Mole of Arsenic (mol)	Concentration of Arsenic (M)
20	2.1	5.15E-03	0.249
40	6.6	0.016	0.731
60	19.7	0.048	1.835
80	39.7	0.097	2.975
95	63.3	0.155	3.854

- In 20 ml 1.0 M sodium hydroxide and 1.0 M sodium sulfide solution under air atmosphere

Table A-15 Solubility of $\text{Na}_3\text{AsS}_4 \cdot 8\text{H}_2\text{O}$ in 1.0 M NaOH and 0.5 M Na_2S solution

Temperature (°C)	Weight of $\text{Na}_3\text{AsS}_4 \cdot 8\text{H}_2\text{O}$ added (g)	Mole of Arsenic (mol)	Concentration of Arsenic (M)
20	2.5	6.13E-03	0.295
40	7.5	0.018	0.821
60	18.5	0.045	1.749
80	36.5	0.089	2.824
95	71	0.174	4.073

A.2.4 Solubility of synthetic crystal #4 (sodium thio-arsenate) in argon

To avoid the oxygen in air, same experiments were done under argon atmosphere. The experimental solubility data is as follows:

- In 10 ml 2.5 M sodium hydroxide and 1.0 M sodium sulfide solution under argon atmosphere

Table A-16 Solubility of $\text{Na}_3\text{AsS}_4 \cdot 8\text{H}_2\text{O}$ in 2.5 M NaOH and 1.0 M Na_2S solution

Temperature (°C)	Weight of $\text{Na}_3\text{AsS}_4 \cdot 8\text{H}_2\text{O}$ added (g)	Mole of Arsenic (mol)	Concentration of Arsenic (M)
20	0.75	1.84E-03	0.179
40	2.5	0.006	0.567
60	7	0.017	1.402
80	14	0.034	2.369
95	28.5	0.070	3.653

2. In 10 ml 2.5 M sodium hydroxide and 0.5 M sodium sulfide solution under air atmosphere

Table A-17 Solubility of $\text{Na}_3\text{AsS}_4 \cdot 8\text{H}_2\text{O}$ in 2.5 M NaOH and 0.5 M Na_2S solution

Temperature (°C)	Weight of $\text{Na}_3\text{AsS}_4 \cdot 8\text{H}_2\text{O}$ added (g)	Mole of Arsenic (mol)	Concentration of Arsenic (M)
20	1	2.45E-03	0.237
40	3.2	0.008	0.711
60	9.5	0.023	1.785
80	19	0.047	2.896
95	29	0.071	3.686

3. In 10 ml 1.0 M sodium hydroxide and 1.0 M sodium sulfide solution under air atmosphere

Table A-18 Solubility of $\text{Na}_3\text{AsS}_4 \cdot 8\text{H}_2\text{O}$ in 1.0 M NaOH and 0.5 M Na_2S solution

Temperature (°C)	Weight of $\text{Na}_3\text{AsS}_4 \cdot 8\text{H}_2\text{O}$ added (g)	Mole of Arsenic (mol)	Concentration of Arsenic (M)
20	1	2.45E-03	0.237
40	3.5	0.009	0.771
60	9.5	0.023	1.785
80	17.5	0.043	2.749
95	34	0.083	3.991

A.2.5 Solubility of synthetic crystal #4 (sodium thio-arsenate) at constant hydroxide and varying hydrosulfide content in argon

1. In 10 ml 2.5 M sodium hydroxide and 1.0 M sodium hydrosulfide solution

Table A-19 Solubility of $\text{Na}_3\text{AsS}_4 \cdot 8\text{H}_2\text{O}$ in 2.5 M NaOH and 1.0 M NaHS solution

Temperature (°C)	Weight of $\text{Na}_3\text{AsS}_4 \cdot 8\text{H}_2\text{O}$ added (g)	Mole of Arsenic (mol)	Concentration of Arsenic (M)
20	0.75	1.84E-03	0.295
40	2.5	0.006	0.721
60	7	0.017	1.319
80	14	0.034	2.310
95	28.5	0.070	2.943

2. In 10 ml 2.5 M sodium hydroxide and 0.5 M sodium hydrosulfide solution

Table A-20 Solubility of $\text{Na}_3\text{AsS}_4 \cdot 8\text{H}_2\text{O}$ in 2.5 M NaOH and 0.5 M NaHS solution

Temperature (°C)	Weight of $\text{Na}_3\text{AsS}_4 \cdot 8\text{H}_2\text{O}$ added (g)	Mole of Arsenic (mol)	Concentration of Arsenic (M)
20	1.5	3.68E-03	0.351
40	3.5	0.009	0.771
60	7.5	0.018	1.482
80	13	0.032	2.250
95	18.5	0.045	2.848

3. In 10 ml 2.5 M sodium hydroxide and 0 M sodium hydrosulfide solution

Table A-21 Solubility of $\text{Na}_3\text{AsS}_4 \cdot 8\text{H}_2\text{O}$ in 2.5 M NaOH and 0 M NaHS solution

Temperature (°C)	Weight of $\text{Na}_3\text{AsS}_4 \cdot 8\text{H}_2\text{O}$ added (g)	Mole of Arsenic (mol)	Concentration of Arsenic (M)
20	2.5	6.13E-03	0.567
40	4.5	0.011	0.964
60	10	0.025	1.857
80	16	0.039	2.593
95	22	0.054	3.164

Part B. EDX analysis of synthetic complexes

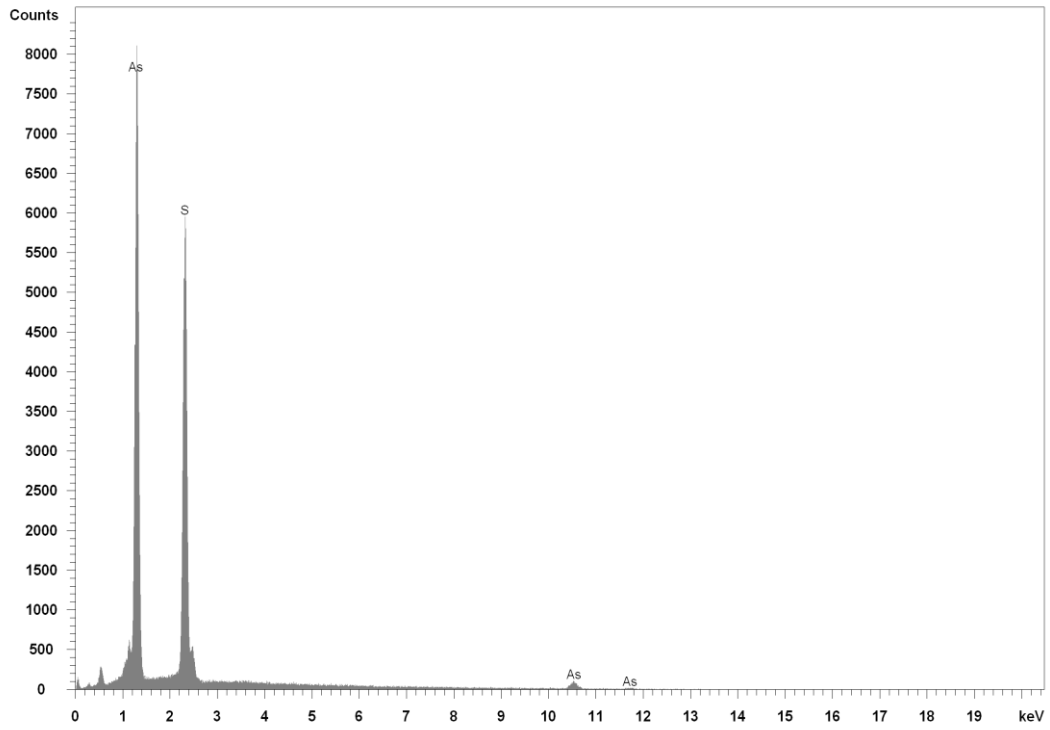


FIGURE B-1 EDX ANALYSIS OF SYNTHETIC AMORPHOUS ARSENIC TRI-SULFIDE

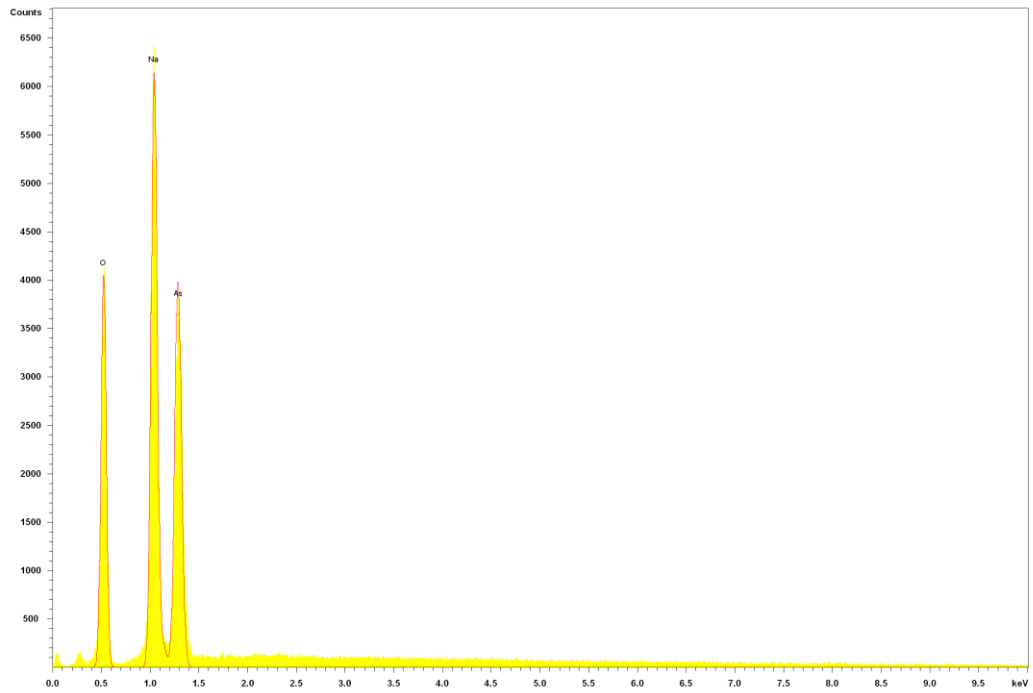


FIGURE B-2 EDX ANALYSIS OF SYNTHETIC SODIUM ARSENATE

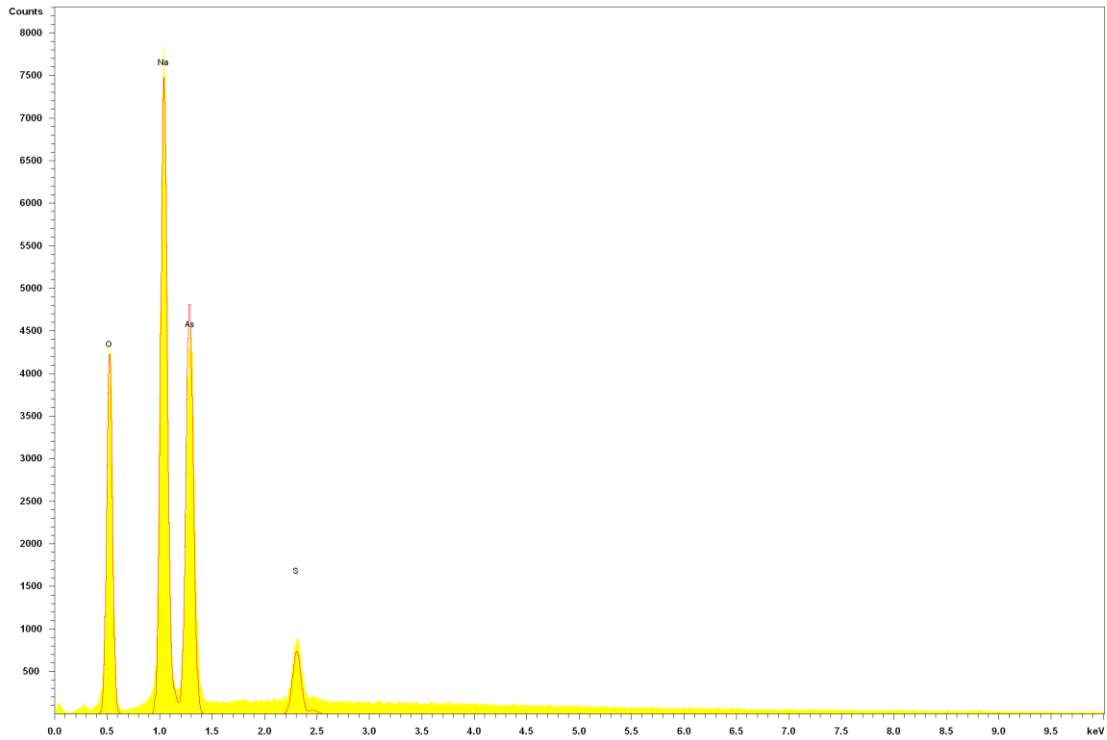


FIGURE B-3 EDX ANALYSIS OF SYNTHETIC CRYSTALLINE COMPLEX #1

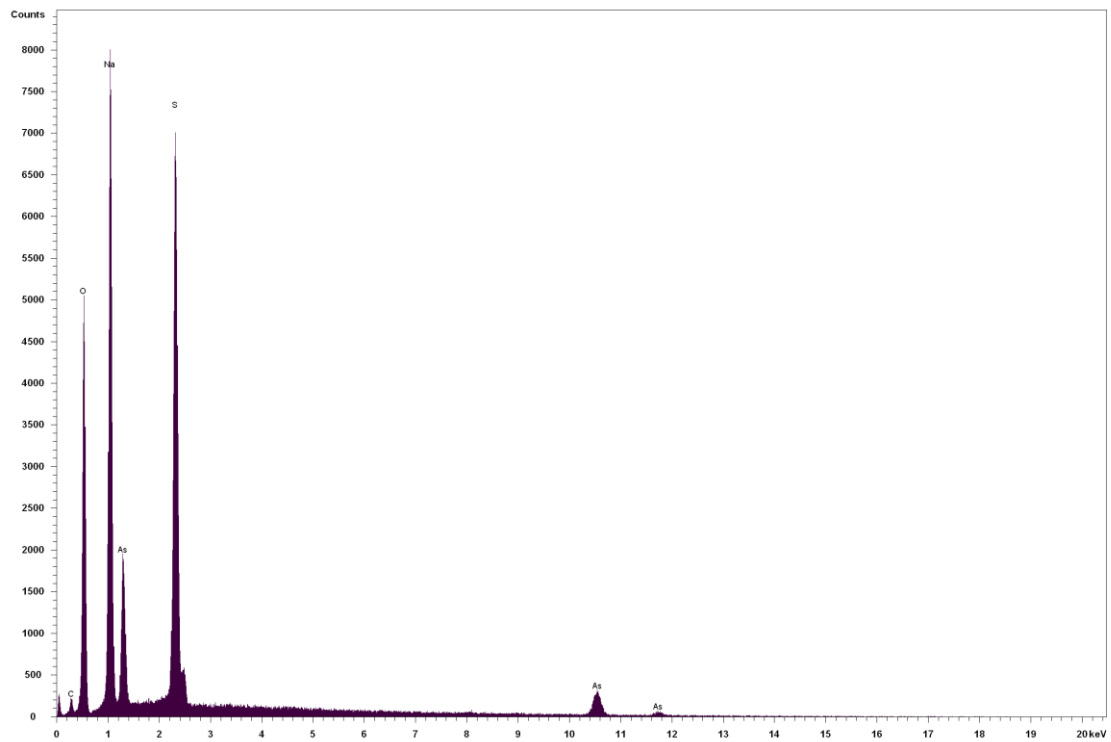


FIGURE B-4 EDX ANALYSIS OF SYNTHETIC CRYSTALLINE COMPLEX #2

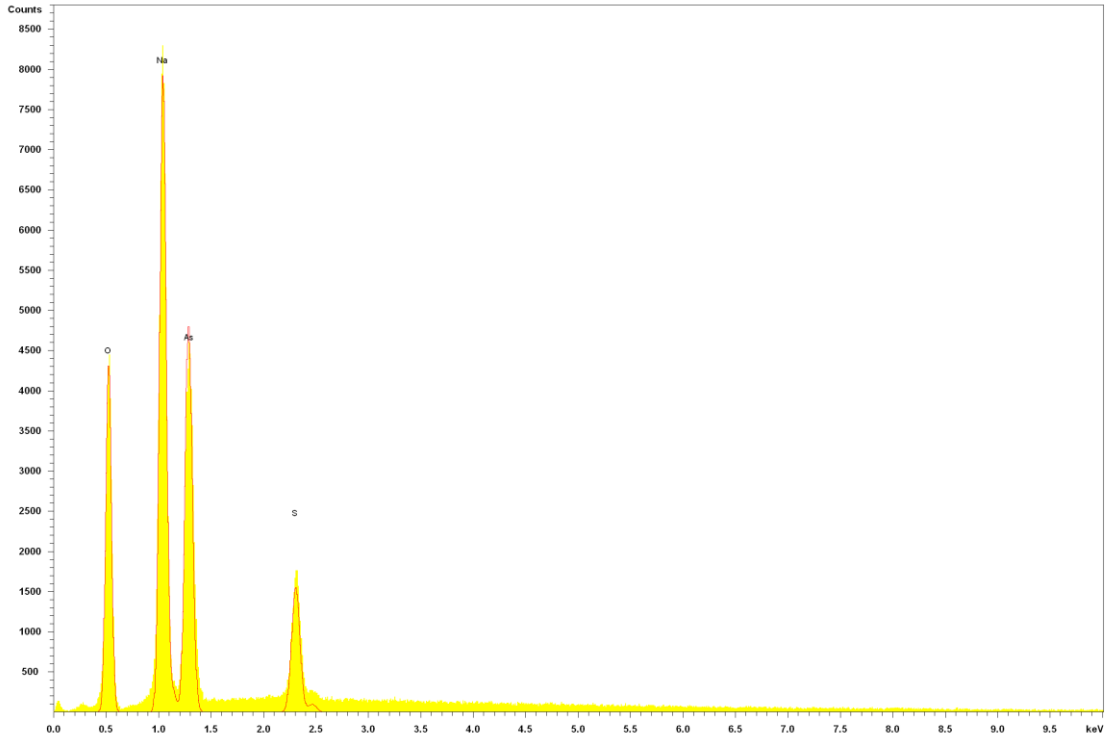


FIGURE B-5 EDX ANALYSIS OF SYNTHETIC CRYSTALLINE COMPLEX #3

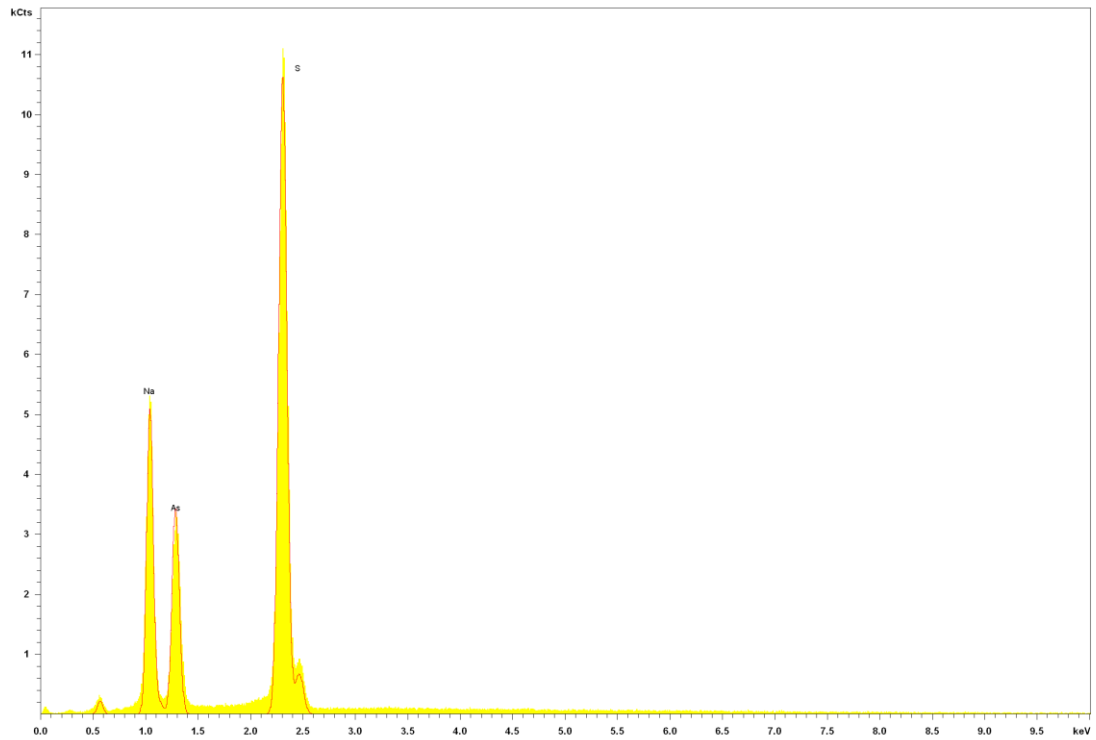


FIGURE B-6 EDX ANALYSIS OF SYNTHETIC CRYSTALLINE #4 (SODIUM THIO-ARSENATE)

Part C. Quantitative x-ray diffraction result of arsenic precipitate from enargite leaching

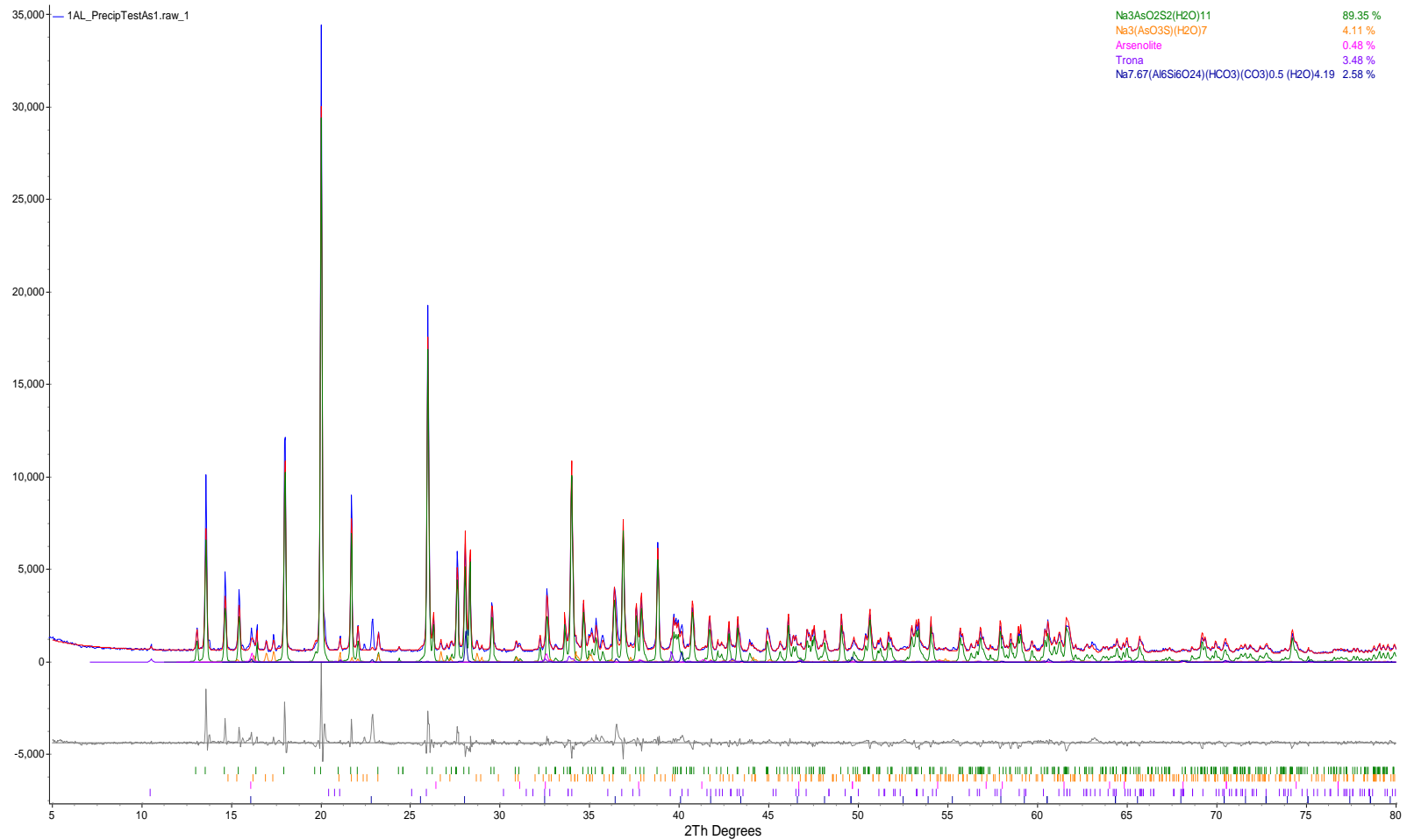


FIGURE C-1 RIETVELD REFINEMENT PLOT OF SAMPLE “AS PRECIPITATE FROM ENARGITE LEACHING WITH Na_2S :ENARGITE ~ 0.130” (BLUE LINE - OBSERVED INTENSITY AT EACH STEP; RED LINE - CALCULATED PATTERN; SOLID GREY LINE BELOW - DIFFERENCE BETWEEN OBSERVED AND CALCULATED INTENSITIES; VERTICAL BARS - POSITIONS OF ALL BRAGG REFLECTIONS). COLOURED LINES ARE INDIVIDUAL DIFFRACTION PATTERNS OF ALL PHASES.

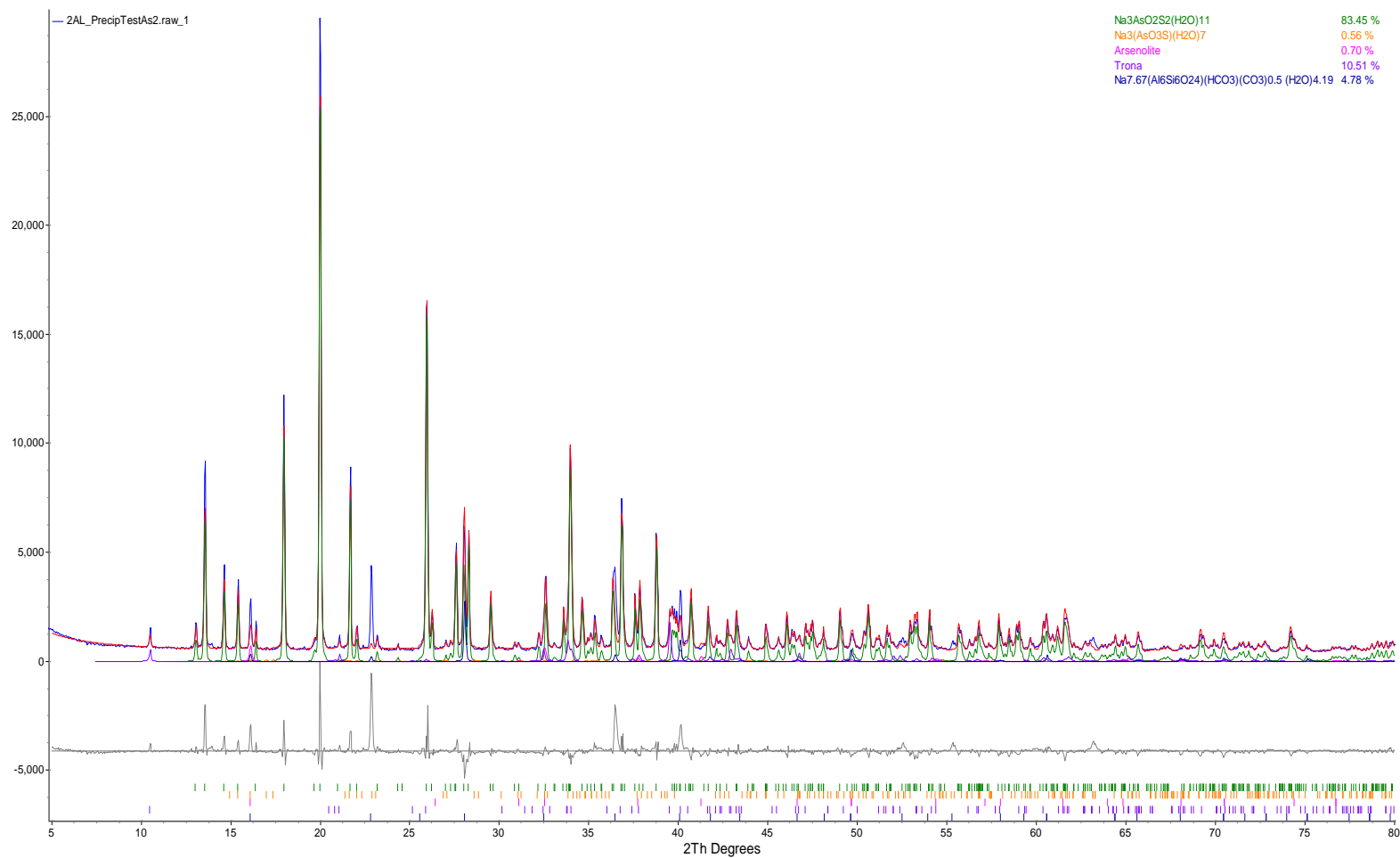


FIGURE C-2 RIETVELD REFINEMENT PLOT OF SAMPLE “AS PRECIPITATE FROM ENARGITE LEACHING WITH Na_2S :ENARGITE ~ 0.324 ” (BLUE LINE - OBSERVED INTENSITY AT EACH STEP; RED LINE - CALCULATED PATTERN; SOLID GREY LINE BELOW - DIFFERENCE BETWEEN OBSERVED AND CALCULATED INTENSITIES; VERTICAL BARS - POSITIONS OF ALL BRAGG REFLECTIONS). COLOURED LINES ARE INDIVIDUAL DIFFRACTION PATTERNS OF ALL PHASES.

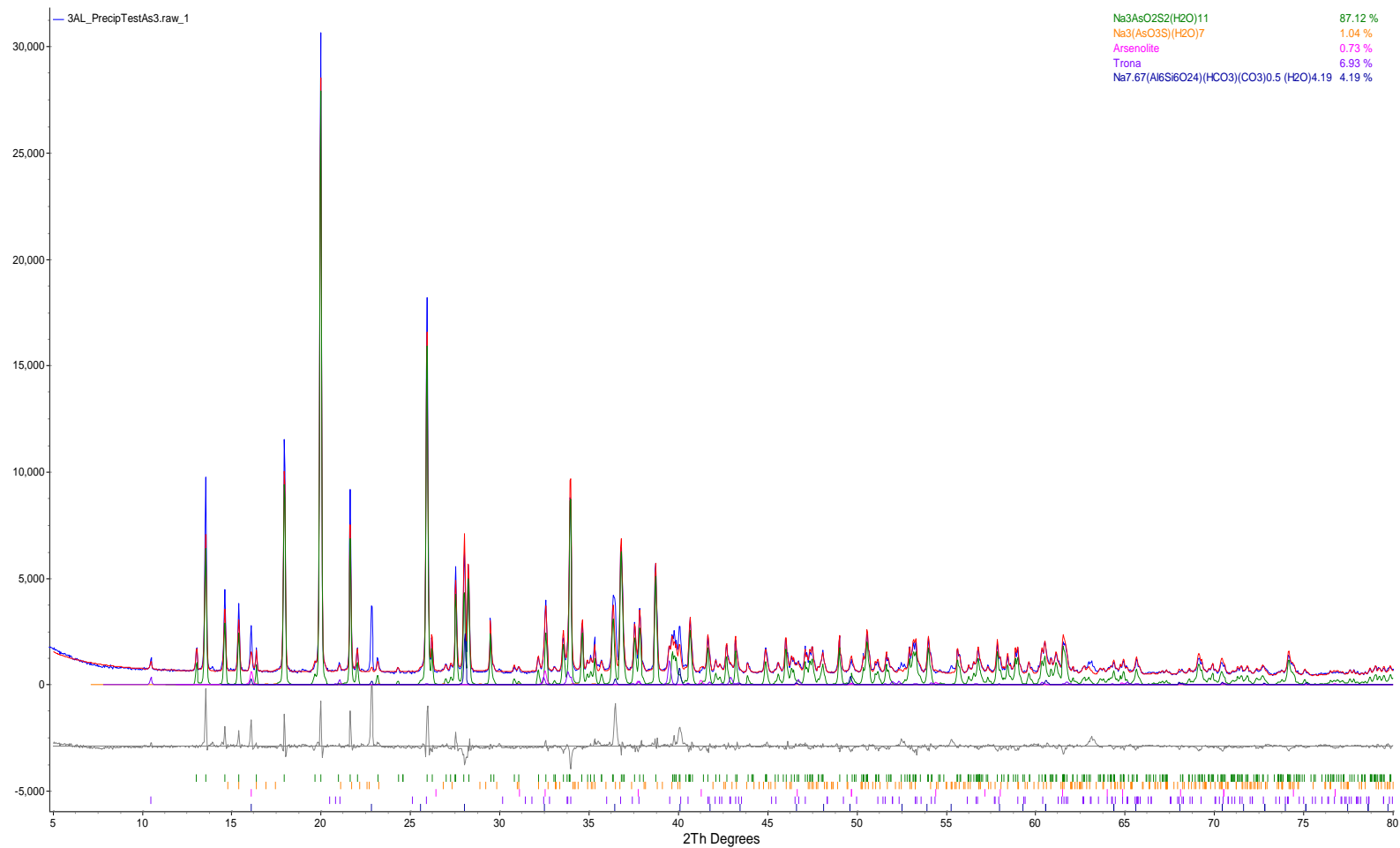


FIGURE C-3 RIETVELD REFINEMENT PLOT OF SAMPLE “AS PRECIPITATE FROM ENARGITE LEACHING WITH Na_2S :ENARGITE ~ 0.648” (BLUE LINE - OBSERVED INTENSITY AT EACH STEP; RED LINE - CALCULATED PATTERN; SOLID GREY LINE BELOW - DIFFERENCE BETWEEN OBSERVED AND CALCULATED INTENSITIES; VERTICAL BARS - POSITIONS OF ALL BRAGG REFLECTIONS). COLOURED LINES ARE INDIVIDUAL DIFFRACTION PATTERNS OF ALL PHASES.